Improving an aqueous two-phase process for C-phycocyanin extraction from *Spirulina*

James Temlett Hockey

Project thesis for the degree of Master of Science

Supervisors: **Prof. Sue Harrison;**
Dr. Marijke Fagan-Endres

Department of Chemical Engineering
Faculty of Engineering and the Built Environment
University of Cape Town

July 2022

Plagiarism Declaration

1. I know that plagiarism is wrong. Plagiarism is to use another's work and to pretend that it is one's own.
2. I have used the UCT Harvard system for citation and referencing. Each significant contribution to, and quotation in, this report from the work, or works, of other people has been attributed, and has been cited and referenced.
3. This report is my own unaided work, except for assistance received from the teaching staff.
4. I have not allowed, and will not allow, anyone to copy my work with the intention of passing it off as his or her own work.
5. This thesis/dissertation has been submitted to the Turnitin module and I confirm that my supervisor has seen my report and any concerns revealed by such have been resolved with my supervisor.

Signed by candidate

Signed *12/07/22*

Acknowledgements

I would like to thank my supervisors, Prof Sue Harrison and Dr Marijke Fagan-Endres, for giving me this opportunity to contribute to the work done by CeBER at UCT. The exposure has been great; it's been a huge learning and growing experience. Thank you, Marijke, for the weekly meetings, helping me stay on track and think through the inevitable stuck-points along the way and the amazing amounts of feedback you've given to me and this work. And thank you Prof Harrison for pushing me to ensure the work was at a high standard, and getting me to think bigger and smarter with your wealth of knowledge.

I am also extremely grateful for the financial assistance of the South African Research Chairs Initiative (SARChI) and the National Research Foundation (NRF), and again to Prof Harrison for making this all happen for so many students, it really is a great privilege.

And thank you to the CeBER bioproducts discussion group, for the invaluable opportunity to discuss our progress and seek help from peers and academics. Particularly Dr Siew Tai, who from my undergrad has been extremely supportive, and is always interested and helpful in discussion groups, and Dr Thanos Kotsiopoulos, who is always helpful even when pretending not to be.

From the lab I would like to thank Emmanuel Nkgoma, Tich Samkange and Sharon Rademayer; they made me feel at home from the first moment I worked in CeBER labs as an undergrad for our 4th year projects. There is not much that can be accomplished without their help, and they are always willing to give it.

To Sue Jobson and Lesley Mostert, for being so helpful, friendly and interested with all the things happening outside the lab. To Catherine Edwards and Muven Naidoo, the up-and-coming academics of CeBER; I've had the privilege to be a TA for courses they have run, and I believe the next generation of undergrads are in good hands.

A huge thanks to my all friends, particularly Matthew (Nithin) George and Sagar Gandhi, who made undergrad an experience I wouldn't trade for anything. Also Frans and Evren, for the daily lunches in the Tea Room, and the fun talks, updates on current events, and the problem-solving sessions. And outside of studies, David, Yann, Meije, Alex, Jaco, Jonno, who have been so loving and supportive, and amazing companions on this journey of life.

And for my family; Mom, Dad, Nicole, Graham, Justin. You have all always been there for me and for some reason never doubted me. Finally, to my beloved fiancée, Nisa, for bringing light into my life. I love you all.

Abstract

Biotechnology and bioprocess engineering have made it possible to expand production of natural compounds, and markets have moved more towards this direction. An example of this is in pigments, where many synthetic pigments have been banned or pulled out of the market due to health concerns, while naturally-derived pigments are growing in popularity. The algal pigment, C-phycocyanin (C-PC) is a blue photosynthetic pigment of the phycobiliprotein family, found in cyanobacteria and red algae. Algal pigments like C-PC have been growing in demand and the market is expected to grow at 5-7 % annually. Phycocyanin has applications as a food and cosmetics dye, a health product with therapeutic uses, and as a diagnostic protein.

Various processes have been studied to recover and purify C-PC from cyanobacteria such as *Arthrospira platensis*, commonly referred to as *Spirulina,* the most used organism for producing the pigment. The C-PC recovery process includes extraction, recovery and purification steps. One recovery and purification step reported in literature is aqueous two-phase separation (ATPS), which is able to produce high purity C-PC with good recovery. At the University of Cape Town (UCT), the Centre for Bioprocess Engineering Research (CeBER) has patented a process for extracting and purifying C-PC from *Spirulina* using a polyethylene-glycol (PEG) and maltodextrin (MDX) ATPS. This is a less-studied form of ATPS, with most C-PC extraction studies using PEG – salt systems. The PEG – MDX system was studied due to challenges faced with C-PC recovery from the PEG phase. The patented CeBER process begins with cell disruption, a period of leaching into a buffered solution followed by cell debris removal. The C-PC is subsequently purified and recovered by the PEG – MDX ATPS and three ammonium sulfate precipitation stages, and finally dried to powder.

The patented process requires optimisation and up-scaling before being commercially applied in industry, the ultimate aim of the greater project. As such, this project aimed to improve the understanding of the overall process for C-PC recovery from *Spirulina* and, in particular, the ATPS step involved, to improve the ATPS performance. The study also sought to produce cosmetic grade C-PC (purity number of > 1.5), and develop process options and simulations for this production based on a combination of literature and experimental results. The work was conducted in view of future up-scaling. This included study of the leaching step with the *Spirulina* used in this project as well as refinement and optimisation of the ATPS step. For the latter, phase diagrams for the PEG – MDX ATPS were produced to inform ATPS refinement and improvement before evaluating its performance. The phase diagrams give an understanding of how the phases partition in an ATPS, allowing prediction and optimisation of top and bottom phase compositions.

Leaching experiments showed that a maximum C-PC concentration was found after 2 h with the *Spirulina* powder used without the need for cell disruption, and that the purity decreased slowly over time (using 100 g/L *Spirulina* powder in 5 g/L citrate buffer at pH 6). This recommended a relatively short leaching time be used compared to previous work using different starting material. The PEG – MDX ATPS phase diagrams produced corresponded

well with similar ATPS data found in literature. The PEG molecular weight was tested for the best performance, finding that PEG 10000 performed slightly better than both PEG 6000 and PEG 20000, achieving a C-PC purification factor of 1.21 ± 0.01 at 9 wt% PEG 10000 and 20 wt% MDX, with a recovery of 95.1 ± 7.8 %. However, the PEG – MDX ATPS for C-PC purification gave lower purification factors compared to PEG – salt ATPS studies from literature.

A two-stage ATPS was therefore considered, with a PEG – citrate ATPS used before the PEG – MDX ATPS. This aimed to take advantage of the good C-PC selective recovery reported in literature for PEG – salt ATPS systems while still using the PEG – MDX to separate the C-PC from the PEG phase. PEG – citrate phase diagrams were produced; these compared well with those found in literature studies. A screening of PEG molecular weights across both ATPS steps found PEG 4000 to be best, mainly due to the performance in the PEG – citrate stage. Using PEG 4000 in two factorial studies on the impact of PEG and citrate concentrations in the first ATPS, and PEG and MDX concentrations in the second ATPS, response curves for the purification, recovery and concentration of the C-PC in the desired phase were produced. A *Statistica* (version 13.5.0.17) model was used to predict a local optimum, where the combination of component concentrations produce C-PC at high purify, recovery and concentration. The PEG – citrate ATPS model predicted the best component concentrations to be 11 wt% PEG and 20 wt% citrate, which gave a C-PC purification factor of 1.63 ± 0.28, at a recovery of 95.6 ± 8.0 %. The PEG – MDX ATPS model predicted a 1.43 ± 0.09 C-PC purification factor and a recovery of 86.8 ± 4.7 %, using a composition of 11 wt% PEG and 22 wt% MDX.

A combination of experimental results and literature data were used to underpin the simulation of five process configurations for C-PC production using *SuperPro Designer* (version 9.5), each targeting a cosmetic grade C-PC product or better. These sought to simplify and improve C-PC production using the PEG – MDX ATPS as the core unit procedure. The first simulation was of the original patented process (cell-disruption, leaching, ATPS, precipitation and finally freeze-drying), with the ATPS operation updated with the best case experimental results obtained in this work. The second and third simulations used the newly proposed two-stage ATPS. In the third option ultrafiltration replaced the precipitation steps. Spray-drying replaced freeze-drying as a faster and more cost-effective means of drying C-PC from the second simulation onward. The fourth simulation incorporated a pre-treatment step, using activated carbon and chitosan to adsorb contaminant proteins and purify the C-PC, before using a single PEG – MDX ATPS. The operation and performance of the pre-treatment step were based on literature information. This model used $(NH_4)_2SO_4$ precipitation as in the original process and required two precipitation stages for final purification. The fifth simulation used the pre-treatment process as in simulation 4, with the second precipitation step replaced with filter-sterilisation, before spray-drying.

The two-stage ATPS processes lead to slightly improved recoveries of 39.1 % and 39.5 % for the second and third of process recommendations, respectively. This is above the original process simulated to recover 38.7 % of the C-PC in the crude starting solution. The two-stage ATPS processes also have lower ammonium sulfate usage due to having fewer precipitation stages, in the case of the second process simulation, and due to replacing precipitation wit ultrafiltration in the third process.

The fourth process showed a higher C-PC purity of > 4.00, compared to the 3.77 simulated for the original process, and a C-PC recovery of 42.7 % from the crude extract. The chemical consumption was similar to the original process, while decreased amounts of ammonium sulfate were required. This process showed the shortest path time of the five options. Of the process configurations presented, the fifth one is best recommended, since it leads to a short batch-time (24.8 h per 3 batches), fewer process units than the original and the lowest overall chemical usage of the five processes. It also produces higher C-PC purification and recovery with reduced complexity compared to the original process. A C-PC purity of up to or above 4.0 is estimated to be achievable with this process, at a recovery of 47.7 % (using the leached C-PC as the starting point). This process produces a C-PC quality well above cosmetic grade. The trade-off between recovery and purity could be explored to achieve a higher recovery of cosmetic grade C-PC.

To summarise, phase diagrams were produced for the PEG – MDX ATPS, and the C-PC leaching was tested on the *Spirulina* used in this project. This ATPS was then tested before moving on to a two-stage ATPS, using a PEG – citrate stage, for which PEG – citrate phase diagrams were produced, before the PEG – MDX stage. This produced better results, comparable to PEG – salt ATPS studies found in literature. Results from the process simulations done on *Superpro Designer* then supported the use of a pre-treatment step before a single-phase PEG – MDX ATPS, followed by precipitation and spray drying, based on information from this study and other literature. This could lead to a feasible design for pilot-testing and a novel process for industrial C-PC production.

It is recommended that the results of the simulations be tested experimentally in further studies. A thorough techno-economic analysis of the proposed processes is also required. The pre-treatment process based on adsorption requires experimental validation and pilot scale confirmation before being applied in industry. Due to the rapidly growing demand for C-PC, a commercial process capable of producing multiple grades of C-PC, from food-grade, to cosmetic-and reagent-grade, could be lucrative for business interests involved.

Table of Contents

List of Figures

List of Tables

List of Acronyms

ATPS	-	Aqueous two-phase system
C-PC	-	C-phycocyanin
CeBER	-	Centre for Bioprocess Engineering Research
DE	-	Dextrose equivalent
GRAS	-	Generally regarded as safe
MDX	-	Maltodextrin
MW	-	Molecular weight
MWCO	-	Molecular weight cut-off
PBP	-	Phycobiliprotein
PEG	-	Polyethylene-glycol
RI	-	Refractive index
SDS-PAGE	-	Sodium dodecyl sulfate–polyacrylamide gel electrophoresis
TLS	-	Tie-line slope
TLL	-	Tie-line length
UF	-	Ultrafiltration
V_R	-	Volume ratio
λ_{max}	-	Absorbance maximum

1 Introduction

1.1 Context and scope of project

Many avenues for research and innovation are opening up in biotechnology due to a move toward sustainable production of useful bioproducts, and the endless quest to discover the extent of nature's ingenuity. An example of this is the increasing demand for natural pigments, since many synthetic pigments are banned due to negative effects on human and environmental health (Kuar *et al.*, 2009). Algal pigments are one such class of complex and useful bioproducts, and are growing in demand while already having a large market value (Dufosse *et al.*, 2005; Griffiths, Harrison, *et al.*, 2016).

Microalgae themselves have a wide range of uses, including health-benefits. As an example, *Arthrospira platensis* (*Spirulina*) is gaining popularity as a 'superfood'. Many of the health benefits of *Spirulina* are being attributed to its blue pigment C-phycocyanin (C-PC) (Kuddus *et al.*, 2013). C-PC is a blue pigment in the phycobiliprotein family. These protein complexes are photosynthetic and are found in various cyanobacteria and rhodophytes. Most phycocyanin is produced photoautotrophically, using energy from the sun and CO_2 as the carbon source, and extracted from *Spirulina*, as it is easy to cultivate in large raceway ponds (Eriksen, 2008). C-PC is used as a natural colourant in food and cosmetics and has proven health-treatment properties which include anti-inflammatory, antioxidant, hepatoprotective and anti-tumor effects (Kuddus *et al.*, 2013). Analytical grade C-PC can be used as a diagnostic chemical and fluorescent tracer in immunological studies (Eriksen, 2008). C-PC is a high-value pigment, costing from US$ 10 to 50 per mg for use as a biomarker and US$ 1 to 5 per gram as a food colourant, due to the different purity requirements (Ramos *et al.*, 2011).

Extraction and purification of C-PC has been done with chromatographic techniques, ammonium sulfate precipitation as well as aqueous two-phase system (ATPS) separations. ATPS is of particular interest, as a liquid-liquid extraction process that makes use of an aqueous polymer-polymer or polymer-salt mixture to selectively partition biomolecules to one phase or the other. These systems are useful for bioseparations due to the mild conditions required, leaving low risk of denaturing the products. ATPS is also cost-effective and relatively easy to up-scale, making use of conventional liquid-liquid extraction equipment (Srinivas, 2000). ATPS technology has been used with success for commercial enzyme separations and much research has been going into using these systems for C-PC extraction and purification (Murty *et al.*, 2012; Wang *et al.*, 2016). The most studied of these systems have been polyethylene-glycol (PEG) as the polymer phase and phosphate salts as the salt phase. High purity C-PC has been achieved.

1.2 Patented CeBER process and operation

1.2.1 Overview

Due to the growing interest in and market for C-PC, as well as research being done on large scale *Spirulina* cultivation, the Centre for Bioprocess Engineering Research at the University of Cape Town (CeBER, UCT) developed and patented a process for the purification and recovery of C-PC from *Spirulina* (Harrison *et al.*, 2019; Patent no. WO2019034955A1). The patented CeBER process makes use of a novel combination polymer-polymer ATPS, using PEG and maltodextrin (MDX), combined with multiple ammonium sulfate precipitation steps for purifying the C-PC. The process operation uses either fresh *Spirulina* or dried powder as the feedstock and includes unit operations for cell disruption (not included in the patent), C-PC extraction from the debris (leaching) and the further extraction and purification by ATPS and precipitation. The ATPS achieves recovery of C-PC in the bottom MDX phase, to avoid the difficulty of separating PEG from the C-PC. This also allows further purification of C-PC by multiple ammonium sulfate precipitations, increasing purity and decreasing microbial contamination of the final product.

Figure 1 shows a simplified diagram of the CeBER process based on the patent developed by Harrison *et al.* (2019) and the project work done in developing the process (Griffiths, Burke, *et al.*, 2016). In this process, the *Spirulina* biomass is disrupted by a bead mill-like process in which attrition of the cells is achieved by agitation with glass beads and left in a citrate buffer solution at pH 6 to leach the C-PC from the disrupted cells into solution. The majority of the cell debris is removed by centrifugation. The crude extract is mixed with MDX and PEG (molecular weight 10000 Da) in an ATPS. The C-PC is recovered into the MDX phase and the phases separated by centrifugation. Following the ATPS, three stages of precipitation with ammonium sulfate are used; both to purify the C-PC product and to reduce the degree of bacterial contamination. Each precipitation step is followed by centrifugation, and the final pellet is freeze-dried to obtain the final C-PC powder in a dry form. The disruption step, the biomass removal by centrifugation and the drying method are not specified in the patent as these are standard unit operations. The patent focused on recovery and purification steps and allows a range of PEG and MDX molecular weights; at least 6000 Da for PEG and from 10 to 20 dextrose equivalent (DE) for MDX (Harrison *et al.*, 2019). The process seeks to produce C-PC of at least cosmetic grade, with a purity number of greater than 1.5 (see Section 2.1.2).

The rationale behind the development of the process was that a PEG – salt system produced C-PC in the top PEG phase, where PEG tended to strongly complex with the C-PC (Griffiths, Burke, *et al.*, 2016). This made it difficult to employ precipitation to recover the C-PC as well as to dry the final product. Having the C-PC report to a MDX bottom phase, however, allowed precipitation with ammonium sulphate. MDX is a good carrier compound, and is generally recognised as safe (GRAS) for food and cosmetic use (U.S. Food and Drug Administration, 2019). MDX has also been found to improve the heat-stability of phycocyanin, allowing more intensive processing and longer shelf-life for the product (Dewi *et al.*, 2016). Using MDX has been shown to reduce the degradation of C-PC when spray-drying, a faster and more economical process for producing phycocyanin powder at large-scale than freeze drying (Purnamayati *et al.*, 2018).

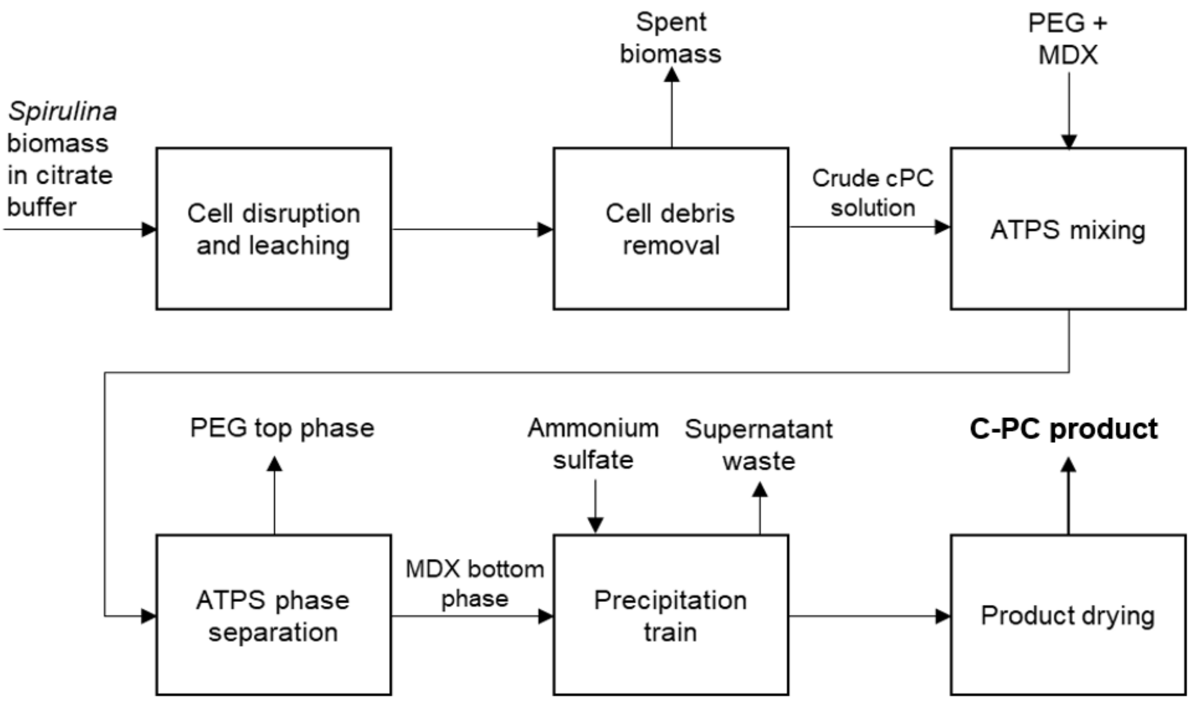

Figure 1. Simplified block diagram for CeBER C-PC process

1.2.2 Gaps identified

This project seeks to build on the process described in the patent to improve the performance of the process.

A PEG – MDX ATPS for C-PC recovery from *Spirulina* has not been been optimised rigorously, making this a key area for optimisation and possible improvement. This polymer-polymer ATPS requires thorough testing to investigate potential improvement to produce phycocyanin at a high purity and recovery. Further, in the process described in the CeBER patent, the ammonium sulphate precipitation contributes substantially to purification. In this study, alternative process options are explored for both improving the extraction of C-PC from the biomass phase for greater recovery, increasing purity achieved prior to precipitation steps and reducing number of unit operations to improve both recovery and product purity.

To optimise the process, and take it to the next steps of upscaling and commercialisation, information on the purity, concentration and recovery of C-PC after each step is necessary. Where this data is relevant and available, it is included in the literature review. The ATPS along with the precipitation steps are key areas where recovery data is important, as this is where the C-PC purification takes place, which needs to be carefully balanced with recovery.

1.3 Dissertation structure

Following the introduction, a literature review (Chapter 2) brings into a broader context the C-PC pigment, its production and potential approaches to improve its extraction, recovery and purification. An overview of the ATPS method and influencing factors is given. Methods of protein precipitation, pre-treatment of crude C-PC solutions and ultrafiltration (UF) that are discussed in literature are presented.

Chapter 3 further explores the various process options for potentially improving the process based on the literature research, as well as discussing the process scale-up considerations. These were given to further the aim of future piloting and commercialisation of the CeBER ATPS process.

Chapter 4 defines the research project, giving the problem statement, project aims and key questions for this project.

Chapter 5 gives the project methodology and experimental design. These methods describe the leaching experiments, the production of phase diagrams for the ATPS processes considered, the use of ATPS on C-PC solutions extracted from *Spirulina* and the investigation of factors to improve their performance. Statistical methods and formulae used are also given.

Chapter 6 seeks to optimise the patented process. First the bead-milling and leaching of C-PC from the *Spirulina* used in this project is tested. Secondly, MDX – PEG phase diagrams were produced before the ATPS was studied for the effect of polymer concentrations on C-PC purity, recovery, and concentration. Finally the effect of using different PEG molecular weights on the ATPS performance is examined.

In Chapter 7 the benefit of employing a two-stage ATPS process is explored, where the first stage is a PEG – citrate system to enhance purification of C-PC and the second is the PEG – MDX system to ensure that the C-PC can be recovered by precipitation and readily dried. To enable design of this system, phase diagrams for the PEG – citrate systems using the different PEG molecular weights were produced.

In Chapter 8, the experimental results obtained are used in conjunction with literature findings to propose improved process routes incorporating ATPS for producing C-PC of adequate purity. A brief comparison between the options is given.

Chapter 9 gives the conclusions of the study and recommendations for further work and for the project going forward.

2 Literature Review

2.1 C-phycocyanin

The product of interest, C-PC, is a protein in the phycobiliprotein (PBP) group, found in various species of cyanobacteria (prokaryotic blue-green algae), rhodophytes (eukaryotic red algae) and cryptomonads (unicellular eukaryotic algae) (Glazer, 1994; Sekar and Chandramohan, 2008). PBPs are a family of pigment molecules involved in light-scavenging during photosynthesis, of which C-PC is a blue-coloured pigment. Other PBPs include phycoerythrin, a red pigment, as well as R-phycocyanin and allophycocyanin, both blue pigments (Kuar *et al.*, 2009). A red fluorescence is also displayed by C-PC, and the protein finds many applications in fluorescent technologies such as immunological studies as a fluorescent tracer (Eriksen, 2008). PBPs make up a larger photosynthetic apparatus known as the phycobilisome: shown in Figure 2.

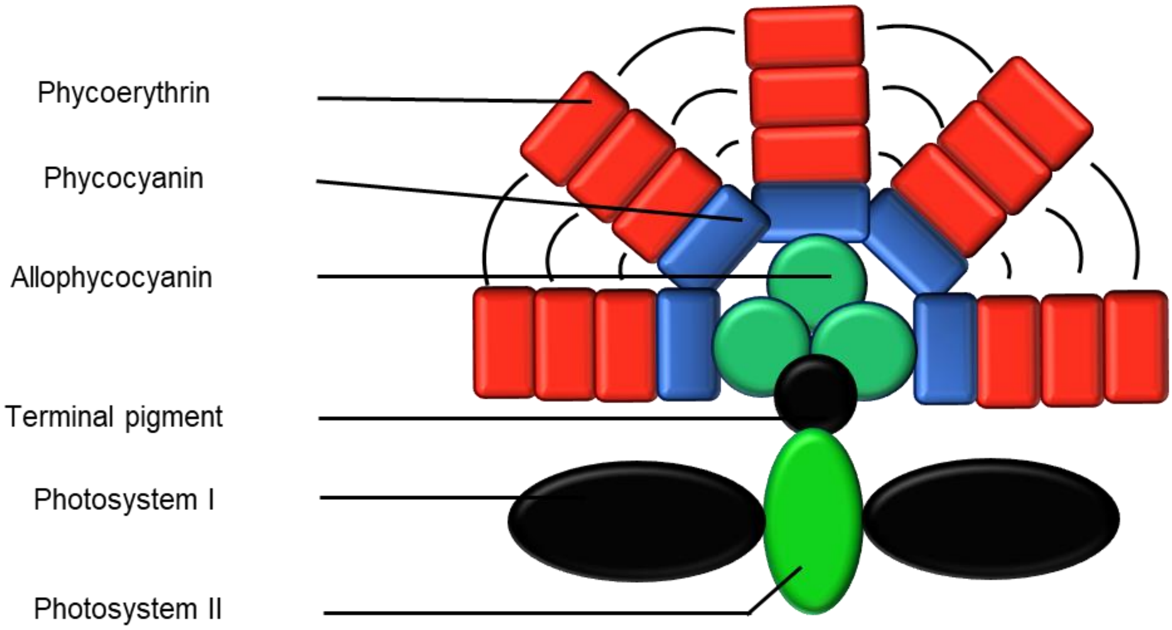

Figure 2. Phycobilisome structure seen in some cyanobacterial species where the photosystems (PS I and II) are attached to the thylakoid membrane and the antenna proteins (PBPs) face outward in the stroma of the chloroplast. Adapted from Kuar *et al.* (2009).

Phycobilisomes are assembled in a regular arrangement on the outer surface of the thylakoid membranes of chloroplasts in these photosynthetic algae. The pigments originate from covalently bound prosthetic groups known as phycobilins, which are open-chain tetrapyrrole chromophores (Eriksen, 2008). PBPs in general are made up of α- and β-chain monomers of around 20 kDa in molecular weight, each with phycobilins attached at different locations on the polypeptide chain (Kuar *et al.*, 2009). The phycobilins include phycocyanobilin (blue-coloured), phycoerythrobilin (red-coloured), phycourobilin (yellow-coloured) or phycobiliviolin (purple-coloured). The chromophores are bound to the polypeptide chain at fixed positions by one or sometimes two cysteinyl thioester linkages

(Glazer, 1994). The type of phycobilin and where it is attached on the α- or β-chain determines the PBP that is produced, its pigment and the structure.

Before discussing the properties and uses for C-PC further, the microbial sources and production of PBPs and C-PC are considered.

2.1.1 Sources and production

Phycocyanin is produced by a variety of microorganisms, and with different systems for production depending on the organism.

Photoautotrophic production has been most popular to date, such as large-scale outdoor cultivation of cyanobacteria (mostly *Spirulina*), where light from the sun is the energy source and CO_2 from air is the source of inorganic carbon (Eriksen, 2008). Production can also be done mixotrophically, where photosynthetic organisms are grown in media fed with organic carbon sources. This approach is usually limited to closed photobioreactors (Kuddus *et al.*, 2013) to limit contamination by heterotrophic bacteria. The organic carbon becomes an extra energy source as well as a carbon source for biomass growth and C-PC production, overcoming mass transfer limitations in surface aerated reactors typical of open cultivation, where there is no head space to enrich with CO_2. Heterotrophic production has also been accomplished using *Galdieria sulfuraria*, where specific strains were used that could grow heterotrophically (only requiring organic carbon for energy) without having lost their photosynthetic apparatus (Sørensen *et al.*, 2013). Recombinant production of C-PC has also been considered in heterotrophic organisms. Some other wild type organisms found to produce C-PC are shown in Table 1.

Table 1. C-phycocyanin producing cyanobacterial and rhodophyte species adapted from Kuddus et al. (2013)

Organism	Dry weight C-PC	Production	Reference
***Anabaena* sp.**	~ 10 %	Photoautotrophic	Moreno *et al.* (1995)
Galdieria sulphuraria	~ 3 %	Heterotrophic	Graverholt and Eriksen (2007)
***Nostoc* sp.**	~ 12 %	Photoautotrophic	Shukia *et al.* (2008)
Phormidium fragile	~ 13 %	Photoautotrophic	Shukia *et al.* (2008)
Spirulina fusiformis	~ 16 %	Photoautotrophic	Minkova *et al.* (2003)
Spirulina maxima	~ 8 %	Photoautotrophic	Herrera *et al.* (1989)
Spirulina platensis	~ 12%	Photoautotrophic/ mixotrophic	Boussiba and Richmond (1979)
***Synechocystis* sp.**	Not quantified	Photoautotrophic	(Rogner *et al.*, 1990)

The vast majority of phycocyanin is produced using *Spirulina* species, with the most widely studied being *Spirulina platensis*, despite not having the highest specific productivity (Kuddus *et al.*, 2013). This is driven by the ease of outdoor cultivation in raceway ponds and large scales at which this can be achieved.

2.1.2 Properties and uses

The two monomer subunits that make up phycocyanin, the α- and β-chains, have molecular weights of about 19.5 and 21.5 kDa, respectively (Sørensen *et al.*, 2013). These subunits most often form trimers ($\alpha_3\beta_3$) and hexamers ($\alpha_6\beta_6$) of C-PC, with the molecular weights being around 113 and 225 kDa, respectively (Stec *et al.*, 1999). There is variation in the phycocyanin produced by different organisms and within the organism. Vernès *et al.* (2015) found phycocyanin to fluctuate in size between 44 and 260 kDa, with the subunits between 15.2 and 24.4 kDa depending on the conditions of growth.

The absorbance maximum (λ_{max}) for C-PC is approximately 620 nm, and it emits fluorescence at 640 nm (Abalde *et al.*, 1998; Vernès *et al.*, 2015). The purity of phycocyanin is quantified according to the purity number, defined as the ratio of the absorbance of the extract at 620 nm (λ_{max} of C-PC) to the absorbance at 280 nm (A_{620}/A_{280}), where A_{280} corresponds to the absorbance maximum used to measure the total aromatic amino acid concentration (Eriksen, 2008).

At 9°C, phycocyanin was found to be stable over a pH range of 5.0 to 7.5, as well as having good stability at temperatures below 40°C (Sekar and Chandramohan, 2008).

Phycocyanin is used in the food and cosmetics industries as a natural blue dye, as well as being a colourant in pharmaceuticals (Dufosse *et al.*, 2005). Many of the health benefits of *Spirulina* can be contributed to the therapeutic properties of C-PC (Vernès *et al.*, 2015). The pigment has been found to have antioxidant, anti-inflammatory and anti-cancer properties (Kuddus *et al.*, 2013). It also acts as a hepatoprotective agent against liver-damage. Highly pure C-PC is used in immunological studies as a fluorescent marker, and in biomedical research as a diagnostic protein (Vernès *et al.*, 2015). This requires analytical-grade C-PC, which has a purity number of greater than 4.0 (Guan, 2016). Food-grade C-PC is of purity 0.7 or greater, while reactive grade is at a purity equal to or greater than 3.9 (Rito-Palomares *et al.*, 2001). Guan (2016) also specified that cosmetic-grade C-PC (for use as a dye) required a purity number between 1.5 and 2.5.

The variety of uses as well as numerous research studies being published on C-PC, has led to a growth in demand for the product (Vernès *et al.*, 2015). Many synthetic dyes are not permissible or desired for use in foods and other applied products, since many have been shown to be carcinogenic, making a natural colourant highly sought-after (Kuar *et al.*, 2009). There have been a large number of patents filed on C-PC: relating to its uses, extraction and purification processes, as well as growth enhancement techniques for higher productivity. A review by Sekar (2008) found a total of 23 patents on phycobiliprotein extraction and purification processes alone. The same review found 213 patents on specific uses of phycobiliproteins, with a further 29 patents on general uses for various applications (Sekar and Chandramohan, 2008). C-PC was not included in all of these patents, but the analysis does indicate the size of the research and commercial interest in this family of pigments. Uses for C-PC have also been discovered more recently than many of the other PBPs, indicating that a growth in demand and commercial applications for C-PC is likely to occur.

In 2017, the global market for phycocyanin was valued at US$ 32.44 million and is expected to reach US$ 66.25 million by the end of 2022, at a compound annual growth rate of 15.35 % over that time period (Report Hive Research, 2019). Food-grade phycocyanin accounted for the highest market share in sales, at 68.03 % in 2017, followed by pharmaceutical grade, accounting for 25.84 % of sales and cosmetic grade with 6.13 % (Report Hive Research, 2019).

2.2 C-phycocyanin extraction

Many processes have attempted C-PC recovery from the various biological producers mentioned, usually done in multiple stages: cell disruption, cell-debris removal, extraction and/or purification steps and finally product recovery. Eriksen (2008) provided a good review of the existing chromatographic processes and aqueous two-phase systems for purifying C-PC. This literature review focuses mainly on the ATPS studies as the central extraction operation, in line with the patented process. It also addresses the extraction steps of cell breakage and leaching (Sections 2.2.1 and 2.2.2), critical for good C-PC recovery, and further processing and recovery options for process improvement in Section 2.4.

2.2.1 Cell disruption and leaching

Extraction of phycocyanin from the cells of cyanobacteria can prove difficult due to the small size of the prokaryotic cells and the multi-layered cell wall providing protection for the cell. Some commonly used methods include ultrasonication (Furuki *et al.*, 2003), bead milling (Scheer and Kufer, 1977), high pressure homogenisation (Abalde *et al.*, 1998), cell breakage by osmotic shock (Boussiba and Richmond, 1979), lysozyme digestion (Stewart and Farmer, 1982), and freezing and thawing (Minkova *et al.*, 2003). A standard technique does not yet exist for the cell disruption of all cyanobacteria, but rather different methods may work for different organisms.

In a study done by Guan (2016), it was found that lysozyme digestion caused the greatest breakage in the *Spirulina* cell wall as compared to freeze-thawing and mechanical methods. Mechanical cell breakage by shear homogenisation was found to be the fastest, but produced the least cell wall breakage in the study. Phosphate buffer solution (PBS) was also found to leach the highest amount of C-PC at the highest purity from the disrupted cells, in comparison to the deionised water and HEPES buffer solution tested (Guan, 2016).

Pott (2018) used bead milling of fresh *Spirulina* biomass to quantify the maximum phycocyanin extracted from the biomass and the conditions for leaching. The greatest extracted amount of around 90% of the phycocyanin was released into solution after 48 h of leaching in a 0.35 M acetate buffer with 0.5 M Ca(II) at pH 6. A minimum ionic strength in the buffer used to extract C-PC from dry *Spirulina* was found to be equivalent to >5 g/L NaCl, which must be maintained to minimize co-extraction of chlorophyll into the leached solution (Li *et al.*, 2020). This same study by Li *et al.* (2020) tested three processing methods for rehydrated dry *Spirulina* powder: high-pressure homogenizing, pulsed electric field and ultrasonication. These were found not to improve the extraction of phycocyanin, while ultrasonication broke down the *Spirulina* to smaller pieces, increasing the amount of impurities in the leached extract (Li *et al.*, 2020). This was likely due to the pre-processing used to dry *Spirulina* into powder, which included spray drying through a small nozzle at high pressure. Most of the phycocyanin in this study was extracted in 3 h by 100mM phosphate buffer only at pH 7.5.

2.2.2 Cell debris removal and extract purification

Cell debris removal is usually the first separation step in downstream processing for bioproducts, removing the larger cell components such as cell walls, membranes and large organelles (Harrison *et al.*, 2013). Commonly used processes are centrifugation (to accelerate gravity settling) which can achieve up to 95 % cell harvest efficiency, and filtration, which excludes the larger cell components from the liquid extract and has been found to achieve microalgae removal of up to 89 % (Uduman *et al.*, 2010). ATPS can also be used as an integrated extraction step, however this is uncommon (Antelo *et al.*, 2010).

Aids to cell debris removal have been used in phycocyanin extraction processes, with good results. Chitosan has been implemented as a flocculating agent for harvesting microalgae, as well as being used to improve the purity of phycocyanin extracts (Wang *et al.*, 2012; Vandamme *et al.*, 2013). Wang *et al.* (2012) found an increase in phycocyanin purity number from 0.89 to 1.57 (a purification factor of 1.76) using chitosan (a natural polymer) at 10 g/L after extraction. The chitosan increased the extract purity by adsorbing some of the contaminating proteins as well as increasing the amount of cell debris removed from solution. Guan (2016) used activated carbon as an adsorbent and found an improvement in C-PC purity number from 0.475 to 0.813, a 1.71 purification factor, at a recovery of 85 %. This was achieved by stirring 80 g/L of activated carbon in the crude phycocyanin solution for 10 minutes. Another study tested the combination of activated carbon and chitosan to purify phycocyanin while improving cell debris adsorption (Fekrat *et al.*, 2019). This found an optimal purification factor of 7.14 using 0.24 % (w/v) chitosan, 8.4 % (w/v) activated charcoal after 10.2 min stirring time, taking the purity number to 3.14 from a crude extract purity of 0.44. The purification achieved in this study was 1.67 times greater than that achieved in a conventional ammonium sulfate precipitation step performed by the researchers (Fekrat *et al.*, 2019). This combination had been used before by Patil *et al.* (2006), using activated carbon and chitosan as adsorbents (amounts not specified) in crude extract pre-treatment, where a purification factor of 3.36 was found at a C-PC recovery of 73.0 ± 1.1 %. It was hypothesised that chitosan acted as a ligand allowing more proteins to be adsorbed into the activated carbon, while also having good binding capacity on its own, having both amino and hydroxyl groups (Patil *et al.*, 2006).

2.3 C-phycocyanin purification

2.3.1 Aqueous two-phase systems

An ATPS is a liquid-liquid extraction system which operates by forming two immiscible aqueous phases with different properties. ATPS processes have found extensive application in separating and purifying various biomolecules, such as enzymes, nucleic acids, antibodies, therapeutic proteins, etc. as well as larger components in biological systems, such as viruses, membranes and cell organelles (Murty *et al.*, 2012). ATPSs usually make use of either two polymer phases or a polymer-salt system for the separation, with the top polymer phase usually being polyethylene glycol (PEG). PEG is almost ubiquitous as a phase-forming polymer due to it being relatively inexpensive, biodegradable, and for its properties in stabilising and refolding proteins (Iqbal *et al.*, 2016). In polymer-polymer systems, the bottom phase is usually dextran, although a very expensive reagent, or maltodextrin, a cheaper alternative derived by hydrolysis of starches. When using a salt phase for the bottom of the ATPS, phosphate or sulfate salts have been widely used; however, this leads to excessive salt-waste to manage. Citrate salts are becoming an attractive alternative, since they are non-toxic and biodegradable (Murty *et al.*, 2012). Polymer-polymer systems have been applied to many bioseparations to reduce the amount of salt waste produced. PEG–dextran systems have extensive application for sensitive bioseparations, with different operating parameters making it more suitable for certain processes than salt systems (Asenjo and Andrews, 2011).

Besides the standard ATPS phase components given above, other systems also exist but have not yet become mainstreamed. Three-phase systems (using three polymers phases), 'single phase' systems (polymer-water) and alcohol-salt systems have been studied, although not as comprehensively (Iqbal *et al.*, 2016).

A major advantage in the application of ATPSs is their use of conventional liquid-liquid extraction equipment, making scale-up simpler and more economical than most bioseparation processes (Srinivas, 2000). Other advantages are the many factors that can be used to influence the partitioning of the proteins to the two phases. This is, however, also a limitation to large-scale implementation of ATPSs, since partitioning behaviour in these systems is not generally well-understood and requires extensive testing to verify performance (Iqbal *et al.*, 2016). Implementation is also limited by the cost of polymers over conventional solvents, making polymer-recycle important to consider.

The general principles of ATPSs is discussed below in some detail. This review will focus on two-phase systems, and specifically those relevant to the extraction and purification of proteins.

2.3.1.1 Two phase formation

The separate phases in ATPSs are formed when the two phase-forming components are mixed in a system in amounts greater than the 'critical concentration' of each component. This leads to incompatibility of the components to form a single phase, due to high ionic strength in polymer-salt systems and phase hydrophobicity and steric effects in a system where two polymers are mixed (Asenjo and Andrews, 2011). When allowed to reach equilibrium, by settling or centrifugation, two phases of different composition as well as density are formed, creating a top and bottom phase with an interface. Phase diagrams can be constructed for polymer-polymer and polymer-salt ATPSs, with a generic example given in Figure 3.

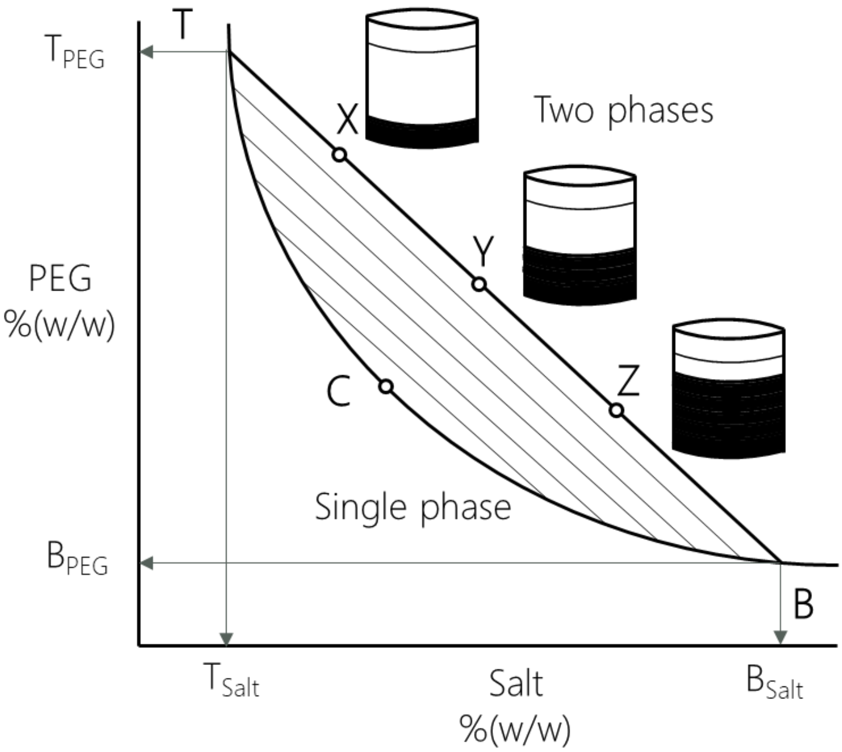

Figure 3. Two-phase diagram for a PEG – salt ATPS showing the binodal curve T-C-B, where C is the critical point, below which the system forms only a single phase. Points X, Y, Z lie on a tie line, with the top and bottom compositions given by T and B. Adapted from Murty *et al.* (2012)

A point on the diagram gives the overall composition of the system (Salt % (w/w); PEG % (w/w)), with any composition below the binodal curve (T-C-B) creating a single-phase system, since the concentrations lie below critical. Points X, Y and Z show systems with different overall compositions, but appearing on the same tie line, indicating that the top- and bottom-phase compositions will be identical, although present at different volume ratios (defined as the ratio of the volume of the top to the bottom phase). The top and bottom phase compositions are given by the intersections of the tie line with the binodal curve; in this case (T_{salt};T_{PEG}) for the top phase and (B_{salt}:B_{PEG}) for the bottom phase for the systems of composition X, Y and Z.

2.3.1.2 ATPS operation

An ATPS process is typically used as a primary purification step in bioseparations. They also generally need to consider and be able to accommodate cell debris that has remained in the extract to be purified (Asenjo and Andrews, 2011). For this reason, small scale ATPSs are always investigated thoroughly before large-scale trials and production. A small-scale ATPS uses a stirred vessel where all the components are mixed with the extract under study. Due to the low density-differences in general, and low interfacial tension, good mixing is almost always expected (Srinivas, 2000). The mixture is left to settle, or centrifuged to produce the two phases, after which the top phase is usually siphoned-off. At large-scale, different configurations are possible and continuous production can be achieved (Cunha and Aires-Barros, 2003). These will be discussed in Section 3.3.

2.3.1.3 Factors influencing ATPS

Many factors influence the operation of ATPSs, protein partitioning as well as the phase diagrams and their tie lines. These factors include temperature of the system, pH, polymer concentration, polymer hydrophobicity, polymer molecular weight (MW), and the type and concentration of salts used (phase forming or supplemental). These factors depend on the type of system being considered.

Temperature

It is essential to have good control of temperature in ATPS operation. Temperature affects the viscosity and density of each component, producing different phase diagrams at different temperatures. Lower temperatures are shown to promote separate phase formation in low concentration polymer-polymer systems, with the opposite occurring in polymer-salt systems (Asenjo and Andrews, 2011). Temperature also affects the partitioning of the biomolecule to be separated, based on the influence in the interaction of the physical and chemical properties involved. These influences are difficult to predict and require trials to determine the responses of the specific system.

Polymer molecular weight and concentration

For the molecular weight of the polymer, in general a higher MW leads to a lower concentration needed to form two phases. With PEG as the top polymer, the higher the MW, the lower the value of the partition coefficient, K (Iqbal *et al.*, 2016). In polymer-polymer systems, the greater the difference between the MW of the polymers, the more asymmetrical the phase diagram curve. Higher polymer concentrations in these systems also lead to lower partitioning to the higher MW phase, while in polymer-salt systems, higher polymer concentrations generally decrease protein partitioning to the polymer phase (Iqbal *et al.*, 2016).

pH

The greatest effect the pH has is on the partitioning of the biomolecules, particularly proteins. If the isoelectric point (pI) of the protein is lower than the pH of the system, the net charge of the protein turns negative (Murty *et al.*, 2012). Reports show that negatively charged biomolecules (due to a higher pH system) increases partitioning to the PEG-rich top phase, due to the positive dipole-moment induced (Iqbal *et al.*, 2016).

2.3.1.4 Phase diagrams

Phase diagram systems relevant to the extraction and purification of C-PC include PEG – salt systems as well as a PEG-maltodextrin ATPS as a cost-effective polymer-polymer ATPS. Figure 4 shows a phase diagram for PEG and maltodextrin, (with a dextrose equivalent of 15) at differing PEG molecular weights. The dextrose equivalent is the average number of bonded glucose (dextrose) molecules per chain of the starch hydrolysate.

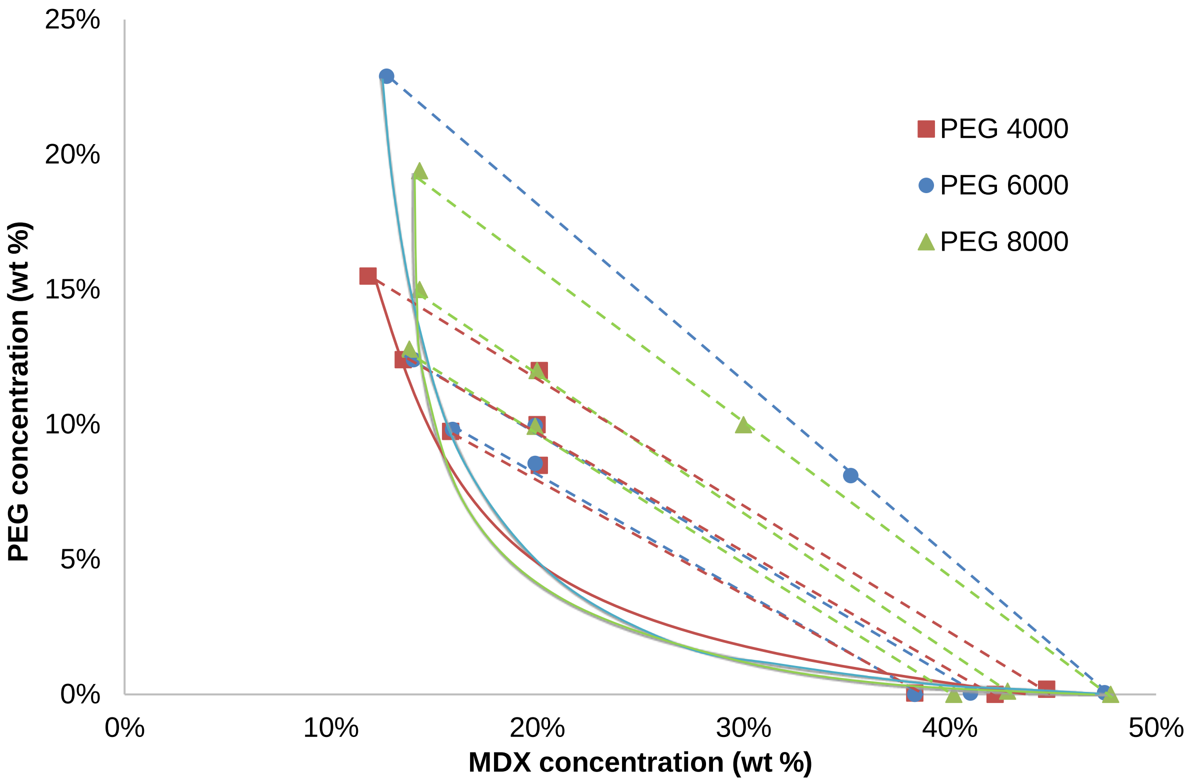

Figure 4. Two-phase diagram for a PEG-maltodextrin (MDX) ATPS showing the binodal curve and tie-lines at different PEG molecular weights with maltodextrin of 15 DE. Adapted from Machado *et al*. (2012).

The experiments performed by Machado *et al*. (2012) showed that a very low recovery of PEG is achievable in the bottom maltodextrin phase in this kind of ATPS, making this system desirable for recovery of biomolecules in the bottom phase. The top phase, however, has a fairly high weight % maltodextrin, which increases as the PEG molecular weight increases. This would affect recovery as well as potentially affecting the recycle of polymers in these systems. Another paper on PEG – MDX phase diagrams looked at different molecular weight PEGs (4000, 6000 and 10000 Da) using the cloud-point method to draw equilibrium curves, seen in Figure 5 (Ramyadevi, Subathira and Saravanan, 2012). This method uses the fact that the solution turns cloudy when the polymers are no longer in solution, leading to a two-phase system. This shows a higher PEG concentration in the bottom phase for PEG 4000 than that shown in Figure 4; this could be due to the different materials and methods used, including the molecular weight of maltodextrin which was not quantified in the study by Ramyadevi *et al.* (2012).

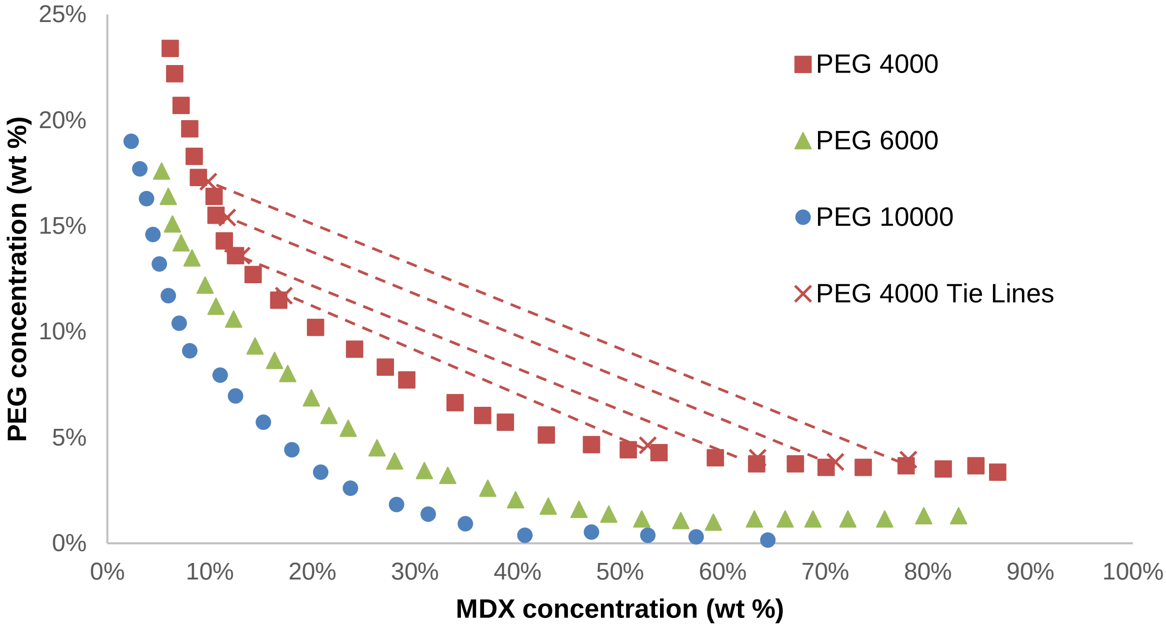

Figure 5. Two-phase diagram for a PEG-maltodextrin (MDX) ATPS showing the binodal curve using the cloud-point method and tie-lines (for PEG 4000) at different PEG molecular weights. Adapted from Ramyadevi *et al.* (2012)

A different ATPS potentially relevant to this project is one using PEG and citrate salt as the phase-forming components, as this was studied in developing the CeBER process (Griffiths, Burke, *et al.*, 2016). Citrate buffer is the extraction medium used for phycocyanin extraction from the dry *Spirulina* in the CeBER process and so could be preferable to use in an ATPS involving the crude phycocyanin extract. Citrate is also biodegradable, non-toxic and can be pH adjusted using citric acid, lessening the environmental burden of the process and reducing the amount of other salts in solution (De Oliveira *et al.*, 2008). Figure 6 shows PEG 4000 – citrate ATPS phase diagrams from different literature sources, which used different pHs in their studies. This comparison shows minimal difference between the different pHs and large agreement between the different studies. The bottom phase for each of the studies reaches about 0 wt % PEG after 18 wt % citrate is reached, which makes it a desirable ATPS to work with, since the bottom phase is polymer-free.

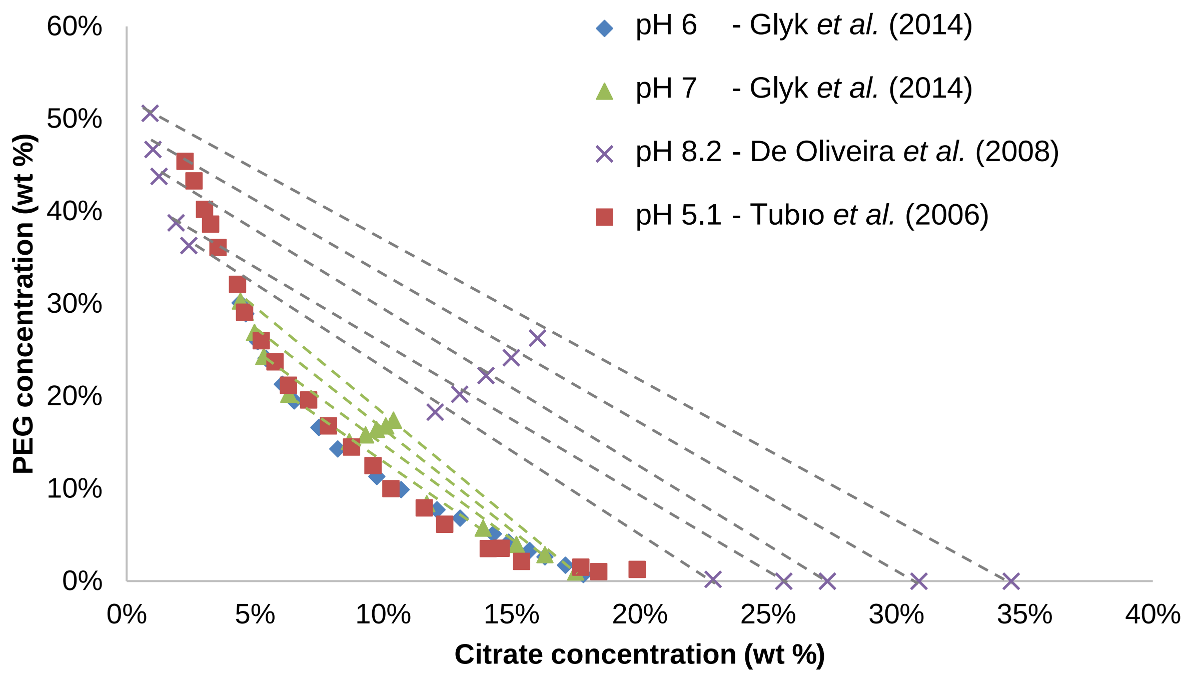

Figure 6. Two-phase diagram for a PEG – citrate ATPS showing the binodal curve using the cloud-point method and tie-lines for PEG 4000 (excepting Tubıo *et al.* (2006), with 3350 Da PEG). Adapted from literature sources shown in the legend.

Figure 7 presents the effect of PEG molecular weight on the phase equilibrium curve in PEG – citrate ATPSs across two different studies. This shows that the two-phase region increases in size as the PEG molecular weight increases, with PEG 8000 reaching 0 wt% PEG at around 15 wt% citrate concentration in the equilibrium curve.

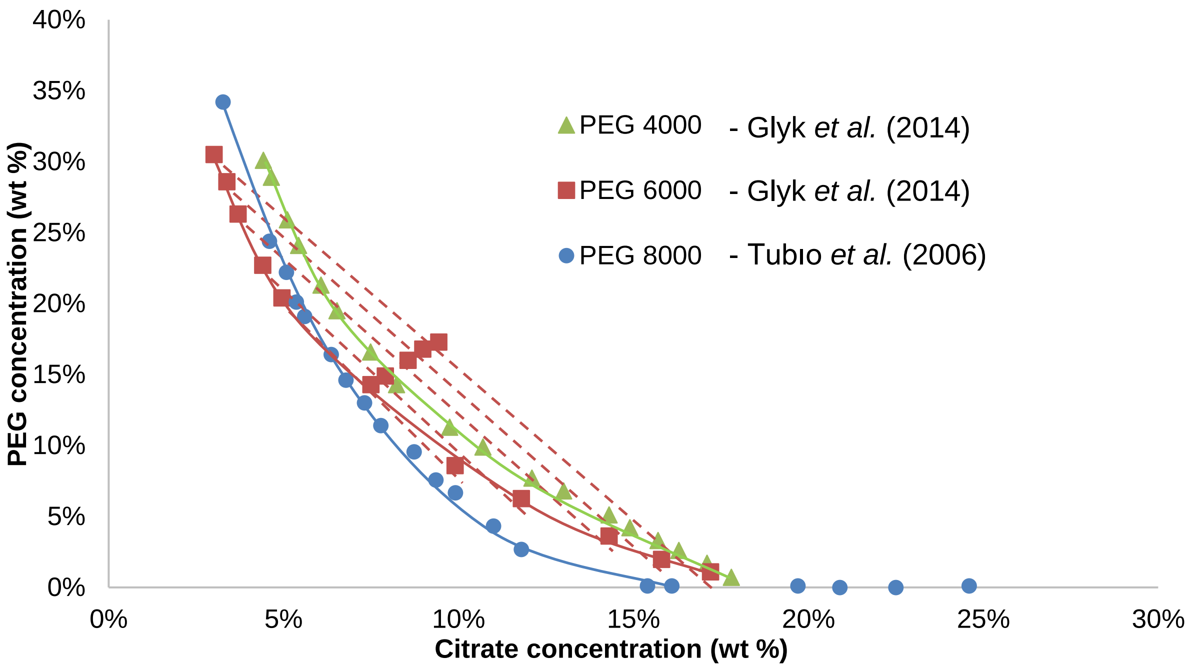

Figure 7. Two-phase diagram for a PEG – citrate ATPS showing the binodal curve using the cloud-point method and tie-lines for different PEG molecular weights. Adapted from literature sources shown in the legend.

2.3.1.5 ATPS for phycocyanin extraction

Many studies have looked at the possibility of purifying C-PC extract by ATPSs. Despite the successful purification of C-PC in these studies, there are no widely known attempts to up-scale and commercialise ATPS technology for producing high purity C-PC. Previous studies have almost exclusively used a low molecular weight PEG top phase usually with a mixture of potassium phosphate salts as the bottom phase-forming component in the ATPS. Table 2 summarises previous studies on PEG – salt ATPS experiments.

Table 2. Summary of ATPS experiments reported for extracting and purifying C-PC using PEG as the polymer phase and phosphate salts as the bottom salt phase

PEG MW (Da)	Polymer / salt concentration (w/w)	Purity before ATPS (A_{620}/A_{280})	Purity after ATPS (A_{620}/A_{280})	Recovery (%)	Reference
1450	7 % / 20 %	0.7	2.1	99.5	Rito-Palomares *et al.* (2001)
1000	-[a]	0.7	2.1	98	Benavides and Rito-Palomares (2005)
4000	12.3 % / 11.6 %	3.96	5.22	66	Patil *et al.* (2006)
4000	-[b]	1.18	3.52	86	Patil and Raghavarao (2007)
4000	5 % / 18 %	0.59	0.79	87	Antelo *et al.* (2010)
4000	12.3 % / 11.6 %	1.1	2.7	88	Sørensen *c* (2013)
4000	14 % / 21 %	1.57	2.49	97	Wang *et al.* (2012)
4000	6 % / 15 %	-[c]	4.32	79	Chethana, *et al.* (2015)
4000	4 % / 21 %	0.55	1.12	100	Antelo *et al.* (2015)

a - TLL = 34 % (Benavides and Rito-Palomares, 2005) b - TLL = 33.5 % (Patil and Raghavarao, 2007) c - Starting purity not given

The studies used PEG as the polymer phase and phosphate salts as the salt phase in the polymer-salt ATPSs. A mixture of potassium phosphate salts (KH_2PO_4 & K_2HPO_4) was used in all the studies. The two older studies achieved extremely high C-PC recoveries of 98 % or greater using low polymer weight PEG (1000 and 1450 Da). Further studies then focused on achieving higher purities of C-PC, opting for PEG 4000, at the cost of a lower recovery in general. Overall protein partitioning is also known to decrease as polymer chain lengths increase, and this trend seems pronounced when considering C-PC partitioning (Iqbal *et al.*, 2016). Within the specific studies, PEG of MW 6000 and above led to decreased purity and recovery of C-PC to the top PEG phase, leading the studies to use PEG 4000 as the optimal molecular weight.

In the follow-on study by Wang *et al.* (2012), sodium citrate was considered as the phase-forming salt in an ATPS for C-PC purification. This found the best final C-PC purity of 2.42 using PEG 4000, followed by 2.37 using PEG 2000 and 2.16 with PEG 6000. The ATPS was carried out at pH 8.3, since only sodium citrate was used without adjusting the pH, and was comparable to the PEG – phosphate ATPS, which had a purity of 2.49 using PEG 4000 (Wang *et al.*, 2012). The phycocyanin recovery using sodium citrate and PEG 4000 was 91.8 %.

These trends are further illustrated when comparing across studies which tested different PEG molecular weights for their effects on C-PC recovery and purity. Figure 8 shows the effect of PEG molecular weight on the C-PC purity number achieved in ATPSs where C-PC was recovered in the top PEG phase.

The purity number of C-PC extracts were found to decrease as PEG molecular weights increased, with an optimal molecular weight usually being at around 4000 Da. This has been attributed to the increased intermolecular forces experienced between polymer molecules of higher molecular weights (Patil and Raghavarao, 2007; Chethana *et al.*, 2015). This decreases the space between the water and polymer molecules in the top phase for the proteins to partition, pushing out the larger protein molecules, like C-PC, and biomass to the bottom phase or the interface between the phases (Grossman and Gainer, 1988).

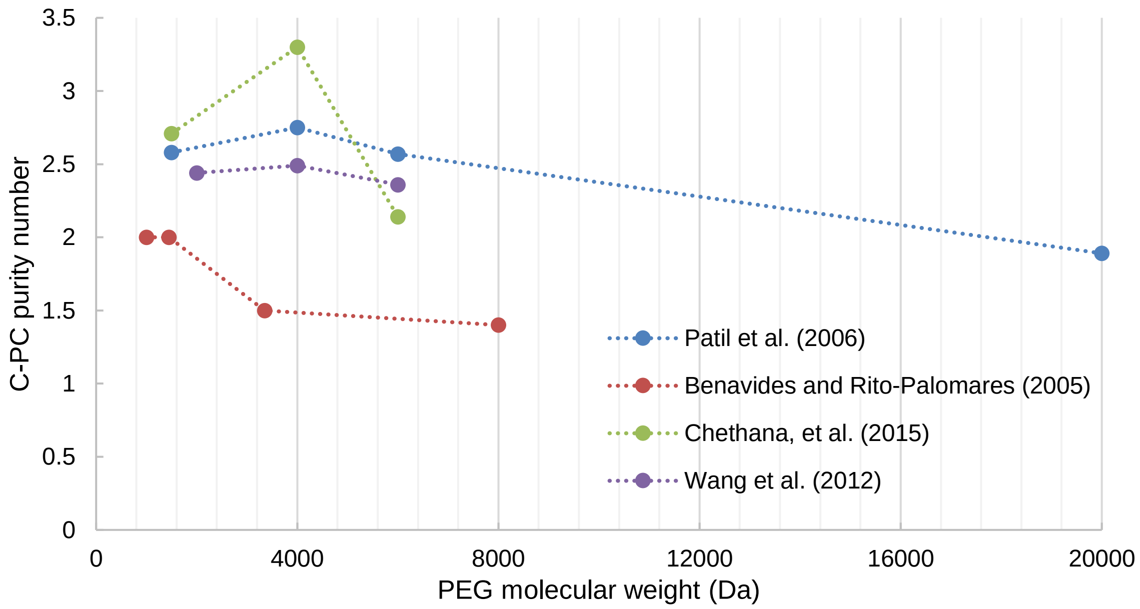

Figure 8. Different studies testing PEG molecular weight and the effect on C-PC purity in PEG-phosphate ATPS. Adapted from literature sources shown in the legend.

A similar effect is seen in the recovery of C-PC as a result of changing PEG molecular weight (Figure 9). Overall phycocyanin recovery was found to decrease as PEG molecular weight was increased. The effects are not as pronounced or reliable, however, as the molecular weight was increased from 6000 to 20000 Da (Patil *et al.*, 2006; Chethana *et al.*, 2015). The study by Antelo et al. (2015) does show a steep drop in recovery between PEG 6000 and PEG 8000, Further supporting the effect. Again, the higher PEG molecular weight, and thus chain length, would increase the intermolecular forces between the polymer and water molecules. The increased intermolecular forces are then assumed to force out more proteins into the bottom phase, decreasing recovery as seen in Figure 9.

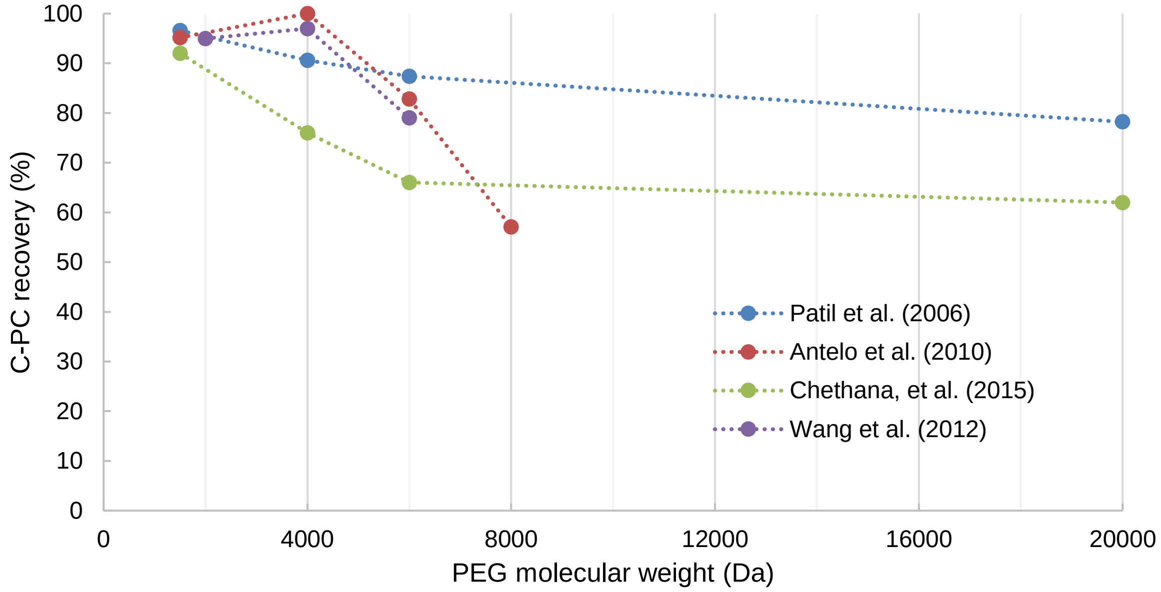

Figure 9. Studies testing the effect of PEG molecular weight on the recovery of C-PC in PEG-phosphate ATPS. Adapted from literature sources shown in the legend.

To date, no studies other than the patent of Harrison et al. (2019) have published results on polymer-polymer ATPS for purifying C-PC. Patil *et al.* (2006) did, however, screen for a PEG – maltodextrin ATPS as an alternative to PEG – salt systems, finding that the resulting purification was around 1.5-fold higher in PEG – salt systems. Experimentally, PEG – salt systems also showed lower viscosity and thus shorter separation-times, which favoured their selection for the study (Patil *et al.*, 2006).

2.4 C-phycocyanin recovery and purification

In C-PC processes using ATPS, post-ATPS processing steps are included to further purify and recover the C-PC to a usable form allowing formulation. After ATPS, most studies report use of ultrafiltration, ammonium sulfate precipitation or chromatographic methods to further recover and purify the product from a PEG phase (Eriksen, 2008). Chromatography methods are not considered further as these are generally expensive ways to produce very high purity C-PC (however, for those interested, see the paper by Eriksen (2008) which reviews many of these methods).

2.4.1 Protein precipitation

Selective protein precipitation is often done by salting-out with ammonium sulfate. When ammonium sulfate is added to a solution containing dissolved proteins, the salt ions out-compete proteins for the water molecules, reducing the hydrophilic interactions that allow the proteins to be in solution (Wingfield, 2016). The result is that the protein molecules precipitate out of solution, and often refold into a more stable form, with the ammonium sulfate still dissolved (Mitchinson and Pain, 1985). Each protein has different hydrophilic interactions, requiring different amounts of ammonium sulfate to precipitate; this can be applied in a process known as fractionation, where different proteins can be selectively precipitated and purified based on the amount of salt added (Song *et al.*, 2013).

In the preceding work done by Griffiths, Burke, *et al.* (2016), precipitation was used for the dual purpose of reducing microbial contamination and purifying the C-PC. Figure 10 shows the effect of multiple precipitations on the colony forming units in the resulting C-PC powder, while Figure 11 shows the increase in purity as a result of the three ammonium sulfate fractionation steps. Ammonium sulfate saturation was at 40 %, 55 % and 30 %, for the first, second and third stages, respectively.

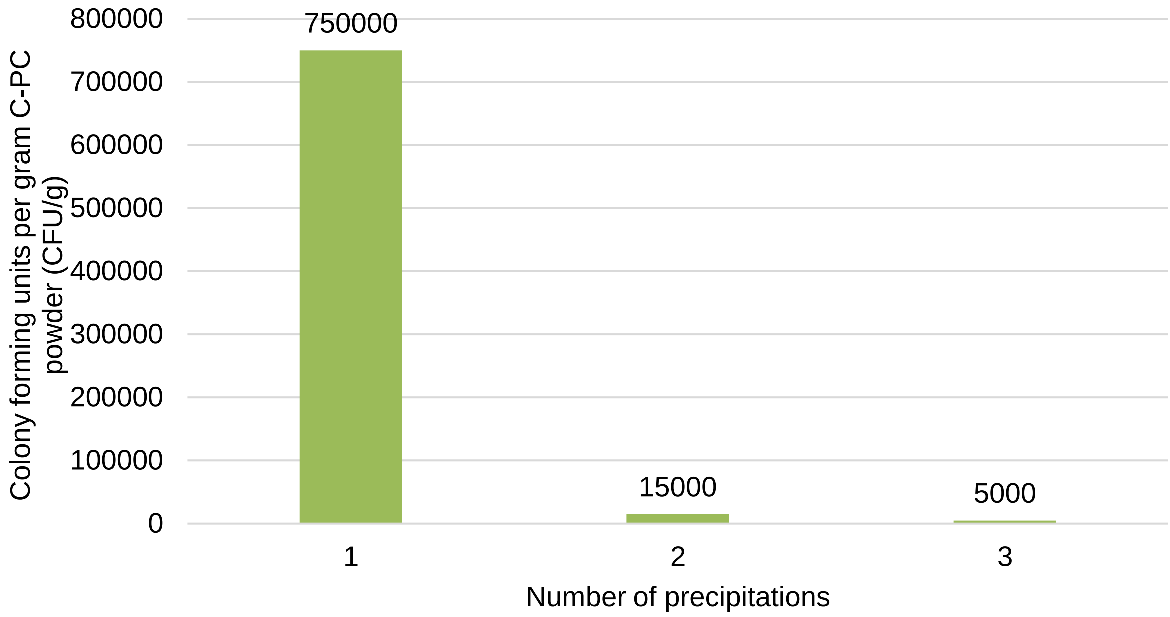

Figure 10. Bacterial contamination in C-PC powder formed after subsequent precipitation steps following ATPS adapted from Griffiths, Burke, *et al.* (2016)

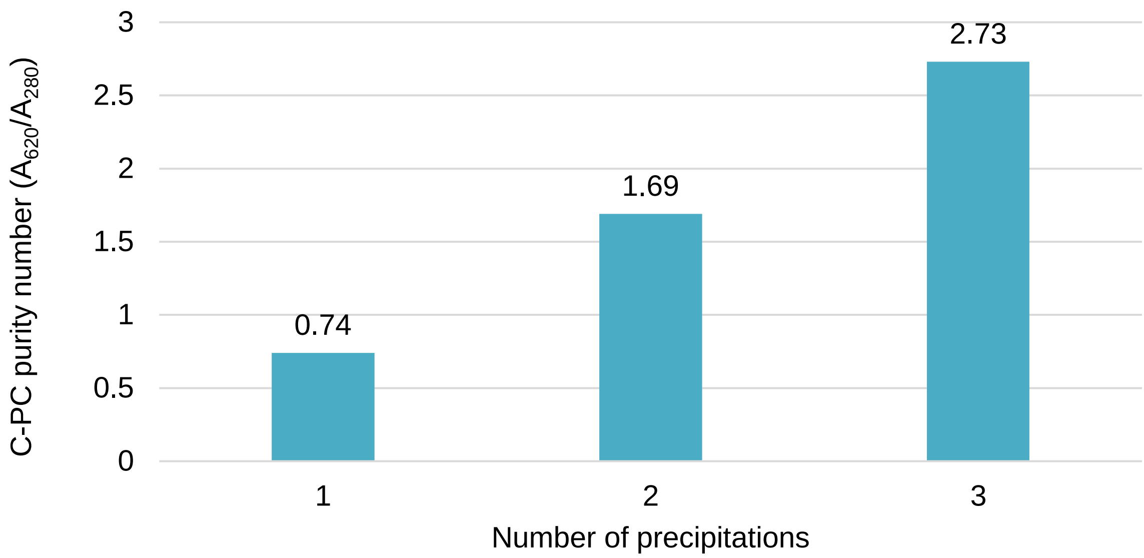

Figure 11. Purity of C-PC produced from subsequent precipitation steps following ATPS adapted from Griffiths, Burke, *et al.* (2016)

The bacterial contamination is reduced from 750000 CFUs/g C-PC powder to around 5000 CFUs/g between the first and third precipitation stages. There is no standard acceptable contamination limit for the different grades of C-PC worldwide, but a lower CFU count is better for shelf-life and where health and safety are concerned.

The purity number increased from 0.74 after the first precipitation to 2.73 after the third stage. This takes the quality of C-PC from the lower range of food-grade to just above cosmetic grade, based on purity number as the criterion. Yield data was not made available for this, which will have an impact on how effective the precipitation is within the process. Previous studies have found C-PC recoveries of between 40 and 70 % per stage of precipitation, but this also depends on the point in the process where precipitation is performed and the protein composition (Rito-Palomares *et al.*, 2001; Sørensen *et al.*, 2013).

Figure 12 shows the effect of different saturations of ammonium sulfate on the fractionation of C-PC. This was done in a step-wise manner, with each point representing a fraction of C-PC precipitated at that saturation, with the solids removed and the saturation increased to precipitate C-PC further. This is shown as a cumulative curve below, with the corresponding purity of the subsequent precipitated fractions shown on the secondary value-axis.

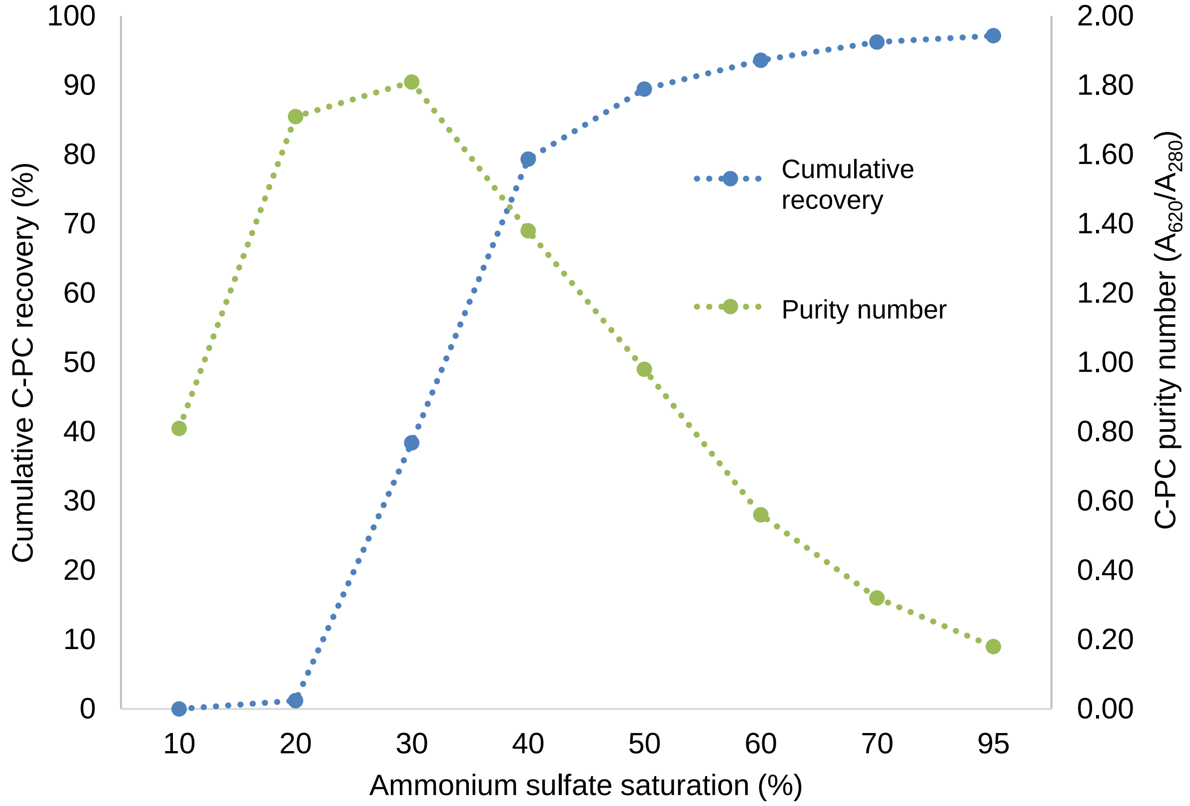

Figure 12. C-PC precipitation by differing saturations of ammonium sulfate with data adapted from Song *et al.* (2013)

A trade-off was shown between purity of C-PC obtained by fractionation by ammonium sulfate at different saturations, and the recovery of C-PC. To increase purity from 0.8 to 1.8, a 39 % recovery of C-PC was found. Alternatively, a roughly 80 % recovery could be obtained if the C-PC recovered was of purity 1.4. Lower recoveries can be expected if the purity requirement increases, however, with a recovery of 48.2 % obtained when purifying C-PC from a purity number of 3.1 to 3.8 (Rito-Palomares *et al.*, 2001). This shows that precipitation results are very much system-specific and should be tested within the system of interest.

2.4.2 Ultrafiltration

Ultrafiltration (UF) is a cross-flow membrane filtration process which operates on the principle of size-exclusion. UF is extremely versatile, with the ability to separate compounds between 1000 and 1000000 Da in molecular size, depending on the pore size of the membrane filter. Pore sizes usually range from 0.001 to 0.1 µm, but units are generally rated by molecular weight cut-off (MWCO), the molecular weight where 90 % of molecules at that size are excluded or retained by the filter membrane. UF can operate at high pressure in various configurations or centrifugally in rotating filter units (Harrison *et al.*, 2013).

Separation of enzymes using aqueous two-phase separation followed with ultrafiltration was performed in a PEG – MDX ATPS system, achieving an overall recovery of 79 % on amyloglucosidase (Tanuja *et al.*, 2000). This showed that PEG and maltodextrin, being a large proportion of the top phase following the ATPS, could be successfully separated from proteins by UF (pore size not given).

Studies have also been performed using ultrafiltration in systems for producing phycocyanin using PEG – phosphate ATPS processes.

In a study by Rito-Palomares *et al.* (2001), a UF filtration unit with a 30 kDa cut-off was used to remove the PEG from C-PC after an ATPS stage. This operated at 40 psi and increased the C-PC purity number from 2.4 (post-ATPS) to 3.1 with a recovery of 70.5 %. Two further studies, those by Patil *et al.* (2008) and Patil and Raghavarao (2007), employed ultrafiltration after ATPS as a means of separating the PEG polymer phase from the C-PC product. These also used 30 kDa membrane cut-offs but used centrifugation at 10000 rpm for the filtration. No increase in purity was obtained, but these were at purities of greater than 4 after the ATPSs (Patil and Raghavarao, 2007; Patil *et al.*, 2008). Sørensen *et al.* (2013) made use of a 50 kDa tangential flow ultrafiltration unit to both remove PEG as well as smaller protein fractions to purify the C-PC product. This led to an increase in purity number from 2.7 to 4.5, at a recovery of 79 %. The increase in purity in this case could be due to the use of a larger molecular size cut-off, as well as *G. sulfuraria* being the source of C-PC, with a different protein composition. No indication of remaining PEG in the C-PC product was given in the above studies.

To employ UF on the top phase after PEG-phosphate ATPS, Sørensen *et al.* (2013) diluted between 4 and 10 mL of the C-PC containing solution to 500 mL, presumably in order to overcome to high viscosity of the PEG phase. The retentate was then repeatedly passed through the filter until the volume was reduced to between 10 and 20 mL. Shkinev *et al.* (1987) found that poly(ethyleneimine) of MW 500000 Da at concentrations higher than 2 wt% drastically reduced permeate flux in UF, leading to the conclusion that viscous polymer solutions be diluted to below 2 wt% to reduce their viscosity.

2.5 C-phycocyanin formulation

To achieve C-PC in powder form, some method of drying is performed on the purified extract. Drying is the final step in many bioprocesses, since solid powdered forms are usually more stable for long-term storage and are easier to transport. Drying refers to removing volatile substances, generally water, by a thermal process or evaporative process to yield a solid product. For drying bioproducts, thermal degradation needs to be considered since many are thermally labile (Harrison *et al.*, 2013). Drying processes that attempt to minimise thermal degradation include: spray drying, vacuum-shelf drying, freeze drying and batch vacuum rotary drying. Depending on the bioproduct to be dried, one or more of these processes are suitable depending on the thermal sensitivity of the product. C-PC in particular shows good stability at temperatures below 40 °C and thermal sensitivity at higher temperatures (Sekar and Chandramohan, 2008).

2.5.1 Freeze drying

Freeze drying is used for very heat-sensitive products, including enzymes, other proteins and some pharmaceuticals, since no thermodegradation occurs during the process (Harrison *et al.*, 2013). Freeze drying also produces a product with a very high specific surface area, allowing rapid dissolution and formulation. The process involves freezing the product mixture rapidly and creating a vacuum, while maintaining temperature below the triple-point of water (0.01°C and 4.6 mm Hg), allowing sublimation of the water from the solid phase. Multiple small-scale studies used freeze drying to produce C-PC powder, to ensure total recovery and product integrity (Herrera *et al.*, 1989; Dewi *et al.*, 2017). Microencapsulation with different materials was tested to produce a powder with a high bulk-density and that would resist oxidation, finding Na-alginate to be the best for this purpose (Dewi *et al.*, 2017). Herrera *et al.* (1989) tested both freeze drying and spray drying, recommending that spray drying be used since it is less energy intensive and has a lower capital investment.

2.5.2 Spray drying

Spray drying occurs where a mixture to be dried is simply sprayed through a nozzle at high pressure with gas, to create atomisation, into a chamber with high temperature co-current air flow (Harrison *et al.*, 2013). This rapidly evaporates the volatile liquids, while the atomised dry powder is blown into a cyclone, allowing the powdered solids to remain in a collection vessel and the humidified air to be taken away. Air temperatures are usually above 100 °C, while the solid product does not reach this temperature, and is allowed to rapidly cool. Counter-current configurations are also used in spray drying. Spray drying has the benefit a higher throughput and a faster drying rate than freeze-drying.

Kurniasih *et al.* (2018) tested spray-drying for producing phycocyanin, using different carriers for microencapsulation since phycocyanin is known to be heat-unstable at temperatures above 40 °C. The study used an air inlet temperature of 130 °C for spray-drying and a combination of maltodextrin and alginate as carriers, finding the combination of 9.4 wt% maltodextrin and 0.6 wt% alginate to be best in terms of colour-intensity and phycocyanin content (by encapsulation efficiency) of those tested (Kurniasih *et al.*, 2018). Purnamayati *et al.* (2018) tested different temperatures of spray drying using 9 wt% maltodextrin and 1 wt% k-carrageenan as carriers, finding 110 °C to perform better than 90 °C and 130 °C in a trade-off between yield and encapsulation efficiency. The microcapsule yield achieved in this study was 27.7 % at 110 °C, in comparison to 40.7 % found in Kurniasih *et al.* (2018) using 130 °C and alginate. Another study used maltodextrin and whey protein isolate, at a ratio of 34 wt% and 66 wt%, respectively, as carrier materials (Ilter *et al.*, 2017). At an inlet temperature of 167 °C, this study found a much higher C-PC encapsulation yield of 87 %. The discrepancies between the different studies on spray drying C-PC could be due to a number of factors, including the chemicals and equipment used, the starting C-PC solution and the measurement of C-PC yield vs encapsulation efficiency. Despite uncertainty with regards to yield, this method is suggested to be faster and more economical.

As a carrier, maltodextrin is known to improve the heat-stability of proteins in spray-drying, hence the use in the above studies. It is also a GRAS compound and used as a carrier in many applications (Dewi *et al.*, 2016). Maltodextrin protects encapsulated material from oxidation and has been shown to protect the antioxidant activity of phycocyanin after spray-drying (Dewi *et al.*, 2016).

3 Potential process improvements and scale-up

3.1 Introduction

Prior to presenting the experimental sections of this dissertation, consideration of potential process improvements, alternatives and scale-up options is presented. Some options for improvement were the ideas of the original authors on the CeBER process patent, while some were found in researching the literature and others arose while performing the experimental work.

3.2 Process improvement options

3.2.1 Multiple ATPS stages

Having multiple ATPS stages may produce an improved process over a single-stage PEG – MDX ATPS, as proposed by Griffiths, Burke, *et al.* (2016). As presented in the literature review, PEG – salt ATPS is most studied for C-PC purification and reported to have a purification up to 1.5-fold higher than the polymer – polymer ATPS in a study by Patil *et al.* (2006). Thus, the inclusion of a PEG – citrate ATPS, in which C-PC reports to the upper PEG phase, can be considered to enhance the performance in terms of purification and recovery, over using the PEG – MDX system alone. The advantages of citrate-salts and the comparable performance to the more-studied phosphate salt systems make this a suitable option for inclusion into the process.

The PEG – MDX is still necessary, however, to overcome the problems reported by Griffiths, Burke, *et al.* (2016) in precipitating the C-PC from the PEG phase when a PEG – salt system is used as well as the difficulty of drying the final product containing PEG. The PEG – MDX ATPS can ensure that C-PC reports to the bottom phase with negligible amounts of PEG.

3.2.2 Ultrafiltration

Ultrafiltration, based on separation by size, may be an alternative to the multiple precipitation stages, based on separation by solubility, for achieving both the desired product purity and quality, in terms of bacterial contamination. As described in the literature review, UF has been used to recover phycocyanin from a PEG phase after ATPS, leading to an increase in purity at a reasonable recovery. C-PC, with a molecular weight of ~225 kDa for its hexamer, has a higher molecular weight than PEG (4 to 20 kDa) and MDX (5 to 10 kDa). Furthermore, the protein fractions in *Spirulina* extracts are largely below the size of 100 kDa based on gel electrophoresis (SDS-PAGE), meaning selective purification of C-PC is possible (Abakoura, 2018).

Figure 13 shows SDS-PAGE results for crude *Spirulina* extract and a blue coloured fraction of the extract (Abakoura, 2018). A limitation of SDS-PAGE is that before staining the protein fractions in the lanes, the disulfide bonds are broken, which may lead to larger proteins breaking up into their component polypeptides. This seems to have happened in

Figure 13, since it shows fractions of below 20 kDa (likely α- and β-subunits of C-PC) but not larger protein fractions which would be the C-PC trimers and hexamers. This does not affect the separation of C-PC by UF; however, it does make it difficult to predict whether C-PC can be purified from other proteins in the mixture.

UF incurs a large capital cost but would likely reduce the running costs of large amounts of ammonium sulfate salts being used. UF can also potentially be used to recycle the polymers in the systems from the ATPS, improving process economics and reducing the waste produced.

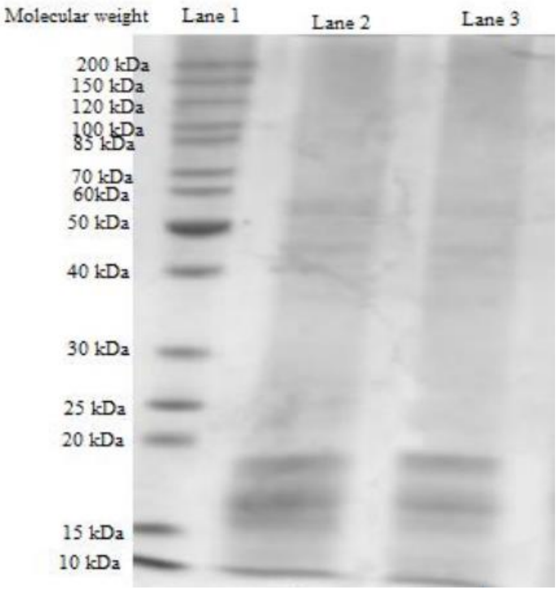

Figure 13. SDS PAGE for *Spirulina* protein fraction in crude extract (lane 2) and a blue (C-PC) colour fraction (lane 3). Lane 1 shows the standard MW markers. Taken from Abakoura (2018)

3.2.3 Polymer recycle

Polymer recycling is a good opportunity to reduce the waste and environmental impact of polymer-use in the process and improve the economic feasibility of producing C-PC. There is a possibility to perform polymer recycling using UF due to the large differences in molecular weights between the polymers and the larger proteins in the process. This should be further considered after initial experiments fill in the gaps in data for the polymer-polymer ATPS. The protein fractions found in the MDX phase in this study will be different to those found in PEG after polymer-salt ATPS experiments. Geckeler and Court (1996) used UF with soluble polymers to adsorb and remove hazardous substances from water, where the MWCO of the UF membrane was lower than the size of the polymer, concentrating the polymer and the bound hazardous compounds. This works only at low polymer concentrations, however, since permeate flux through the membrane is decreased as polymers reach higher concentrations (Geckeler and Court, 1996). Shkinev *et al.* (1987) found a 50 % reduction in permeate flux from 1 to 0.5 L/min.M^2 when the concentration of a poly(ethyleneimine) polymer was increased from 2 to 4 wt%. This was due to the increased viscosity of polymer solutions at higher concentrations. If such low concentrations of polymer in solution is the limiting factor for UF, some other concentrating step, such as evaporation, would be needed to recycle at a higher concentration.

In a pilot-plant study, Papamichael *et al.* (1992) implemented PEG recycling in an ATPS where fumarase enzyme was purified into the bottom potassium phosphate phase. The PEG top phase was simply fed back into the make-up feed mixture for the ATPS, with a bleed to reduce the build-up of contaminants. This reduced the PEG requirements by 50 % and the potassium phosphate used by 12 % (Papamichael *et al.*, 1992). Since PEG is also the non-enriched phase in a PEG – MDX ATPS, there is also the possibility of feeding the top phase back into the pre-mixture for the ATPS, as this would contain PEG as well as some MDX and C-PC. While the purity of C-PC produced may be affected and would need careful monitoring in this set-up, it is well worth considering.

3.2.4 Salts recycle

Salts that remain in solution after precipitation can be purified by dialysis membranes and then recycled for further precipitation. Including this step would reduce the salt waste produced in the process as well as reducing the running costs of the process. This step will be essential if precipitation remains a part of the process, and can also recover salt from ATPS steps. Tan *et al.* (2012) coupled a PEG – NaH_2PO_4 ATPS and dialysis for extracting and purifying aloe polysaccharides and proteins. In this ATPS, the salt-rich bottom-phase was sent through a dialysis tube to recover the salt into deionised water, leaving behind the polysaccharides. This also led to a large dilution of the salt, which was not discussed in the paper, and would require concentrating the salts to be reused in the process.

Hustedt (1986) used UF to recycle the potassium phosphate salt in a PEG – salt ATPS where fumarase enzyme was recovered in this bottom salt phase. The PEG phase was also recycled back directly to the start of the process, as in the study by Papamichael *et al.* (1992). The PEG could be recycled 4 times in this study with no deleterious effects on the recovery or activity of the enzyme, with a 95 % recovery of PEG to the fresh feed (Hustedt, 1986). The salt recycling does not perform as well, with a 45 % loss per stage. This opens the possibility of implementing UF to recover citrate salt in a PEG – citrate ATPS if it were implemented in the current process, which does not have the limitations of polymer solutions with respect to extremely low concentration requirements.

3.3 Considerations for scale-up

3.3.1 Cell disruption and leaching

Scale-up for cell disruption and leaching depends on the process selected following preliminary studies and economic analyses. For bead milling, as used in the preceding laboratory work underpinning the patent, the geometry of the vessels would remain proportional as the scale increases, with the bead to volume ratio remaining constant. Rotational speed of the impeller would initially remain constant and depend on the operation of the up-scaled system. As the process is up-scaled, cooling might be necessary to keep the temperature below 40 °C, since large amounts of heat can be built up by the friction of glass beads during milling.

3.3.2 Centrifugation or other cell debris removal

A continuous decanter centrifuge system could be used to up-scale the centrifugation operations in the process. If another process (such as filtration) were used for cell debris removal, this process would be scaled-up by the installation of a larger throughput filtration unit, or using multiple smaller filtration units to process the entire volume. Either of these methods would allow for the continuous removal of cell debris in the process.

3.3.3 ATPS

ATPS has successfully been conducted at large scale for decades for various systems and both Raghavarao *et al.* (1995) and Cunha and Aires-Barros (2003) have written comprehensively on aspects of scale-up in ATPS processes. Many options are available for large-scale aqueous two-phase systems, due to their ability to exploit equipment for conventional liquid-liquid extractions.

The industrial implementation of large-scale systems for aqueous two-phase separations have mainly been limited by the theoretical understanding of phase equilibria and partitioning in different systems, their selectivity, as well as the high cost of polymers (Cunha and Aires-Barros, 2003). One of the advantages for these systems is that a short period of gentle stirring, usually a few minutes, is enough to achieve phase and partition equilibrium. This is due to the low interfacial tension between the phases, which allows small bubble-formation with low energy input and thus a large area for mass transfer (Raghavarao *et al.*, 1995). Fast settling systems (like PEG – salt systems) can achieve phase separation using various kinds of gravity settlers, while different columns and conventional centrifugal separators can achieve continuous phase separation depending on the needs of the process. Since in this study polymer mixtures are being separated as opposed to different phases being contacted, the two most relevant unit operations will be described, namely mixer-settlers and disk stack centrifuges. Other ATPS options for large scale include a variety of column operations where a light and heavy phase are contacted in counter-current flow or bubbling for mass transfer.

- Mixers-settlers: This consists of two vessels, one with a mixer to equilibrate the phases and a second to settle the mixture into phases (Figure 14). This may be run in batch operation or continuously. It may also be arranged in multiple counter-current unit, arranged vertically in a cascade or horizontally in batteries.
- Mixer-disk stack centrifuge: For systems where the separation time is too long by gravity, a disk stack centrifuge can be used to speed up the continuous separation of phases (Figure 15). Multiple centrifuges can also be used in a counter-current operation to increase recovery and/or purity of the product. The equilibrated mixture is fed through a central stationary pipe into a rotating bowl, where the phases separate due to the speed at which they rise through channels in the disks and are separated by narrow disks in the chamber.

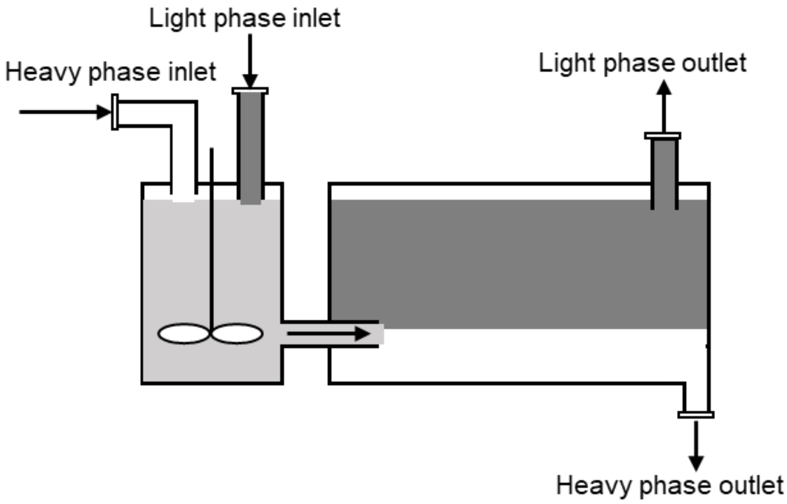

Figure 15. Mixer-settler unit for industrial ATPS with the mixture entering a settling vessel for easy separations. Adapted from Cunha and Aires-Barros (2003).

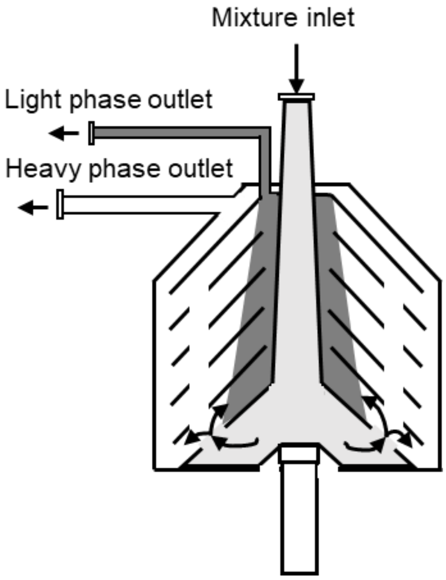

Figure 14. Disk-stack centrifuge for rapid separation of phases in ATPS. Adapted from Cunha and Aires-Barros (2003).

3.3.4 Precipitation and ultrafiltration

For precipitation stages, continuous decanter centrifuges could be used in scale-up to allow continuous production at high throughput, instead of small, batch centrifugation after each precipitation stage.

Were UF to be employed, a longer processing cycle would be required to process larger volumes of liquid in an up-scaled process. Since UF units have a very high cost, this would need to be well thought out and researched before committing to using it in the scaled-up process, as purchasing separate units for small scale tests would likely not be appropriate.

3.3.5 Drying

At larger scales, spray drying would be preferential to freeze drying. Freeze drying is less economical at a large scale, and spray drying can effectively be applied to larger volumes of product. The MDX present after ATPS would act as an effective carrier as well as stabiliser, protecting the C-PC from heat degradation during spray-drying and oxidation during product storage.

3.4 Conclusions

To conclude the discussion on possible improvements to the original process, C-PC can be successfully extracted and purified using various ATPS processes. The main variables for ATPS optimisation include polymer (PEG) chain length and the concentrations of the top and bottom phases, which determines the tie-line on which the ATPS falls on the system phase diagram. To date, only PEG – salt systems have been reported in the open literature for separating C-PC from crude protein solutions. These found that C-PC recovery to the top phase generally decrease as the PEG chain length is increased above 4000 Da. This was attributed to increased intermolecular forces between polymer molecules of increasing chain length, pushing out larger proteins, like C-PC to the bottom phase or phase interface.

The application of PEG – citrate ATPS is a consideration to take into account, since these have been found to produce high purity C-PC at high recoveries, and could be used in combination with the PEG – MDX ATPS, explored by Griffiths, Burke, *et al.* (2016). The latter gives the advantage of recovering C-PC from the MDX phase, allowing precipitation, while the former favours increased purification at the cost of C-PC reporting to the PEG phase which precludes precipitation and negatively affects drying.

Precipitation by ammonium sulfate has been studied for purifying and recovering C-PC, including after ATPS. This showed varying results in terms of recovery, ranging from below 50 % to above 70 % per precipitation stage. Precipitation was found to be able to improve purity of C-PC as well as reduce bacterial contamination, in the process studied in this thesis (Griffiths, Burke, *et al.*, 2016).

Ultrafiltration has been used with success for separating C-PC from the PEG phase after ATPS. UF does not always result in an increased purity of C-PC, however, since this depends on the size fractions of proteins present at that stage in the process, as well as the pore size of filter membrane used. One factor to consider with implementing UF is that for solutions containing polymers, a very low polymer concentration (<1-2 wt%) is allowable in a UF unit, due to the high viscosity causing decreased permeate flux. Raw material recycle should be possible based on the performance of the system and configuration of the process, as demonstrated in other ATPS processes where salts were recycled by either dialysis or UF, and polymers by feeding back with some amount of bleed. This would need verification, since it depends on the composition of the phase fractions separated after the ATPS.

Considering the process to be studied, there are gaps in knowledge of the process as well as limitations in literature. Recovery and purity data are not available for each step in the process, and these must be determined before considering alternative experimental approaches. Contamination data is also not available, making it difficult to determine the point of ingress for the high bacterial colony forming units in the product after ATPS. This is, however, likely if a long period of leaching is used and nutrients from the disrupted cells remain available in the buffer solution. The PEG – MDX ATPS has also not been reported in literature, making optimisation more challenging since partitioning is affected by many variables, and considering how important the starting point for optimisation could be.

Scaling-up the process will require further literature research, feasibility and economic study, and experimental results at progressively increasing scale.

4 Defining the Research Project

4.1 Problem Statement

The CeBER, UCT patented process for C-PC recovery and purification from *Spirulina* (Harrison *et al.*, 2019) has to-date demonstrated its effectiveness for a limited set of conditions and configurations, and only at laboratory scale. The process will benefit from further optimisation before its economic feasibility can be determined, and it can be upscaled for commercial production. Factors identified for further testing and optimisation include: the initial leaching step after cell disruption with the aim of minimising its duration to restrict undesired microbial growth and contamination; further characterisation and optimisation of the ATPS; and the chemicals and polymer use which could be further minimised, improved or considered for recycling, for a more cost-effective and resource-efficient process.

4.2 Research Project Objectives

- Refine the disruption step and leaching time for the dry *Spirulina* sample used
- Quantify and so improve understanding of the impact of the component concentrations in ATPSs on the purity and recovery on phycocyanin produced, while ensuring recoverability
- Develop a greater understanding of the mass balance around the ATPS
- Identify possible process route improvements which incorporate scale-up considerations
- Investigate the possibility of polymer recycling
- Propose and simulate possible process route options for phycocyanin extraction and recovery, based on desired outcome and of the process and C-PC produced

4.3 Key Research Questions

- How can the C-PC leaching rate be improved, and contaminant ingress be reduced?
- Does increasing PEG molecular weight increase 2-phase area in PEG – MDX phase diagrams?
- Do recovery and purity of C-PC improve as PEG molecular weight increases in the PEG – MDX ATPS?
- Would a 2-stage ATPS using PEG – salt ATPS improve the overall process?
- Can ammonium sulfate use be reduced, or the precipitation step be replaced by UF or an alternative process?
- Can UF or other means be used to recycle PEG and maltodextrin?
- What process route configuration allows for the most resource-efficient C-PC production using ATPS?
- Will process simulation help produce useful process flow diagrams for this project and future work?

5 Method

5.1 Approach & research methodology

The approach to the project was based on improving key aspects in the process, focused mainly on the use of ATPS for C-PC purification. This involved critically evaluating the patented process and the decisions made in developing it, as well as reviewing literature for ideas on how to improve the process, and comparisons to test results against. Options were considered for recycling components in the system, reducing the chemical usage, and pre-treatments for improving the purity of the phycocyanin extracted and produced in the process.

For the experimental work, a largely iterative approach was used, as there were multiple options for improving the performance of an ATPS and the mechanism behind different protein partitioning in these systems is not well understood. The results were used to simulate improved scenarios using statistical tools and process simulation software, guided by experimental results and literature values where these fell outside of the scope for experimental work.

5.2 Experimental approach

The experimental research approach includes four main activities:

1. Understanding the mass balance and equilibrium curves associated with the ATPS through production of phase diagrams
2. Optimising the ATPS and key procedures for purity and recovery of C-PC
3. Determining an improved purification procedure, and considering alternative steps in developing an overall flowsheet for C-PC production from *Spirulina*
4. Adequately simulating various process routes to aid future research into potential upscaling

5.3 Experimental methods

5.3.1 Materials used

The dry *Spirulina* powder used in this project was purchased from Green Create Nutra (GC Nutra) in Mauritius. The *Spirulina* grown by GC Nutra had been rapidly mixed in a vessel before being fed into a spray dryer with a small orifice nozzle to produce the powdered form (Griffiths, personal communication 2020, January 8). Ampicillin (Merck) was used as a biocide in the leaching tests to prevent bacterial overgrowth and foaming at 100 mg/L.The *Spirulina* powder used in the development of the patent was purchased from Superfoods SA, which imported it from India.

The chemicals used in the experimental work were from various sources, which will be named as the chemicals are given in the methodology below. All the deionised water used was from a Millipore Elix 3 unit, using electro-deionisation and reverse osmosis.

5.3.2 Original process experimental basis

Figure 1 shows the simplified block diagram for the original process to produce C-PC powder, the starting point of this project. The experimental procedure is given here, as per the close-out report for the previous project (Griffiths, Burke, *et al.*, 2016).

5.3.2.1 Cell disruption and leaching

Dry *Spirulina* powder was bead-milled in a 3 L plastic beaker with 1 kg of 1 mm diameter borosilicate glass beads (purchased from MilliporeSigma). An overhead stirrer (Dillon RDM-100A 14” drill press) was used, operating at 180 RPM. 100 g dry *Spirulina* was loaded with a 5 g/L citrate buffer at pH 6, confirmed using a Lasec pH 50+ DHS probe. The citrate buffer was made using a mixture of 92 % sodium citrate (Kimix Chemicals, South Africa) and 8 % citric acid (Sigma-Aldrich) by mass. Weighing was done using a Radwag PS 4500.R2 balance. The volume was then topped up with deionised water to 1 L. The mixture was milled for 15 minutes with the liquid suspension then poured off and left to soak for a further 48 h to leach the C-PC from the cell debris.

5.3.2.2 Cell debris removal

The biomass was removed by centrifuging at 7000 g for 20 minutes in 500 mL centrifuge bottles. A Beckman Avanti J-25 centrifuge was used. The supernatant was poured off, to be used in further processing, and the biomass pellet was discarded.

5.3.2.3 Aqueous two-phase separation

The ATPS was performed by adding 1 L of the crude extract, which is the supernatant after centrifugation, to a 3 L plastic beaker, with the addition of 77 g of PEG (Sigma-Aldrich, MW ≥ 10000 Da) and 460 g of maltodextrin (Supplement World, South Africa). This translated to roughly 5 wt% PEG and 30 wt% maltodextrin as the ATPS composition. This was mixed using the overhead stirrer at 180 RPM for 30 minutes or until well mixed. The mixture was spun again in 500 mL centrifuge bottles at 7000 g for 40 minutes. The bottom phycocyanin-rich maltodextrin phase was siphoned-off using clear tubing. The ATPS was carried out at a pH of 6 and 25 °C.

5.3.2.4 Precipitation train

Three precipitation stages were used in the patented process. Each used ammonium sulfate (Kimix Chemicals, South Africa) at decreasing amounts in order to selectively precipitate C-PC, thereby increasing purity and decreasing bacterial contamination. After each stage the mixtures were left to stand for at least 1 h and then centrifuged at 7000 g in 500 mL bottles for 15 minutes. The supernatant was then drawn off and the precipitated pellets redissolved.

The first precipitation used 1 L of the bottom phase from the ATPS with 298 g of ammonium sulfate. After centrifugation, the bottom clear phase formed was removed by peristaltic pump and the pellet resuspended in water up to 80% of the initial phase volume.

The second precipitation used 1 L of the previous resuspension and an added 410 g of ammonium sulfate. After centrifuging at 7000 g for 20 minutes in 500 mL centrifuge bottles, the supernatant was discarded and the pellet redissolved to 1 L with deionised water.

The final precipitation used 223 g ammonium sulfate in the 1 L from the previous stage, with the clear supernatant being poured off and discarded.

5.3.2.5 Drying

Freeze-drying was used in the initial stages of the project, with the final pellet after precipitation being placed in a freeze dryer for 12 h or until completely dry. An Instruvac vacuum freeze-dryer was used.

5.3.3 Cell disruption and leaching test for C-PC

For the experimental system, the dry *Spirulina* powder was bead-milled according to the protocol above (5.3.2). A control experiment was run where the 100 g of *Spirulina* powder was mixed by the overhead stirrer in 1 L of citrate buffer at 5 g/L as above, without glass beads. This was done to compare the leaching of the phycocyanin into solution without any additional cell disruption. Regular measurements, every 2 to 3 hours, were taken for analysis of C-PC concentration and purity, from which the recovery could be determined (see C-PC quantification methods found in Section 5.4.1). See appendix A.1 for raw data.

The dry *Spirulina* was then suspended in citrate buffer to observe the cells under microscope. These can be seen in Section 6.2.1.3, where an Olympus, CX-41 epifluorescence microscope was used at 100 times and 1000 times magnification, with the 1000 times magnification done under oil immersion.

5.3.4 PEG – MDX phase diagrams

5.3.4.1 Equilibrium curves

Phase diagrams were produced using the methods from the textbook: Aqueous Two-phase Systems: Methods and Protocols (Hatti-Kaul, 2000) and a paper which produced phase diagrams with a PEG – MDX system (Machado *et al.*, 2012).

For three PEG molecular weights: 10000, 12000 and 20000 Da, systems of varying PEG and MDX concentrations (Table 3) were prepared. These were then centrifuged at 4000 RPM for 30 minutes in 15 mL Falcon tubes. A Hettich Universal 320 centrifuge was used for this. The phase volume ratios were read off from the graduations on the tube, and each phase was further diluted into 2 mL Eppendorf microcentrifuge tubes for analysis of the polymer concentrations. See appendix A.2 for raw data.

Table 3. Phase diagram mixtures for the PEG – MDX ATPS phase diagrams

ATPS mixture	PEG concentration (wt%)	MDX concentration (wt%)
1	5	25
2	10	25
3	10	30
4	15	30
5	20	30

5.3.4.2 Maltodextrin quantification

The MDX concentration was quantified using the method developed by Dubois *et al.* (1956). Standard curves were produced using MDX in a range of amounts from 20 to 190 µg in 2 mL of solution in test tubes. To each sample tube, 0.4 mL of 20 % (w/w) phenol solution (Sigma-Aldrich) was added. Under a fume hood, 5 mL of concentrated sulfuric acid (Kimix, South Africa) was pipetted into the centre of the liquid layer of each test tube, to ensure good mixing. The test tubes were then left for 10 minutes under the acids fume hood before being mixed by vortex and put in a warm water bath at 25 – 30 °C for 20 minutes. The sample absorbances were then read using a FLUOstar Omega spectrophotometer at 488 nm (BMG-Labtech). The experimental samples were diluted with deionised water before performing the colourimetric assay to fit within the range of the analytical curve produced. Each sample was analysed in triplicate.

5.3.4.3 PEG quantification

The PEG concentrations were quantified using the refractive indices (RIs) of each polymer, read using a HI 96800 Refractometer (Hanna). Analytical standards were produced for PEG and MDX by obtaining the refractive index of each standard concentration in a range using a refractometer. For the experimental samples, the overall RI was determined. The MDX concentration, found by the method above (5.3.4.2), was then translated to the RI contributed by that concentration in the overall mixture, since RIs are additive. The remaining contribution to the refractive index was due to the PEG content, which then allowed the quantification of PEG in each phase. Each sample was analysed in triplicate.

5.3.4.4 Water quantification

The water content of each sample was obtained by mass balance, since only three compounds (MDX, PEG and water) were present in the mixtures.

5.3.5 PEG – citrate phase diagrams

PEG and citrate salts at pH 6 were used to produce the phase diagrams for this ATPS. These phase diagrams were produced using the method adapted from Glyk *et al.* (2014). The different molecular weight PEGs were used to produce standard solutions. A refractometer was used to produce standard curves for refractive index against PEG concentration in wt%. The same was done for mixtures of citrate salts, using sodium citrate and citric acid at varying ratios to achieve a pH of 6 at different concentrations in wt%.

For the two-phase systems, different PEG and sodium citrate concentrations were mixed in 15 mL Falcon tubes and then adjusted to pH 6 with a 50 wt% citric acid solution (Table 4). These were allowed to fully dissolve and were then shaken to mix the phases that had started to settle and separate. Once fully dissolved, the tubes were centrifuged at 4000 g for 30 minutes, producing two clear phases with a sharp interface. The volumes of each phase were then read off the graduations on the tubes for the volume ratios.

About 5 mL were drawn up from the top and bottom phases by a Pasteur pipette for measuring the densities of the phases. 0.5 mL of these phases were diluted by adding 1.5 mL of deionised water before the refractive indices were measured. Some were also diluted with water and weighed before freeze-drying, to determine the water content. Based on the refractive indices of the top and bottom phases, and their respective water concentrations from freeze-drying, the composition of each of the three components in each phase could be determined. This was done using the formula below, due to the additive nature of refractive indices (Glyk *et al.*, 2014).

$$n_D = a_0 + a_1 w_{PEG} + a_2 w_{cit} \qquad \text{Equation 1}$$

Where a_0 is the RI for deionised water, and a_1 & a_2 were the gradients from standard curves produced for RI vs PEG and citrate concentrations, respectively. See appendix A.3 for raw data.

Table 4. Phase diagram mixtures for the PEG – citrate ATPS phase diagrams

ATPS mixture	PEG concentration (wt%)	Citrate concentration (wt%)
1	15	10
2	17	12
3	19	14
4	23	18

5.3.6 Polymer concentration studies

Tests were performed to examine the effect of polymer concentrations on C-PC partitioning. At a constant concentration of 30 wt% for maltodextrin, the PEG 10000 concentration was increased from 5 wt% to 7 wt% and then 9 wt % to test the effect of PEG concentration on the partitioning of C-PC. The PEG 10000 concentration was then kept at 9 wt% while the maltodextrin concentration was lowered to 25 wt% and then 20 wt%.

This set of experiments was carried out at the scale mentioned in Section 5.3.2, starting with 1 L of buffered *Spirulina* suspension, followed by leaching and cell debris removal. The ATPS were carried out in duplicated experiments and analysed in triplicate. The results were used to inform the further studies on PEG molecular weight, based on the best performing combination in terms of C-PC purity and recovery. See appendix A.4 for raw data.

5.3.7 PEG molecular weight studies

Tests were performed to examine the effect of PEG molecular weight on C-PC partitioning. Three different molecular weights of PEG were used: 6000, 10000 and 20000 Da. Following from the previous experiment, the best-performing concentration combination was used, 9 wt% PEG with 20 wt% maltodextrin. The ATPS were again carried out in duplicated experiments and analysed in triplicate. Comparisons were made based on C-PC recovery, concentration and purity.

5.3.8 Two-stage ATPS studies

A two-stage ATPS was investigated by employing a PEG – citrate ATPS followed by a PEG – MDX ATPS (see Figure 16 and Figure 17 for examples of the two ATPS stages). The first testing step involved screening the two-stage ATPS for the best PEG molecular weight at high and low concentration combinations. This was followed by factorial studies for the separate stages of the ATPS. These factorial studies were performed at a reduced scale, in which 50 mL falcon tubes were used for each experiment rather than the 1 L working volume at which the previous ATPSs were investigated.

5.3.8.1 Screening for PEG molecular weight

Higher and lower component concentrations were used for the PEG – citrate ATPS to screen for PEG molecular weight. The second ATPS was performed using the top PEG phase from the first stage mixed with maltodextrin to form a PEG – MDX ATPS. PEG of molecular weights of 4000, 6000 and 10000 Da were used in the screening.

The low concentration screening test used 13 wt % PEG and 11 wt% citrate at pH 6. The balance was an extract solution containing phycocyanin, where 3 mL of crude extract was added to 27 mL of deionised water, as per the extraction method outlined above (5.3.2). This was done due to the colour intensity of the phases when the undiluted crude extract was used, which made it difficult to accurately differentiate the phases. The high concentration test used 22 wt% PEG of different molecular weights and 14 wt% citrate, also at pH 6. This combination was chosen as similar concentrations have been successfully implemented in other studies on these ATPSs and the two combinations have similar estimated volume ratios based on the asymmetrical phase diagrams produced for PEG – citrate ATPS.

The second stage for each of the above ATPSs involved taking a specific mass of the top (PEG- and phycocyanin-rich) phase and mixing this with deionised water and maltodextrin. The final maltodextrin concentration was 20 wt% while the PEG concentration aimed for was

15 wt%. The PEG concentration was estimated based on phase diagrams for PEG – citrate ATPS. The top and bottom phases from each of the ATPSs were analysed for C-PC concentration and purity and the volumes were read from the graduations on the 50 mL Falcon tubes used. See appendix A.5 for raw data.

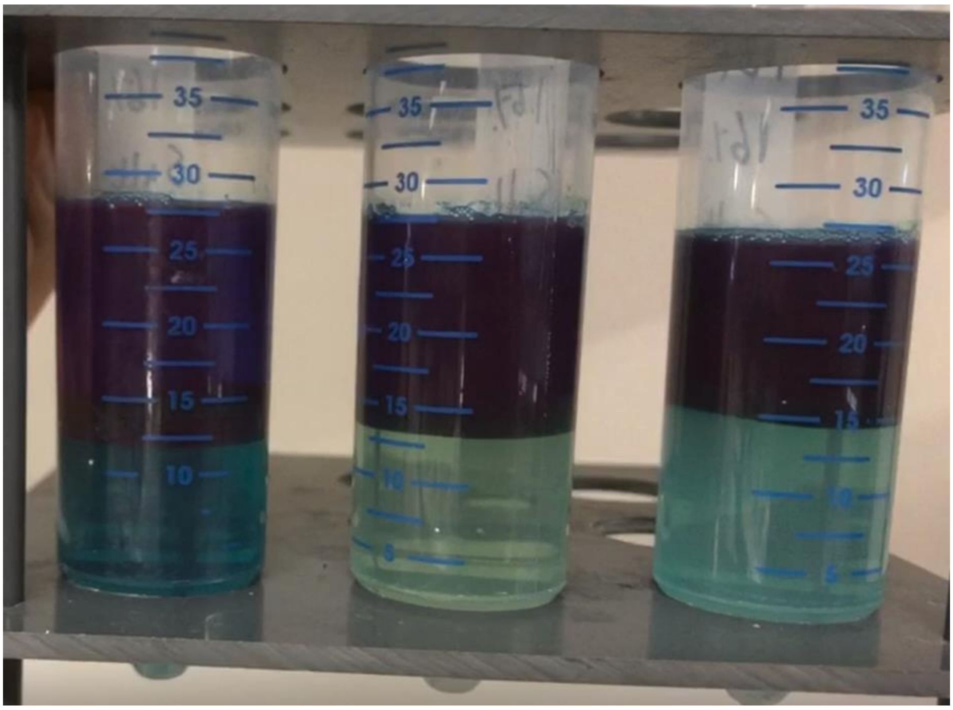

Figure 16. PEG – citrate ATPS after phase separation, with C-PC partitioned to the top phase

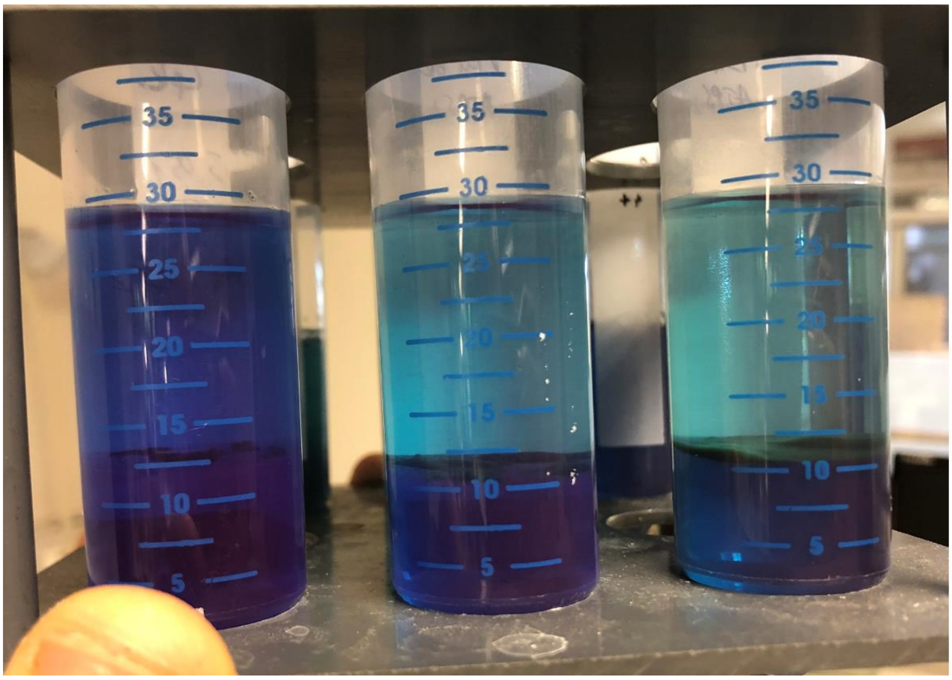

Figure 17. PEG – MDX ATPS after phase separation, with C-PC partitioned to the bottom phase

5.3.8.2 PEG – citrate ATPS factorial experiment

Using the best-performing PEG identified from the screening experiments, different component concentrations were used in a PEG – citrate ATPS factorial experiment. The factorial experiment varied two factors: PEG and citrate concentration. This was done at three concentration levels, evenly spaced. Both PEG and citrate concentrations were varied between 12, 16 and 20 wt %, with the sodium citrate and citric acid being used to ensure pH 6 was used in each ATPS. The balance was again made up of a phycocyanin-containing crude solution made up of crude extract diluted with deionised water to aid visual discernment of the different phases formed. The top and bottom phases were analysed for C-PC concentration and purity, as well as density. The volumes were again read off the graduations on the 50 mL falcon tubes used. See appendix A.6 for raw data.

5.3.8.3 PEG – MDX ATPS factorial experiment

Different polymer concentrations were used in a PEG – MDX ATPS factorial experiment, using the best-performing PEG from the screening experiments. This factorial experiment had PEG and maltodextrin concentration as factors, each with 3-levels. The PEG concentrations used were 12, 16 and 20 wt%, while the MDX concentrations were 20, 25 and 30 wt%, due to the different phase-forming characteristics of this ATPS. The balance for each combination was a phycocyanin-containing crude solution made up of crude extract diluted with deionised water to allow visual discernment of the different phases. The top and bottom phases were analysed for C-PC concentration and purity, and the volumes were read off the graduations on the 50 mL falcon tubes used. See appendix A.7 for raw data.

5.4 Analytical methods and data handling

5.4.1 C-PC descriptors

For each experiment where the purity number, recovery and concentration of C-phycocyanin were relevant, the following formulae were used. In each case, the sample was appropriately diluted with deionised water, centrifuged in 2 mL Eppendorf microcentrifuge tubes at 13000 RPM in a microcentrifuge (Eppendorf MiniSpin plus), and then the absorbances were read by spectrophotometer. Each sample had absorbance quantified at 280, 620 and 650 nm, the maximum absorbance wavelengths for proteins, C-phycocyanin and allophycocyanin, respectively. The total volume from which the sample was taken was also quantified and used to determine the total phycocyanin content, which could be used to determine recoveries at each step.

5.4.1.1 C-PC Purity

The purity of C-phycocyanin is by convention given as the purity number. This is the ratio of the absorbance at the maximum absorbance for C-PC (620 nm) to the maximum absorbance for the total amino acids present in solution (280 nm). The spectrophotometer was used to determine this ratio, using microplates for the sample readings.

$$C - PC\ purity = \frac{\mathrm{A}_{620}}{\mathrm{A}_{280}} \qquad \text{Equation 2}$$

Where A_λ is the absorbance under a spectrophotometer at λ, the wavelength in nm.

5.4.1.2 C-PC concentration

The concentration of C-PC is found by the formula below, using the absorbances at 620 nm and 650 nm, to account for the amount of allophycocyanin in the solution (Yoshikawa and Belay, 2008):

$$[C-PC]\ (mg/mL) = 0.162 * A_{620} - 0.098 * A_{650} \qquad \text{Equation 3}$$

Where [C-PC] is the C-PC concentration

5.4.1.3 C-PC recovery

The recovery of C-phycocyanin was calculated as the fraction of the amount of C-PC recovered in a stage relative to that from the previous step. This was calculated using the values of C-PC concentration from the previous and subsequent steps, and the respective volumes that were recovered.

$$C-PC\ recovery\ (fraction) = \frac{[\mathrm{C-PC}]_2 \mathrm{V}_2}{[\mathrm{C-PC}]_1 V_1} \qquad \text{Equation 4}$$

Where V is the volume, and 1 refers to the previous or first step, and 2 refers to the subsequent step.

5.4.2 Phase diagram calculations

5.4.2.1 Tie lines

The tie-lines were produced by drawing straight lines from the top-phase composition, through the initial mixture composition, to the bottom-phase composition. The tie-line slope (TLS) is usually constant, since tie-lines are approximately parallel in most phase diagrams, and the average was found for each of the phase compositions to make assumptions for novel mixtures. TLS was calculated using the equations below for the different ATPS.

$$TLS = \frac{w_{PEG}(top) - w_{PEG}(bottom)}{w_{MDX}(top) - w_{MDX}(bottom)} = \frac{\Delta \mathrm{w_{PEG}}}{\Delta \mathrm{w_{MDX}}} \qquad \text{Equation 5}$$

And:

$$TLS = \frac{w_{PEG}(top) - w_{PEG}(bottom)}{w_{citrate}(top) - w_{citrate}(bottom)} = \frac{\Delta \mathrm{w_{PEG}}}{\Delta \mathrm{w_{citrate}}} \qquad \text{Equation 6}$$

The tie-line length (TLL) was calculated using the compositions of the top and bottom phases of each ATPS, with a greater length showing that the compositions are further apart on the phase equilibrium curve. The TLL was found using the equation below.

$$TLL = \sqrt{(w_{PEG}(top) - w_{PEG}(bottom))^2 + (w_{MDX}(top) - w_{MDX}(bottom))^2} \qquad \text{Equation 7}$$

And:

$$TLL = \sqrt{(w_{PEG}(top) - w_{PEG}(bottom))^2 + (w_{citrate}(top) - w_{citrate}(bottom))^2} \qquad \text{Equation 8}$$

5.4.2.2 Phase volume ratios

The phase volume ratios (V_R) were read off graduations in the falcon tubes used after centrifuging to separate the phases. The phase volume ratios could also be estimated by the inverse lever rule, using the tie-lines and phase equilibrium curves obtained, and then compared to the phase volume ratios observed visually. The volume ratio is defined as the ratio of the volume of the top phase to the volume of the bottom phase in a given ATPS.

$$V_R = \frac{\mathrm{V_{top}}}{\mathrm{V_{bottom}}} \qquad \text{Equation 9}$$

The inverse lever rule can be used to estimate the volume ratio, knowing the starting, top phase and bottom phase compositions in an ATPS. Equation 7 was adapted as an example of the distance formula for calculated the required lengths in the equation below.

$$\frac{\mathrm{V_{top}}}{\mathrm{V_{bottom}}} = \frac{Length(starting - bottom\ phase\ composition)}{Length\ (starting - top\ phase\ composition)} \qquad \text{Equation 10}$$

5.4.2.3 Phase densities

The phase densities were determined by pipetting out 0.5 mL of the phase solutions into Eppendorf microcentrifuge tubes and weighing the volumes on a fine balance (Ohaus Adventurer Analytical). Experiments were carried out in triplicate.

5.4.2.4 Experimental data fitting

Sigmoidal equations have been proposed for modelling the equilibrium curves for aqueous two-phase systems (Hu *et al.*, 2004; Glyk *et al.*, 2014). The equation below was used to fit the data obtained, with the results being evaluated visually since it is a non-linear relationship:

$$w_{PEG} = \mathrm{a} + \mathrm{b}(w_{MDX})^{0.5} + \mathrm{c}w_{MDX} + \mathrm{d}(w_{MDX})^2 \qquad \text{Equation 11}$$

And:

$$w_{citrate} = \mathrm{a} + \mathrm{b}(w_{PEG})^{0.5} + \mathrm{c}w_{PEG} + \mathrm{d}(w_{PEG})^2 \qquad \text{Equation 12}$$

Where a, b, c and d are fit parameters. w_{MDX} is the concentration of MDX in wt % (where MDX is interchangeable with PEG and citrate).

5.4.3 ATPS performance parameters

5.4.3.1 Partition coefficient

The partition coefficient is the ratio of the concentration of a specific component in the top and bottom phases of an ATPS after mixing and settling. In this report these are either based on C-PC concentrations or total proteins, based on the absorbance at 280 nm.

$$K_{cPC} = \frac{[C-PC]_{top}}{[C-PC]_{bot}} \qquad \text{Equation 13}$$

Where K_{cPC} in the partition coefficient for C-PC and top and bot refer to the top and bottom phases of the ATPS after settling.

$$K_{protein} = \frac{A_{280,top}}{A_{280,bot}} \quad \text{Equation 14}$$

Where $K_{protein}$ in the partition coefficient for total protein.

5.4.3.2 Purification factor

The purification factor in this report always refers to phycocyanin and is the ratio of the C-PC purity before and after the ATPS. This allows a comparison with literature experiments where different starting purities were used and allows comparisons across different ATPS.

$$Purification\ factor = \frac{C\text{−}PC\ purity\ after\ ATPS}{C\text{−}PC\ purity\ before\ ATPS} \quad \text{Equation 15}$$

Where C-PC purity before ATPS refers in most cases to the purity number of the crude extract used in the ATPS and C-PC purity after ATPS refers to the purity number in the phase where C-PC partitions to, depending on the system.

5.4.3.3 Concentration factor

The concentration factor also refers to phycocyanin and is the ratio of the C-PC concentration before and after the ATPS, where the value after is taken to be the concentration of the phase where phycocyanin partitions to, as above when calculating purification factor.

$$Concentration\ factor = \frac{[C\text{−}PC]_{after\ ATPS}}{[C\text{−}PC]_{before\ ATPS}} \quad \text{Equation 16}$$

5.4.4 Data analysis and interpretation

5.4.4.1 Programs used

For the general data handling and calculations, Microsoft Excel (Version 2002; Build 12527.21416) was used. All graphs except those produced in Sections 7.3.2 and 7.3.3 were produced in Excel. The problem solver function was used for the phase diagrams in 5.3.5.

Statistica (version 13.5.0.17) was used in Chapter 7 for the interpretation and modelling of the factorial experiments in that section (more details in 7.1). *SuperPro Designer* (version 9.5) was used to simulate the process route options given in Chapter 8.

5.4.4.2 Experimental error

Experimental error has been estimated and presented as standard deviation between analytical repeats, where these were done, and experimental repeats. In tables and text, these were given as the uncertainty in the data, using the uncertainty sign, ±. In graphs these were shown using error bars, which give the type of experimental error (whether based on analytical repeats or repeated experiments). Where raw data was used in further analysis and calculations, the error was propagated depending on the manipulations used and the input values with their respective uncertainties.

6 Evaluation of the patented process unit operations

6.1 Introduction

The aim of first part of the project was to evaluate the performance of the patented process unit operations, focusing on the PEG – MDX ATPS as well as the leaching of the phycocyanin from the disrupted *Spirulina* cells.

To support the ATPS research, different PEG molecular weights were investigated through producing phase-diagrams for improved understanding of the ATPS and determination of a range of polymer concentrations which could be utilised to access the two-phase area of this system.

In the development of the patent process, PEG with MW of 10000 Da (the highest that was tested) was found to be best for C-PC partitioning to the lower phase in a PEG – MDX system. In a PEG – salt system, PEGs of lower molecular weight have a higher protein recovery into the PEG phase. It would be expected, therefore, that in a PEG – MDX system, a higher MW PEG would have a lower protein recovery in the PEG phase and have a higher recovery to the MDX phase, which is where C-PC is recovered in these ATPSs. The previous research was limited in its testing of higher molecular weight PEGs, and thus this was identified as a critical variable which required further investigation.

Phase diagrams are essential to understanding the phase compositions in an ATPS, and are unique to each combination of chemicals, in this case, polymers. Phase diagrams were thus generated for the specific polymers used in this ATPS study, and compared to other phase diagrams produced in literature. This was done, as opposed to the common approach assuming phase compositions from those in literature, since it was also necessary to understand the ATPS in terms of a mass balance and as part of a larger process.

The initial leaching step was investigated in order to reduce the long leaching time previously reported as required . During cell disruption and leaching, the cell contents from the *Spirulina*, which are extremely rich in nutrients, are released into the buffered solution. This allows bacteria to thrive under long leach times, exacerbated by the fact that *Spirulina* biomass carries endemic microbes from the growth environment. Reducing the leaching time would reduce the risk of contaminant bacterial growth, making the process safer and more hygienic. This has the additional benefit of reducing the burden on later sterilisation steps required to produce a safe product. A faster leaching step would also reduce down-time for the other steps in the process or the scale of the leach process or both, allowing it to handle more continuous C-PC production. A study was performed to find the changes in C-PC purity and concentration in the buffer solution over time following the initial cell disruption step. This was to determine the effect of cell disruption and the duration of bead-milling necessary for the dry *Spirulina* powder used in this thesis.

6.2 Results and discussion

6.2.1 C-phycocyanin leaching studies

6.2.1.1 Cell disruption and leaching time effect on C-PC concentration

Figure 18 presents the C-PC concentrations measured in buffer solution following rehydration of the dried *Spirulina* powder and disruption of the cells by bead-milling. Results of a negative control in which no bead-milling was used are also given.

With the dry *Spirulina* used in this study, there was no significant difference between the C-PC concentration in the control test and the bead-milled sample. This was an unexpected result because C-PC is an intracellular compound and thus disruption of the cell is required for its liberation. This result may have been because the *Spirulina* drying process, which included vigorous mixing and spray drying, caused enough cell-disruption to permit phycocyanin leaching to occur when the dried *Spirulina* was rehydrated. Spray-drying processes force a suspension through a small aperture under high pressure, the basic mechanism of cell disruption by high pressure homogenisation.

A large amount of the C-PC (5.14 ± 0.66 g/L) was already leached out of the *Spirulina* by 2 hours. The concentration flattened off from 7 hours into the leaching, at which time the control test had a C-PC concentration of 5.68 ± 0.09 g/L. The C-PC concentrations then remained in the range of 5.5 – 5.8 g/L until the sampling ended at 26 hours. Due to uncertainty shown by the error bars, 2 hours may be sufficient to leach out most of the leachable C-PC available in the *Spirulina* sample. The C-PC leached at this time is equivalent to an extraction of 51.4 ± 6.6 $mg_{C\text{-}PC}/g_{dry\ biomass}$.

This result can be compared to a study done by Pott (2018), where continuous bead-milling was done to determine the maximum C-PC in a fresh *Spirulina* sample. It was found that maximum C-PC concentration was found after around 5 hours of continuous milling. It was also noted that the heat generated from the milling degraded C-PC and the concentration decreased steadily after the 5 hour point, where the maximum extraction achieved was around 180 $mg_{C\text{-}PC}/g_{dry\ biomass}$. Guan (2016) found that using mechanical shear and constant stirring, 54.5 ± 0.1 $mg_{C\text{-}PC}/g_{dry\ biomass}$ could be achieved after 15 minutes.

The C-PC leached was thus lower than the extraction achieved by Pott (2018) using constant milling, while comparable to that achieved by Guan (2016) using mechanical shear and stirring. This was most likely due to the *Spirulina* samples used having a lower C-PC content, since the prolonged leaching did not increase the C-PC concentration, and there was no difference between the bead-milled and negative control experiments in this study. The comparisons also indicated that differing methods of mechanical cell disruption can have a great influence on the time taken for leaching to occur, as well as whether the samples used were freshly disrupted or had been dried by some process, as in the present study, and by which process it was dried.

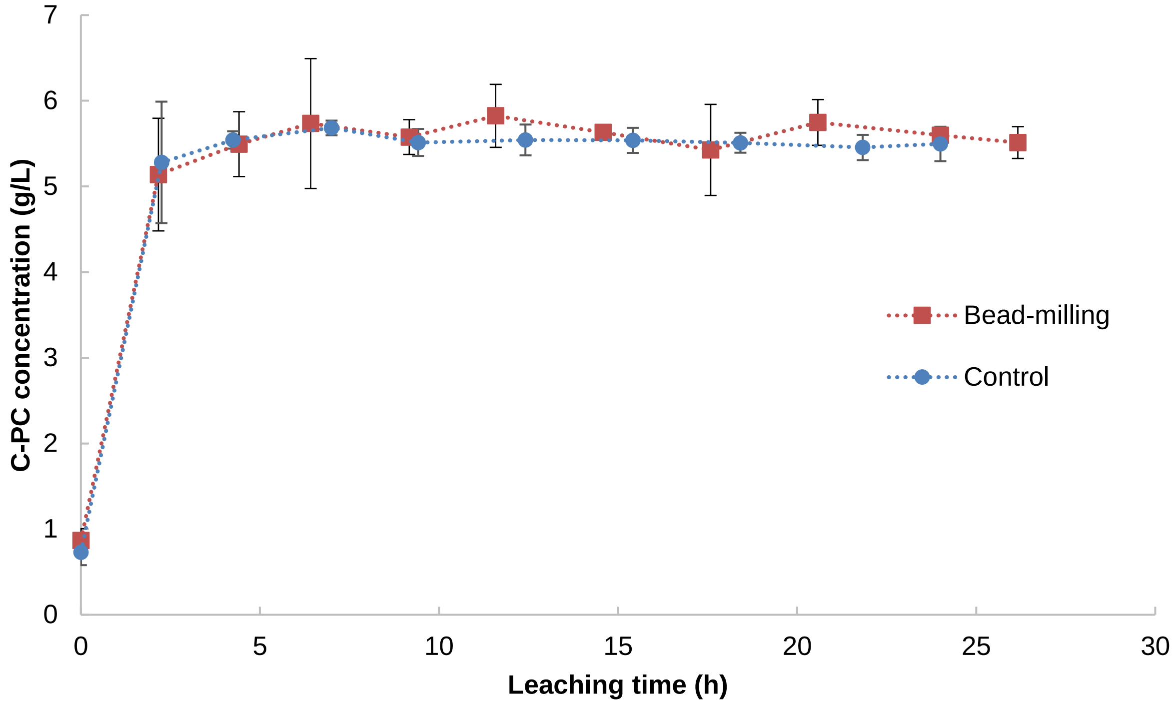

Figure 18. Phycocyanin concentration in crude solution during leaching in citrate buffer, with and without cell disruption by bead-milling. Error bars indicate standard deviation in triplicate analyses.

6.2.1.2 Cell disruption and leaching time effect on C-PC purity number

The C-PC purity number for the bead-milled and control experiments are presented in Figure 19. As observed for C-PC concentration, there was no significant difference between the bead-milled and negative control.

Both tests saw their maximum C-PC purity number at 2 hours after leaching started. The maximum purity number in the bead-milled and control experiments were observed after 2 hours, at 0.70 ± 0.05 and 0.71 ± 0.05 respectively. The purity number decreased in a seemingly linear trend after the maximum at 2 hours. After 26 hours, the C-PC purity number was 0.63 ± 0.03. The decrease in purity number would have been caused by an increase in total proteins and amino acids leaching into solution relative to the C-PC. This indicates that the other contaminating proteins leach at a slower rate than C-PC.

Crude extract purities vary widely from study to study, due to differences in method and *Spirulina* samples used. Guan (2016) found a purity of 0.42 using mechanical shear and 0.48 using a freeze-thaw method (both in phosphate buffer). Rito-Palomares *et al.* (2001) found a crude C-PC purity of 0.70 ± 0.07 using bead grinding in $CaCl_2$ solution, and Wang *et al.* (2012) achieved a purity of 0.89 using a freeze-thaw method in distilled water. This shows that results can vary depending on the study, based on different starting materials and methods of extraction. It also shows that the details of disruption method should be tailored to the specific sample that is being used for the process.

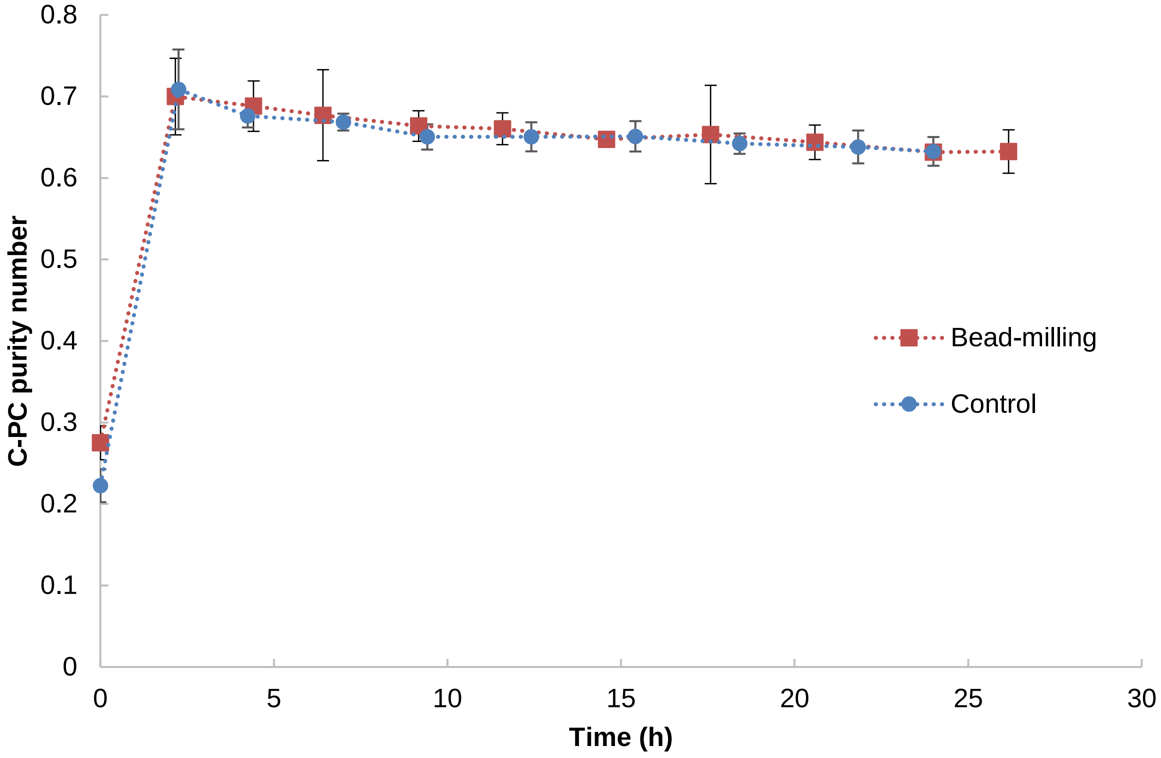

Figure 19. Phycocyanin purity number in crude extract solution during leaching in citrate buffer, with and without cell disruption by bead-milling. Error bars indicate standard deviation in triplicate analyses.

6.2.1.3 Morphology of the dry Spirulina powder

The dry *Spirulina* used was observed under microscope after being resuspended in buffer solution to confirm why bead-milling had no influence on the rate of leaching. The pictures taken under microscope can be seen in Figure 20 and Figure 21.

Figure 20 shows the dry *Spirulina* powder resuspended at 100 times magnification, where it is possible to see both the cell fragments and the more integrated spiral shapes, classic of *Spirulina* before it has been disrupted. This shows substantial disruption of the *Spirulina* before it has undergone bead-milling, with the majority of the cells being fragmented into short straight segments.

Figure 21 is further magnified under oil immersion to 1000 times, to look closer at the individual segments. This showed even further disintegration within those segments, with most of the cells showing complete breakage, where the cell walls are seemingly ruptured, and the internal contents exposed to the surrounding solution.

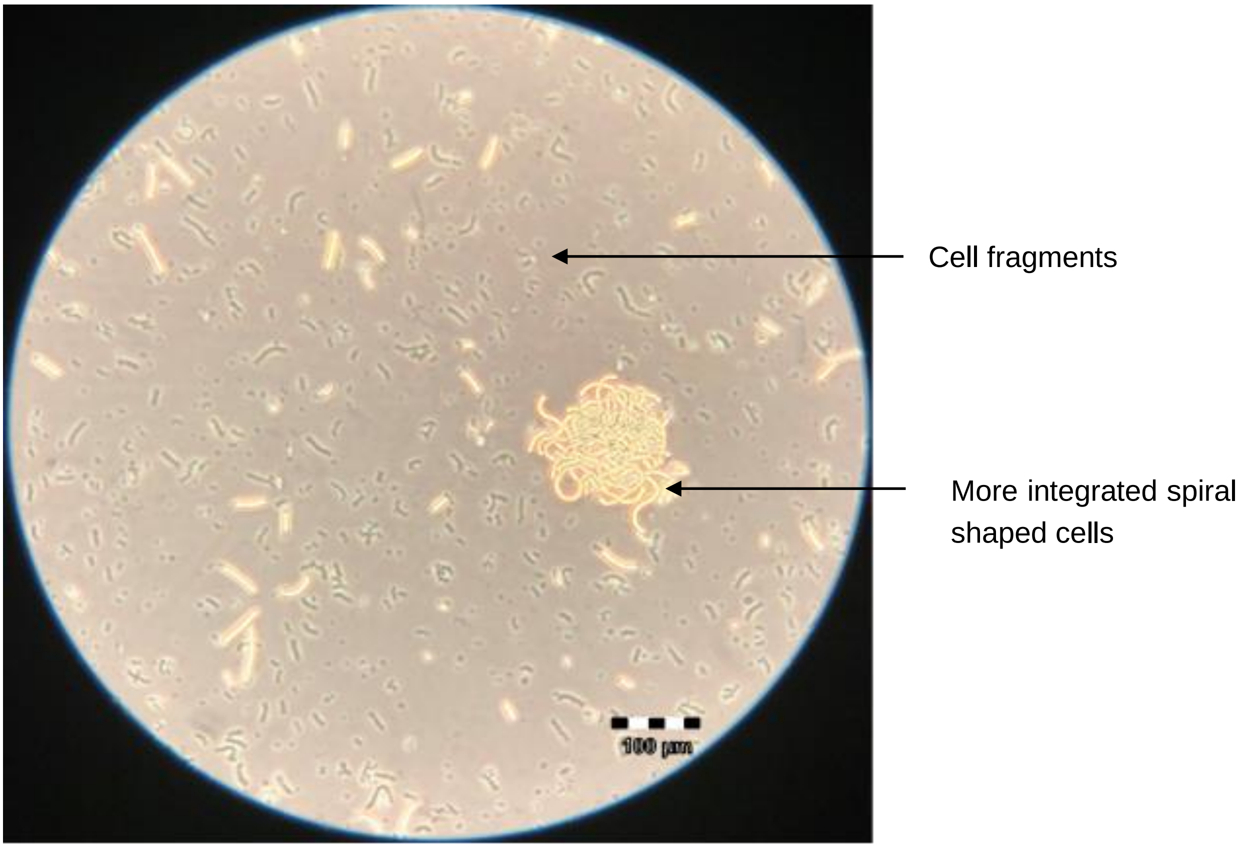

Figure 20. Resuspended dry *Spirulina* powder (without bead-milling) at 100 × magnification

Figure 21. Resuspended dry *Spirulina* powder (without bead-milling) at 1000 × magnification under oil immersion

6.2.2 PEG – MDX ATPS phase diagrams

The phase diagrams produced using PEG of different high molecular weights (10000, 12000 or 20000 Da) and maltodextrin as the other phase-forming component are presented in Figure 22, Figure 23 and Figure 24, respectively.

The bottom phases of all initial mixtures had near zero PEG as wt%, indicating that almost all PEG was excluded from this maltodextrin-rich phase. This agreed with studies performed by Machado *et al.* (2012), Silva and Meirelles (2001) and Ramyadevi *et al.* (2012) in which they found that the equilibrium curve of PEG 10000 and maltodextrin phase diagrams reached a near-zero PEG composition at MDX concentrations greater than 35 wt%. This indicated that the bottom phase after separation would contain almost no PEG for certain starting compositions. Using the tie-line slope, these conditions can be approximately found, where a tie-line is drawn through a theoretical starting composition, at the correct slope, to intersect with the equilibrium curve. The two points of intersection will then give a good estimate of the composition of the top and bottom phases once these are allowed to separate.

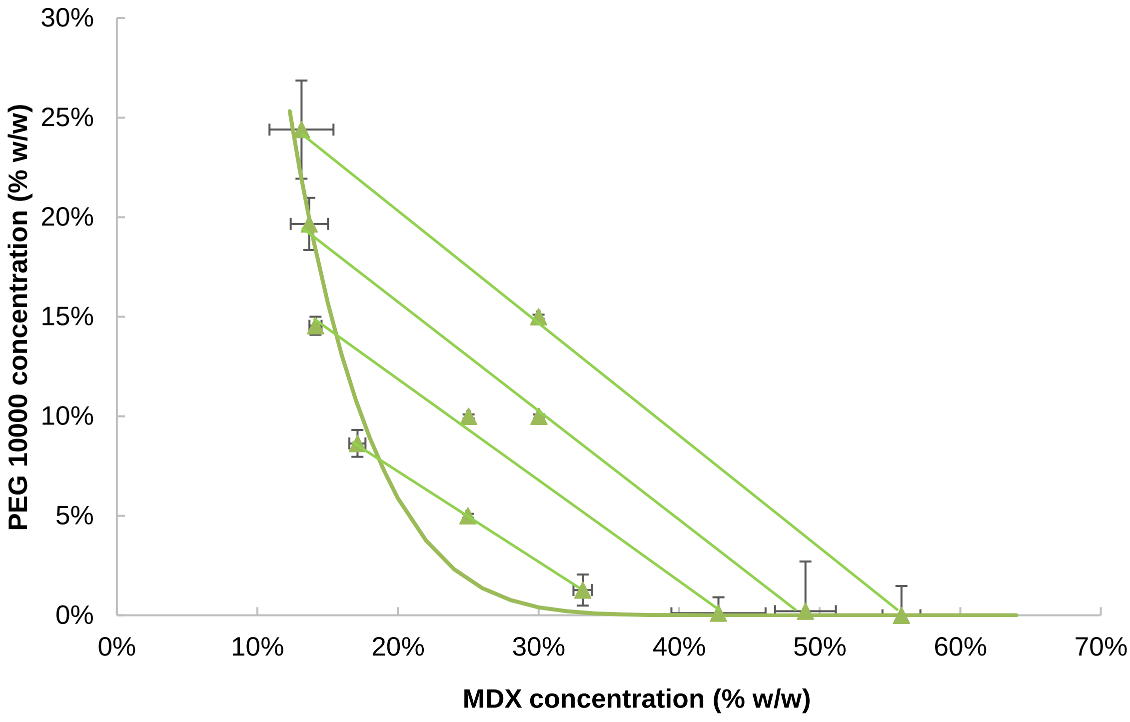

Figure 22. PEG 10000 – MDX phase diagram with tie-lines. Points indicate experimental data findings and the line is the model fit (Table 5). Error bars show standard deviation based on triplicate analysis.

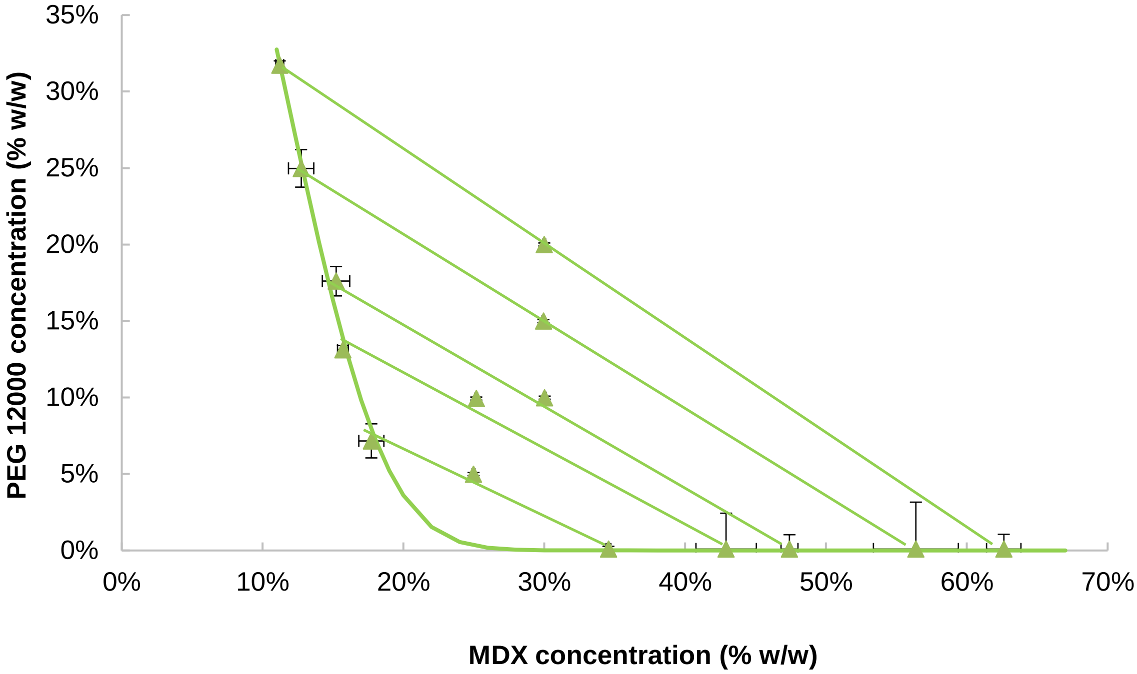

Figure 23. PEG 12000 – MDX phase diagram with tie-lines. Points indicate experimental data findings and the line is the model fit (Table 5). Error bars show standard deviation based on triplicate analysis.

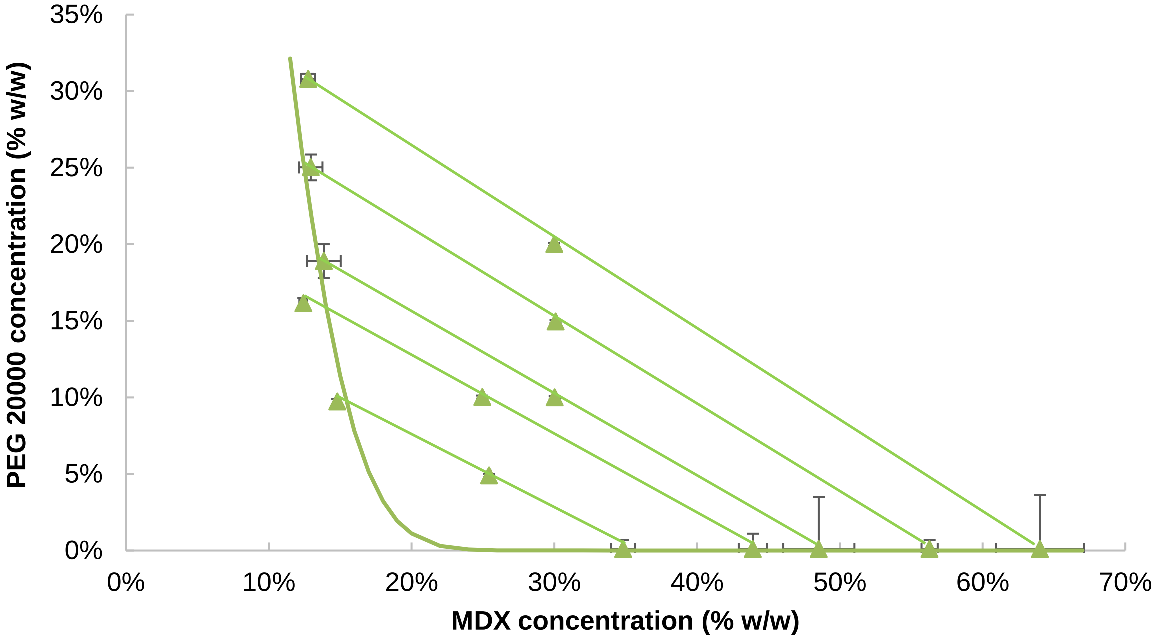

Figure 24. PEG 20000 – MDX phase diagram with tie-lines. Points indicate experimental data findings and the line is the model fit (Table 5). Error bars show standard deviation based on triplicate analysis.

6.2.2.1 Comparison of PEG – MDX phase equilibria

Figure 25 presents the 3 phase diagrams superimposed onto one set of axes. The equilibrium curves show minimal deviation from one another. A noteworthy difference between the phase diagrams though, is that the greater the PEG molecular weight, the larger the biphasic area on the phase diagram. Similar trends were found by Silva and

Meirelles (2001) and Ramyadevi *et al.* (2012), where the biphasic area increased as the PEG molecular weight increased up to 10000 Da. This manifests as a decrease in the polymer concentrations needed to form two phases as the molecular weight increases, based on the model, and only within the range of MDX concentrations between ~15 and 30 wt%. This does not, however, have a great effect on the compositions in the phases once they have separated.

This shows the likelihood of very similar polymer compositions being seen in the top and bottom phases when the same initial composition is used, regardless of the polymer length of PEG (10000, 12000 or 20000). This is backed up by the fact that each mixture produced a similarly pure MDX bottom phase (<1 wt% PEG), once the mixtures produced a bottom phase of greater than 35 wt% maltodextrin. The average TLS for each phase diagram, given in Table 5, was also not significantly different.

These factors make it reasonably clear that any difference noted in C-PC purity, recovery or partitioning between the phases is due to the nature of the interaction between the proteins and the polymer chains of different lengths, and not due to any differences that can be noted in the phase compositions or volume ratios produced.

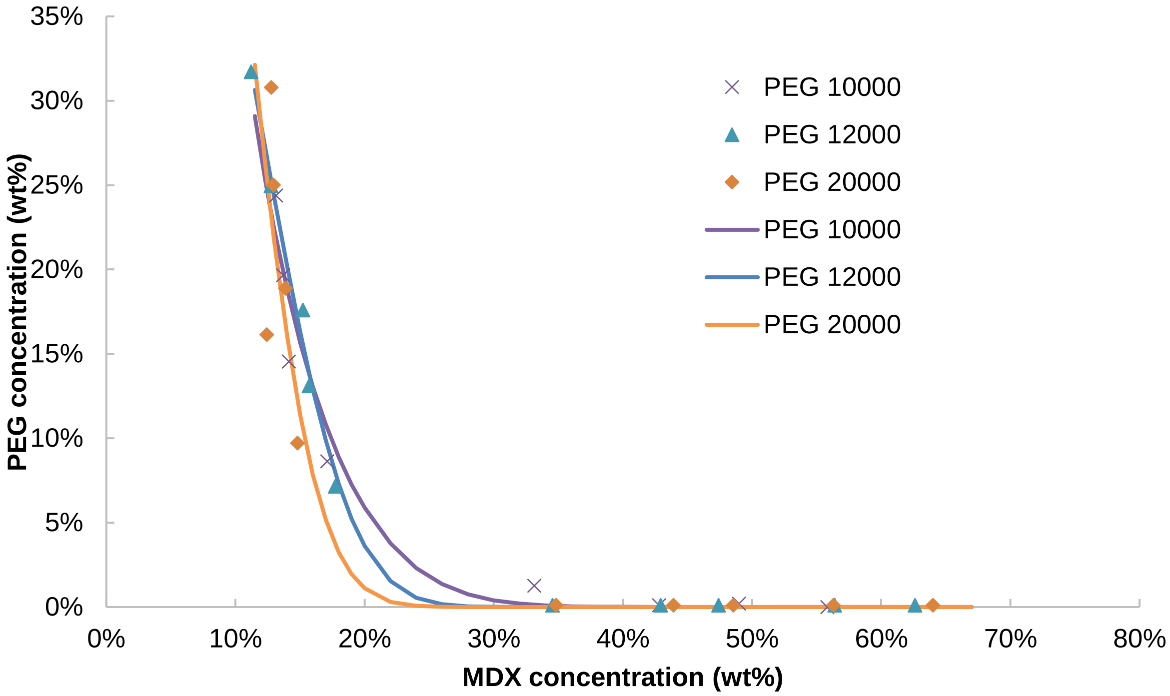

Figure 25. PEG – MDX phase diagram comparing PEG molecular weight. Points in the legend indicate experimental data findings and the lines are the model fits to each dataset (Table 5).

Table 5. Tie-line slope averages and model parameters for PEG – MDX ATPS varying PEG molecular weight

PEG molecular weight (Da)	**Average TLS (%/%)**	**Equilibrium curve model parameters (5.4.2.4)**			
		a	b	c	Sum of squared errors
10000	-49.1 ± 4.7	0.674	0.912	315	5.55E-04
12000	-52.5 ± 8.0	7.71	9.25	92.4	2.59E-03
20000	-54.1 ± 5.0	2.51	4.03	453	1.64E-02

6.2.2.2 PEG – MDX phase equilibria comparison to literature

Figure 26 presents a comparison between the PEG 10000 – MDX phase diagram produced in this work to those found in literature with the most similar conditions. These were phase diagrams produced by Machado *et al.* (2012), Silva and Meirelles (2001) and Ramyadevi *et al.* (2012). The highest molecular weight PEG tested by Machado *et al.* (2012) was 8000 Da, using maltodextrins of two different DEs (10.5 and 15). Ramyadevi *et al.* (2012) used PEG 10000 with an unidentified molecular weight of MDX, and Silva and Meirelles (2001) used PEG 10000 with MDX with a DE of 22.

The phase diagram in this study most closely resembled that produced by Machado *et al.* (2012) using PEG 8000 and MDX with a DE of 15. It also had a greater two-phase area than that produced by Silva and Meirelles (2001) but smaller than the one that Ramyadevi *et al.* (2012) produced. The differences between these phase diagrams can likely be accounted for in the different chemicals procured, whether the PEG molecular weights were different between the sources and the different maltodextrins used. The comparison likely indicated that the DE of the maltodextrin used in this study was lower than 22. This showed the importance of producing these phase diagrams for the ATPS study that followed.

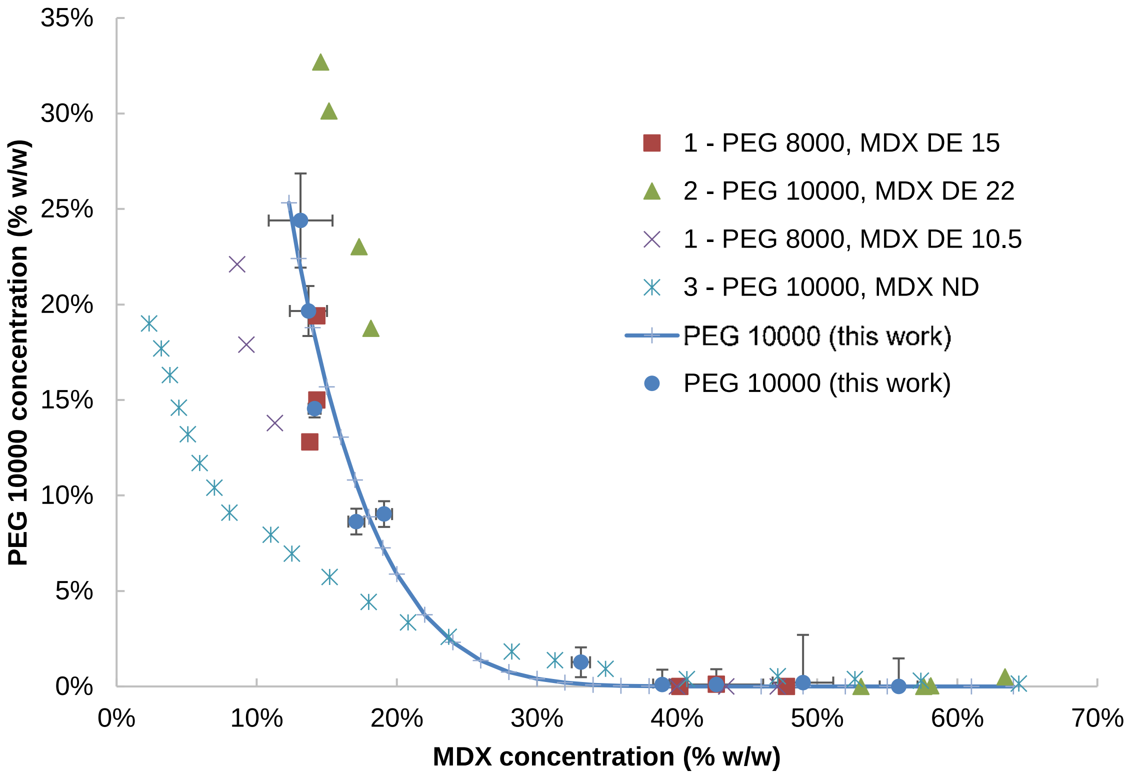

Figure 26. Comparison with similar phase diagrams in literature. Points indicate experimental data and literature findings and the line is the model fit for the PEG 10000 data (Table 5). Literature sources in legend: 1 - Machado *et al.* (2012) 2 - Silva and Meirelles (2001) 3 - Ramyadevi *et al.* (2012). Error bars show standard deviation based on triplicate analysis.

6.2.3 C-phycocyanin separation using PEG – MDX ATPS

6.2.3.1 Method improvement and polymer concentration screening

An initial screening stage was done to improve the C-PC separation performance and method by ATPS before testing the different polymer lengths. Formalised experimentation had not been done previously to vary polymer concentrations, leaving possible room for improvement. Using the phase diagrams produced, feasible starting concentrations could be used that would form two phases when left to separate. PEG 10000 was used in this screening study, being the one used in the previous work.

The starting concentrations from the previous work were 5 wt% PEG and 30 wt% MDX. This produced a system where there was a low volume ratio (estimated as 0.195) and thus a large MDX volume compared with the PEG phase. This is not desirable as the concentration of C-PC decreased, due to the addition of a large amount of polymer increasing the total volume of the system. Shown in Table 6 below, the purity remained about the same between the crude extract and the MDX phase, indicating that no purification occurred using these concentrations. Recovery of C-PC in the PEG phase, however, was less than 1 %, indicating that almost no C-PC reported to the top phase. The loss in recovery in the MDX phase was assumed to be due to volume loss when separating the phases and transferring the viscous liquid from vessel to vessel, as almost 100 % recovery would be expected if no volume loss occurred. This meant that increasing the volume ratio, by increasing the volume of the PEG phase in relation to the MDX phase, would concentrate the C-PC in the bottom phase while still having minimal recovery to the PEG phase, possibly increasing the purity. This was tested by increasing the PEG wt% in the next two experiments.

Table 6. Stepwise results for the patented process using 5 wt% PEG and 30 wt% MDX

	C-PC concentration (g/L)	Recovery (frac.)	Purity number
Leach	5.30 ± 0.30	-	0.606 ± 0.005
Cell-debris removal	5.58 ± 0.35	0.633 ± 0.057	0.604 ± 0.004
MDX phase	4.84 ± 0.54	0.975 ± 0.158	0.581 ± 0.008
PEG phase	0.05 ± 0.02	0.001 ± 0.001	0.028 ± 0.014

Table 7 and Table 8 show the process results when the MDX concentration was kept constant at 30 wt% while the PEG concentration was increased to 7 wt% and 9 wt%. The purity of C-PC in the MDX phase was slightly improved in the case where 7 wt% PEG was used (from 0.581 ± 0.008 to 0.634 ± 0.033) however no improvement was seen in the case where 9 wt% PEG was used. C-PC recovery in the PEG phase was almost zero in both cases, and the recovery in the bottom MDX phase was very high in each case (100 ± 14 % for 7 wt% PEG and 97 ± 16 % for 9 wt% PEG).

The increase in PEG concentration did not produce desirable results and the mixtures became more viscous and difficult to transfer and measure. The volume ratios were also not improved, with extremely small PEG phases and similarly low C-PC concentrations in the MDX phase due to the high volumes present. It was thus decided to reduce the MDX concentration; attempting to increase the volume ratio, mixture viscosity and concentration of C-PC in the bottom phase.

Table 7. Stepwise results for the patented process using 7 wt% PEG and 30 wt% MDX

	C-PC concentration (g/L)	Recovery (frac.)	Purity number
Leach	5.17 ± 0.14	-	0.585 ± 0.004
Cell-debris removal	5.75 ± 0.22	0.673 ± 0.045	0.592 ± 0.004
MDX phase	5.15 ± 0.64	1.000 ± 0.140	0.634 ± 0.033
PEG phase	0.07 ± 0.01	0.000 ± 0.000	0.031 ± 0.011

Table 8. Stepwise results for the patented process using 9 wt% PEG and 30 wt% MDX

	C-PC concentration (g/L)	Recovery (frac.)	Purity number
Leach	5.17 ± 0.14	-	0.585 ± 0.004
Cell-debris removal	5.75 ± 0.22	0.673 ± 0.045	0.592 ± 0.004
MDX phase	5.15 ± 0.64	1.000 ± 0.140	0.634 ± 0.033
PEG phase	0.07 ± 0.01	0.000 ± 0.000	0.031 ± 0.011

Table 9 and Table 10 show process results when operating at 9 wt% PEG and decreased MDX concentrations of 25 wt% and 20 wt%, respectively. Based on the phase diagrams produced, 9 wt% from the previous experiments was used going forward, as this would allow lower MDX concentrations to be used while still forming two phases.

The mixtures were found to be less viscous in mixing and pouring and the volume increase was lower upon adding the polymers due the smaller amount of MDX. The loss of C-PC to the top PEG phase was very low again, around 1 % for both mixtures. The recoveries to the bottom MDX phase were correspondingly around 99 %. Both processes using the lowered MDX concentrations increased the purity of C-PC, to 0.754 ± 0.003 for 25 wt% MDX and 0.736 ± 0.010 for 20 wt% MDX. This achieved food grade purity (purity number >0.7). These systems also increased C-PC concentrations in the MDX phase, with a maximum of 10.50 ± 0.60 mg/mL found in the 20 wt% MDX and 9 wt% PEG system. This ATPS mixture concentrated the C-PC by a factor of 1.9 and had a purification factor of 1.22.

Table 9. Stepwise results for the patented process using 9 wt% PEG and 25 wt% MDX

	C-PC concentration (g/L)	Recovery (frac.)	Purity number
Leach	4.82 ± 0.11	-	0.565 ± 0.004
Cell-debris removal	5.18 ± 0.12	0.652 ± 0.000	0.565 ± 0.003
MDX phase	8.39 ± 0.46	0.992 ± 0.089	0.754 ± 0.003
PEG phase	0.07 ± 0.02	0.008 ± 0.002	0.020 ± 0.023

Table 10. Stepwise results for the patented process using 9 wt% PEG and 20 wt% MDX

	C-PC concentration (g/L)	Recovery (frac.)	Purity number
Leach	5.08 ± 0.13	-	0.584 ± 0.005
Cell-debris removal	5.54 ± 0.19	0.698 ± 0.026	0.603 ± 0.004
MDX phase	10.50 ± 0.60	0.989 ± 0.054	0.736 ± 0.010
PEG phase	0.09 ± 0.01	0.011 ± 0.002	0.060 ± 0.010

Table 11 shows the summarised results for the different MDX and PEG concentrations used in this initial stage of the project for screening and improving the method. Higher purification factors and volume ratios were seen in the two ATPS mixtures with 25 wt% and 20 wt% MDX. The higher the volume ratio, the more the C-PC was concentrated as well, with the highest concentration being found in the mixture with 20 wt% MDX and 9 wt% PEG, at a volume ratio of 1.22 ± 0.04. This is good from a processing point of view, since it would use less ammonium sulfate to precipitate the protein in a subsequent downstream processing step, due to the lower volumes and higher C-PC concentrations involved. The purity achieved in this system was above food-grade and with a purification factor of 1.22 over the crude solution, making it suitable for moving forward to testing different PEG MWs.

Table 11. Comparison of results for the varied ATPS polymer concentrations

MDX wt %	PEG wt %	Volume ratio	Purification factor	C-PC partitioning ($1/K_{C\text{-}PC}$)	Protein partitioning ($K_{protein}$)
30	**5**	0.19 ± 0.03	0.97 ± 0.06	29.7 ± 4.3	0.373 ± 0.064
30	**7**	0.15 ± 0.02	1.07 ± 0.06	71.5 ± 18.1	0.311 ± 0.062
30	**9**	0.14 ± 0.00	0.96 ± 0.01	99.4 ± 11.1	0.270 ± 0.044
25	**9**	0.78 ± 0.13	1.33 ± 0.01	122 ± 32.8	0.248 ± 0.020
20	**9**	1.22 ± 0.04	1.22 ± 0.02	118 ± 19.6	0.207 ± 0.016

6.2.3.2 Variation of PEG molecular weight

Following the study done on varying the polymer concentrations and improving the method of extraction and measurement, the MW of PEG was varied at a fixed polymer concentration of 20 wt% MDX and 9 wt% PEG, to determine the influence this factor had in a PEG – MDX ATPS. PEGs of MW 6000 and 20000 were used to compare ATPS performance with PEGs of longer and shorter chain lengths to PEG 10000.

The results in Table 12 and Figure 27 show that PEG 10000 performed somewhat better than both PEG 6000 and PEG 20000 on the three most consequential factors for the extraction process: C-PC purification factor, C-PC concentration factor and C-PC recovery.

The greatest recovery was found with PEG 10000, at 95.1 ± 7.8 % followed by PEG 20000 at 93.6 ± 6.7 %. At these polymer concentrations, PEG 6000 had the lowest C-PC recovery of 84.4 ± 11.6 %, substantially lower but still within the uncertainty bounds of the other two MW PEGs.

The highest concentration factor was 1.65 ± 0.10 for PEG 10000, followed by 1.50 ± 0.16 for PEG 20000 and 1.45 ± 0.08 for PEG 6000. A possible explanation for this is the fact that PEG 10000 was found to have the highest volume ratio, and thus the highest ratio of top to bottom phase volume. This would mean that, if all else were equal, the C-PC concentration in the bottom phase would be higher, due to the lower volume in that phase. This does not explain the fact that PEG 20000 has the lowest volume ratio and yet has a greater concentration factor than PEG 6000.

Purification factor varied to a small extent between the different MW PEGs, with PEG 10000 again the highest at 1.21 ± 0.01, followed by PEG 20000 and PEG 6000, at 1.17 ± 0.01 and 1.13 ± 0.02 respectively. The purification factor for PEG 10000 agreed with that found in the previous work (1.22 ± 0.02 from Table 11) and was generally found to be robust upon repeats, seen in the low uncertainty values. However, these purification factors are still far below those seen in other, more widely studied, ATPS types. Sørensen *et al.* (2013) found a C-PC purification factor of 2.45 at a recovery of 88 % using PEG 4000 and potassium phosphate salts in an ATPS study which used 12.3 wt% PEG 4000 and 11.6 wt% salts to produce the two phases. Another study found a purification factor of 2.04 at a recovery of 100 % using 4 wt% PEG 4000 and 21 wt% potassium phosphate salts (Antelo *et al.*, 2015).

The partition coefficient for C-PC, taken as the inverse ($1/K_{C\text{-}PC}$) due to C-PC partitioning to the bottom phase, was seen to be higher as the PEG molecular weight increased. This indicates that the ratio of C-PC concentration in the bottom to the top phase was the highest for PEG 20000. The total proteins partition coefficient was also higher in PEG 20000 than the others, although not substantially so. This indicates a slightly higher ratio of total protein concentration in the top phase over the bottom phase. The end result did not have a great impact on the recovery and purification of C-PC over the PEG 10000 – MDX ATPS, likely due to the lower volume ratio observed. These factors also do not translate into performance as do the C-PC purity number, recovery and concentration, but rather give an indication about how the different compounds react to the phases in the ATPS. This could explain, however, why PEG 20000 still outperformed PEG 6000 while having a lower volume ratio.

Table 12. Comparison of results of different PEG MWs in ATPS with 20 wt% MDX and 9 wt% PEG

PEG MW (Da)	Volume ratio	Purification factor	$1/K_{C\text{-}PC}$	$K_{protein}$
6000	1.15 ± 0.08	1.13 ± 0.02	31.1 ± 10.9	0.248 ± 0.062
10000	1.19 ± 0.12	1.21 ± 0.01	107.6 ± 13.6	0.251 ± 0.082
20000	0.98 ± 0.01	1.17 ± 0.01	157.9 ± 66.6	0.263 ± 0.049

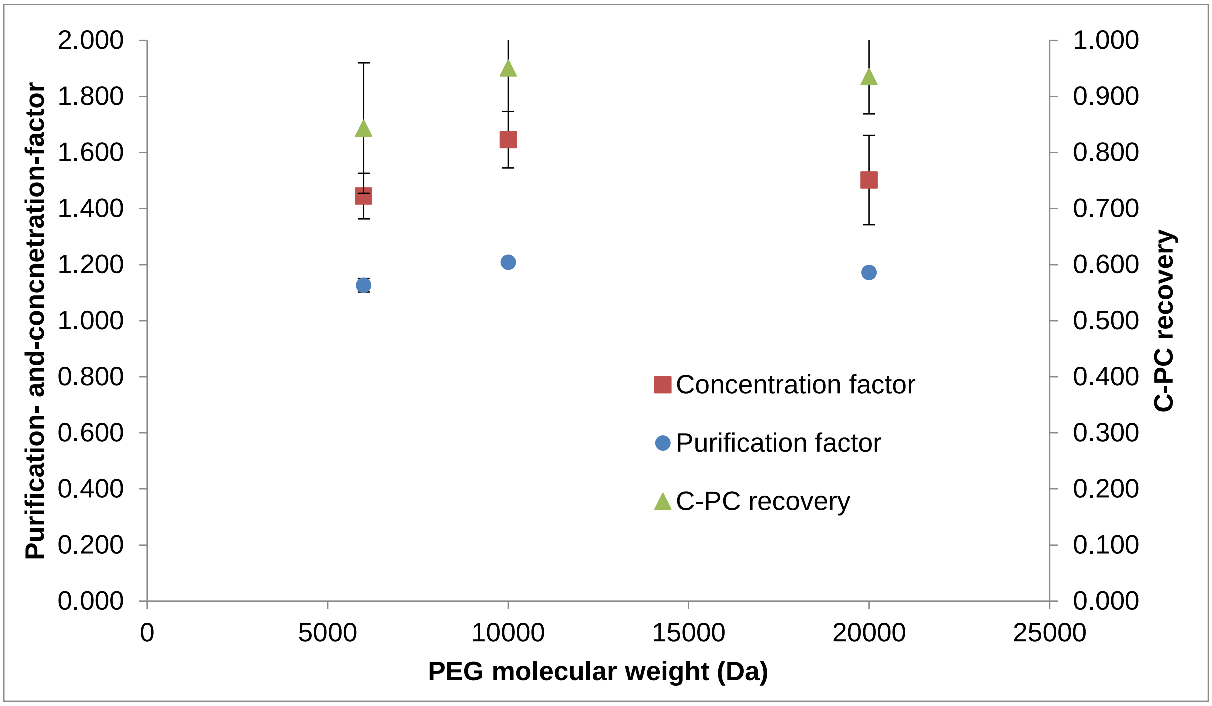

Figure 27. Comparison of MDX – PEG ATPS results for purifying C-PC with varying PEG molecular weight. Error bars show standard deviation based on duplicated experiments.

6.3 Conclusions

This chapter investigated the leaching time required and the effect of bead-milling for the dry *Spirulina* sample used for this study. Following that, phase diagrams were produced for three PEG and maltodextrin ATPS systems using different molecular weights of PEG. Also investigated were the effects of polymer concentrations and PEG molecular weights on a PEG – MDX ATPS for purifying C-PC from the leached *Spirulina* supernatant.

It was found that 2 hours was most likely the optimal leaching time for the dried *Spirulina* sample used in this study. The C-PC concentration did not increase substantially after 2 hours of leaching, reaching 5.14 ± 0.66 g/L at 2 hours and remained in the range of 5.5 – 5.8 g/L until the end of the experiment, at 26 hours. The C-PC purity number was at a maximum after 2 hours, at 0.70 ± 0.05, with a slow linear decline until the experiment was ended at 26 hours. There was no clear difference between the bead-milled sample and the control sample, which was leached with no bead-milling. This was likely due to the spray-drying process used to produce the *Spirulina* powder, which involved high pressure pumping through a small nozzle. Significant cell-disruption was confirmed by the microscope pictures of the non-bead-milled sample which showed small disintegrated segments of the algae. The decline in purity number with time was likely due to the C-PC leaching faster than other proteins in the *Spirulina,* causing the purity to be highest at the start and slowly decline as other proteins go into solution. These results were used for this thesis but is not a universal recommendation for the process, as it depends on the specific *Spirulina* sample used.

For the phase diagrams produced, the three PEG molecular weights used (10000, 12000 and 20000 Da) had similar top and bottom phase compositions. Based on the models used for the phase equilibrium curves, however, there seemed to be an increasing biphasic area as the PEG molecular weight increased. This translates to a larger area of component compositions for PEG – MDX mixtures to separate into two phases after mixing. The bottom phase of all the phase diagrams reached near-zero wt% PEG after the MDX concentration exceeded 35 wt%, which agreed with other PEG – MDX phase diagrams found in literature. The PEG 10000 – MDX ATPS used in this study most closely resembled a PEG 8000 – MDX phase diagram where the MDX had a DE of 15 (Machado *et al.*, 2012). The phase diagram from this study using PEG 10000 had a greater biphasic area than one produced using PEG 10000 and a MDX with a DE of 22 (Silva and Meirelles, 2001). This indicated that the DE of the MDX used in this study was lower than 22. The literature comparisons thus showed the necessity of producing phase diagrams with the specific chemicals procured when doing work with ATPS.

After testing different polymer concentrations for the ATPS, it was found that lower MDX concentrations and higher PEG 10000 concentrations improved performance over the original composition of 30 wt% MDX and 5 wt% PEG. This was observed in the tests done where the purification factor for the composition of 20 wt% MDX and 9 wt% PEG 10000 had a 1.22 ± 0.02 purification factor and final C-PC concentration of 10.5 ± 0.6 g/L, compared to the original composition which had a 0.97 ± 0.06 purification factor and a C-PC concentration of 4.28 ± 0.44 g/L in the MDX phase. This was most likely due to the higher volume ratios when decreasing MDX concentration and increasing PEG concentration, since there would be more of the top phase-forming component (PEG) and less of the bottom phase-forming component (MDX) present. This would increase the volume of the top phase, possibly allowing more proteins to partition there, while the C-PC is still drawn to partition mostly to the bottom phase. The volume ratio of the 20 wt% MDX and 9 wt% PEG ATPS was 1.22 ± 0.04 while for the original composition (30 wt% MDX and 5 wt% PEG) it was 0.19 ± 0.03.

This better-performing composition was used to test different (lower and higher) PEG molecular weight options: 6000, 10000 and 20000 Da. PEG 10000 was found to perform the best of the three tested, with a C-PC purification factor of 1.21 ± 0.01, a C-PC recovery of 95.1 ± 7.8 % and a C-PC concentration factor of 1.65 ± 0.10. PEG 20000 performed second-best on all the factors, likely due to the higher partition coefficients for C-PC and total proteins, despite having the lowest volume ratio.

Comparatively these purification factors are much lower than those seen in PEG – salt systems, which have been found to reach purification factors of 2.45 with 88 % C-PC recovery and 2.04 at 100 % recovery, both using PEG – 4000 and potassium phosphate salts. These achieve a purer product using a smaller total amount of polymer (12 wt % and 4 wt%, respectively), with the bottom phase-forming component being a salt. It cannot be said at this point whether these would result in the need for fewer downstream processing steps, but it does point to the need to rethink the current ATPS mode and look for ways to improve the effectiveness of this step in the process, such as the use of a compatible two-stage ATPS process.

7 Investigation of a two-stage ATPS

7.1 Introduction

Following the results seen in Section 6.2.3, it was decided to consider alternative modes of operation for the ATPS used in the process. In developing the patented process, a PEG – citrate ATPS was considered, before discovering issues with attempting to precipitate the C-PC from the PEG phase (Griffiths, Burke, *et al.*, 2016). Due to the poor purification factor in the polymer-polymer ATPS, however, the PEG – citrate ATPS is proposed in this chapter as the first stage of a two-stage ATPS process. The second stage employs a PEG – MDX ATPS to recover the C-PC to the bottom MDX phase, to enable more options for product recovery.

Design of the first step involved producing PEG – citrate ATPS phase diagrams for three molecular weights of PEG: 4000, 6000 and 10000 Da. The phase diagrams were produced using a mixture of citric acid and sodium citrate, to produce the phase diagrams at a pH of 6. These three PEGs were chosen due to the lower molecular weight PEGs having better reported results in PEG – salt ATPS in general, with PEG 4000 usually being found to perform the best (see Section 2.3.1.5). Since a second step of PEG – MDX ATPS will be used, the PEG molecular weight was taken up to PEG 10000, with that being found to perform the best in a PEG – MDX ATPS.

The three PEG molecular weights were then tested in a two-stage ATPS process for C-PC purification. Screening experiments were done using a ‘high’ and ‘low’ concentration combination of PEG and citrate in the first stage. This was then followed up by a PEG – MDX ATPS using the top phase of the first stage, adding MDX and diluting with water to achieve a constant MDX concentration, while attempting to achieve a consistent PEG concentration.

After the screening experiments, the best-performing PEG molecular weight was used for two factorial experiments based on varying the respective polymer concentrations. The first used the PEG – citrate ATPS in a 3-level 2-factor analysis of the effect of PEG and citrate concentrations on C-PC purification, concentration and recovery. The other was a 3-level 2-factor analysis of the PEG – MDX ATPS with the factors being the concentrations of the two polymers. This was again tested for the polymer concentration effects on the purification, concentration and recovery of C-PC. These were analysed using the statistical analysis program *Statistica* to produce response curves and to simulate the response variables with changes to the input concentrations. This was used to improve data on the process so that further options for optimisation and downstream processing could be explored.

7.2 Results and discussion

7.2.1 PEG – citrate phase diagrams

Presented in Figure 28, Figure 29 and Figure 30 are the phase diagrams for PEG – citrate ATPS, using the different molecular weights of 4000, 6000 and 10000 Da, respectively. The phase diagrams produced were asymmetrical, as can be seen by the different scales of the two axes, with the highest concentration point reaching above 45 wt% PEG in each case while the citrate concentration reaches under 34 wt% in each phase diagram. This is also clear from the average tie-line slopes, which range from -177 ± 19 for PEG 4000 to -186 ± 30 for the PEG 10000 phase diagram (Table 13). These large negative slopes indicate that the change in PEG concentration is greater that the corresponding change in citrate concentration.

The phase diagrams also indicated that the bottom phase could achieve a very low concentration of residual PEG, shown by each of the equilibrium curves reaching the bottom axis with a ~0 wt% PEG. This occurs at different citrate concentrations for the three phase diagrams. For the PEG 4000 – citrate ATPS, a near zero PEG concentration is reached in the bottom phase at around 28 wt% citrate, according to the model equilibrium curve. The PEG 6000 – citrate phase diagram reached the ~0 wt% PEG mark at around 25 wt% citrate, and the PEG 10000 – citrate phase diagram reached the bottom axis even earlier, at 19 wt % citrate.

Also observed was that the higher the PEG molecular weight, the lower the citrate concentration in the top phase at high PEG concentrations. The top point on the phase equilibrium curve was 3.9 wt % citrate and 45.2 wt% PEG 4000, 3.0 wt% citrate and 47.2 wt% PEG 6000, and 2.8 wt% citrate and 46.6 wt% PEG 10000 for the different PEG molecular weights, from the same starting composition in each case. This indicated that the higher the PEG molecular weight, the purer the top and bottom phases were in PEG and citrate, respectively. This difference was very slight, however, and was accentuated at the points mentioned above.

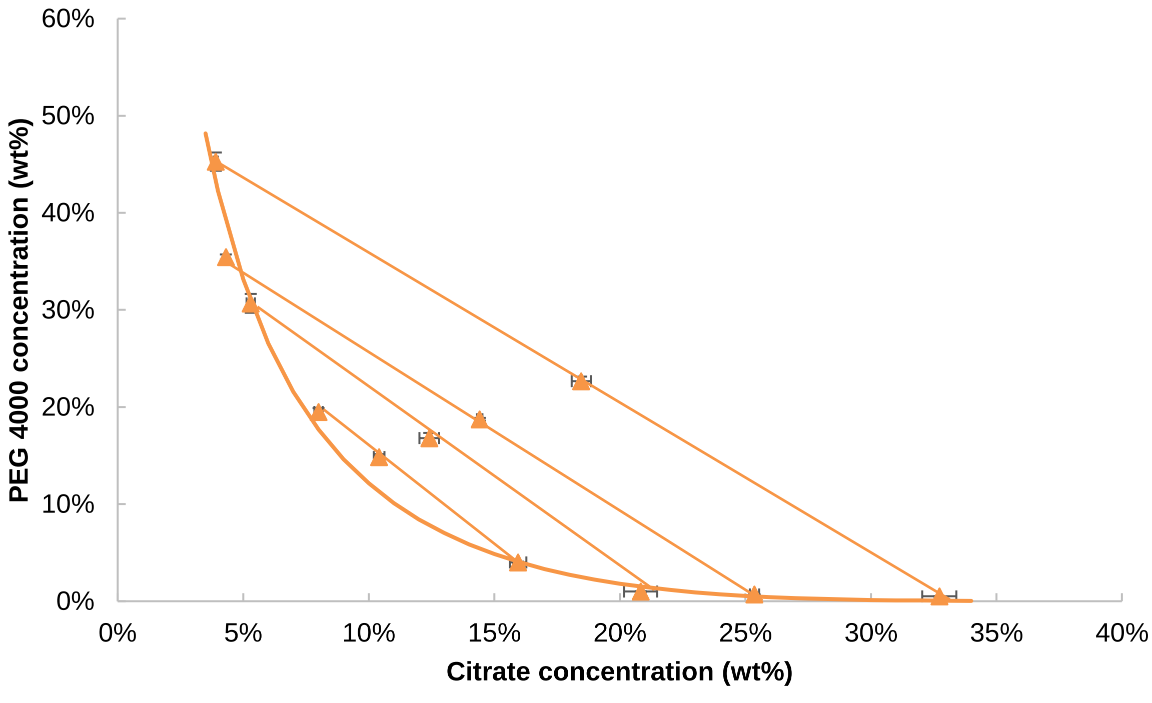

Figure 28. PEG 4000 – citrate phase diagram with tie-lines. Points indicate experimental data findings and the line is the model fit (Table 13). Error bars show standard deviation based on triplicate analysis.

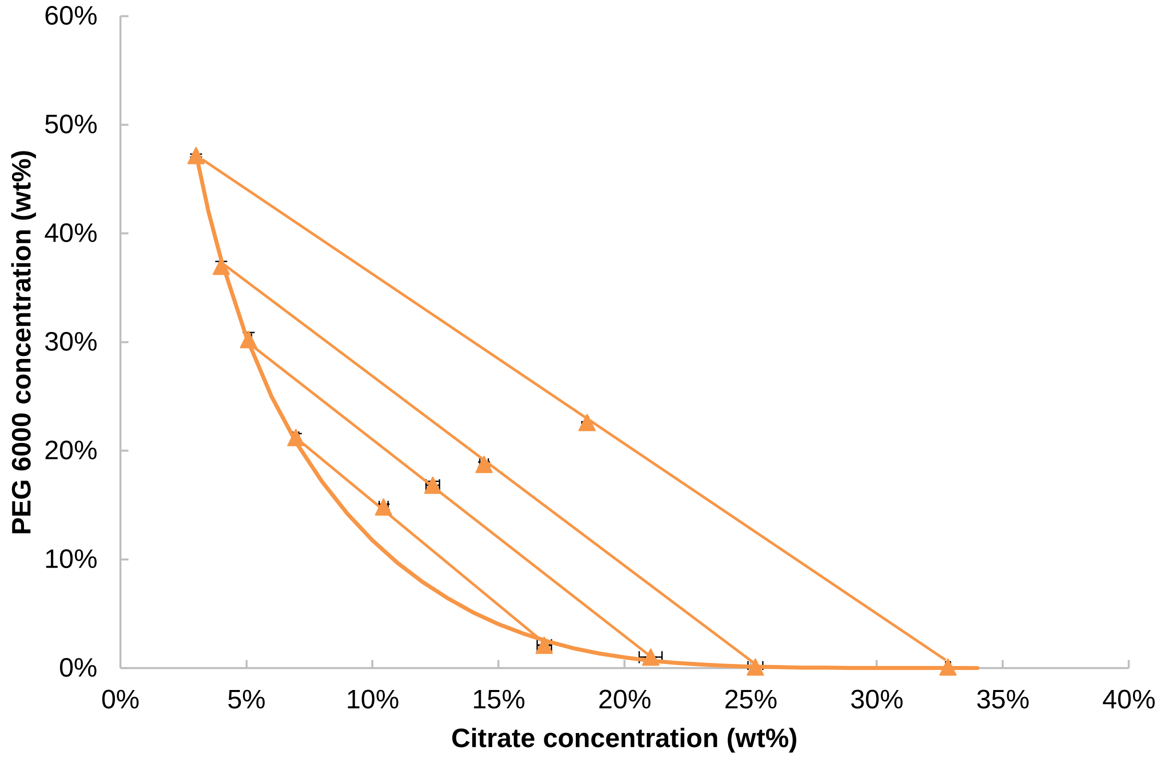

Figure 29. PEG 6000 – citrate phase diagram with tie-lines. Points indicate experimental data findings and the line is the model fit (Table 13). Error bars show standard deviation based on triplicate analysis.

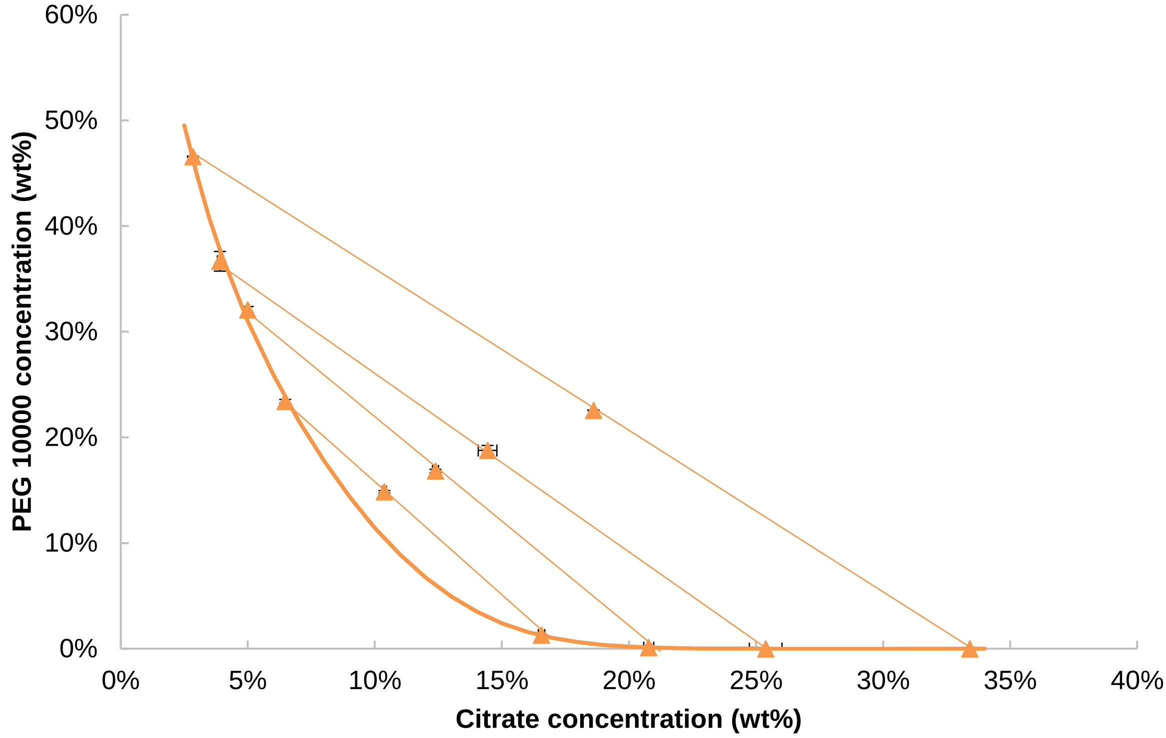

Figure 30. PEG 10000 – citrate phase diagram with tie-lines. Points indicate experimental data findings and the line is the model fit (Table 13). Error bars show standard deviation based on triplicate analysis.

7.2.1.1 Comparison of PEG – citrate phase equilibria

In comparing the three PEG molecular weights, the higher the molecular weight, the greater the biphasic area (Figure 31). The difference was slight, however, and could be seen mainly where the PEG concentrations were high (>25 wt%) and where the citrate concentration reached above 10 wt%. This presented as the tendency for the higher molecular weight PEG systems to reach the bottom axis at a lower citrate concentration, which modelled the point at which the bottom phase contained ~0 wt% PEG.

The model produced agrees well with the plotted experimental points in each of the cases, seen with the low sum of squared errors used in fitting the model (Table 13). The tie-lines slopes were not substantially different for each of the PEG molecular weight systems, although these were found not to be perfectly parallel, based on the large standard deviation of the TLSs and seen visually in the tie-lines drawn. This was likely due, in part, to the asymmetry in the phase diagrams, and thus as the tie-lines drew closer to the equilibrium curve, the gradient of the tie-lines increased.

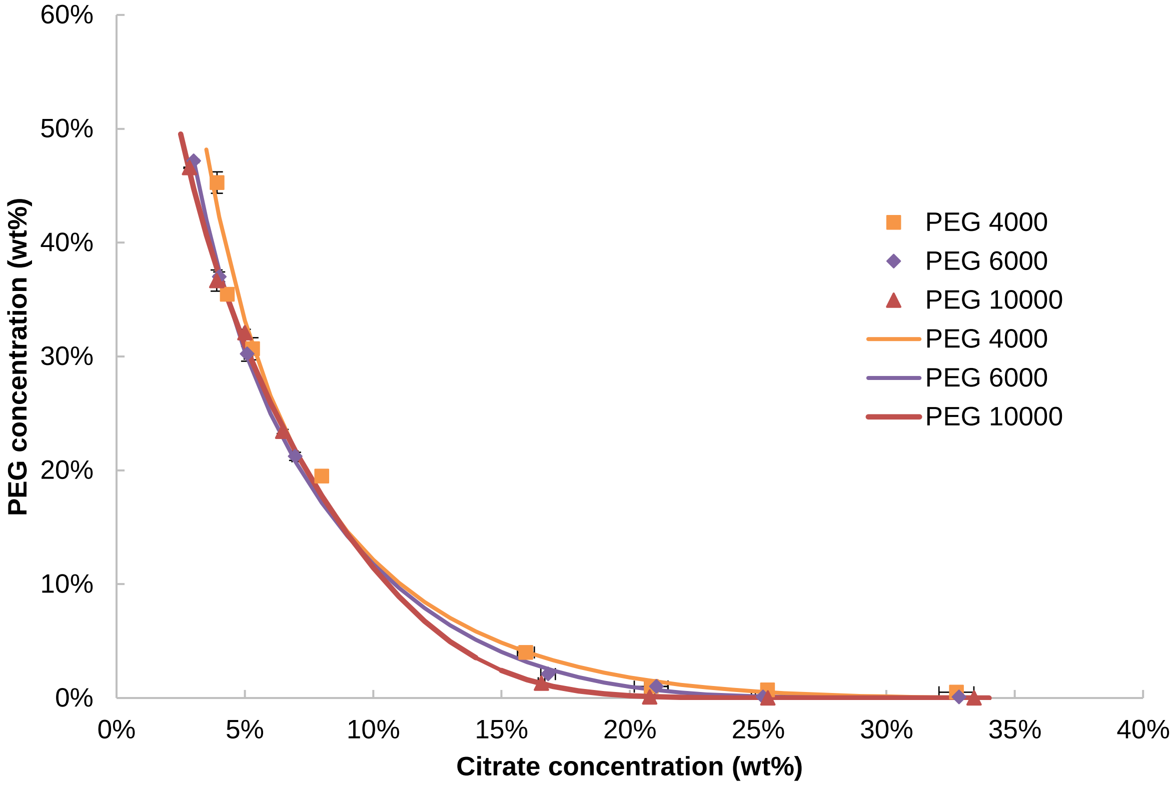

Figure 31. PEG – citrate phase diagram comparing PEG polymer lengths. Points in the legend indicate experimental data findings and the lines are the model fits to each dataset (Table 13). Error bars show standard deviation based on triplicate analysis.

Table 13. Tie-line slope averages and model parameters for PEG – citrate ATPS varying PEG molecular weight.

PEG molecular weight (Da)	**Average TLS (%/%)**	**Equilibrium curve model parameters (5.4.2.4)**			
		a	b	c	Sum of squared errors
4000	-177 ± 19	3.17	10.1	84.2	2.12E-03
6000	-177 ± 15	2.03	8.38	198	8.89E-05
10000	-186 ± 30	1.37	6.38	462	2.64E-04

7.2.1.2 PEG – citrate phase equilibria comparisons to literature

Comparing the phase diagrams to literature, only the PEG 4000 and PEG 10000 ATPS phase diagrams were used, as the equilibrium curve for PEG 6000 fell between these. The comparison showed a very close agreement between the phase diagrams produced in this work and those produced by Glyk *et al*. (2014) and Tubıo *et al.* (2006). The highest PEG molecular weight tested with citrate in an ATPS was found to be PEG 8000, by Tubıo *et al.* (2006) and so this was included in the comparison, although the pH of the system was 5.1 in their study.

A similar trend was seen in both the literature comparisons, where a higher PEG molecular weight system led to a greater biphasic area. The results from Glyk *et al*. (2014), using PEG 4000 at pH 6 agreed well with that from Tubıo *et al.* (2006) using PEG 3350 at pH 5.1, showing that results were not greatly affected by pH across these two studies, and that the comparisons were valid. The greatest deviations were seen where the PEG 6000 and PEG 8000 phase diagram points from the literature examples showed a gap as citrate concentrations decreased from 10 wt%.

This also related to the point at which each phase diagram reached the bottom axis, indicating a near 0 wt% PEG in the bottom phase solution. Findings from this study were similar to those observed by Glyk *et al*. (2014), where the point at which the equilibrium curve reached the bottom axis was around 20 wt% citrate for the phase diagram using PEG 4000 and 18 wt% citrate for PEG 8000. The study was done at varying pH using the cloud-point method. Other studies found similar results, where a near zero concentration of PEG was achieved in the bottom phase on the equilibrium curve (Tubıo *et al.*, 2006; De Oliveira *et al.*, 2008). These results were in a similar range, with PEG 8000 from the Tubıo *et al.* (2006) study reaching the bottom axis around 16 wt% citrate, while the lower MW PEG of 3350 Da reached a near 0 wt% PEG at around 20 wt% citrate. This was another example which showed the greater biphasic area with increasing PEG molecular weight.

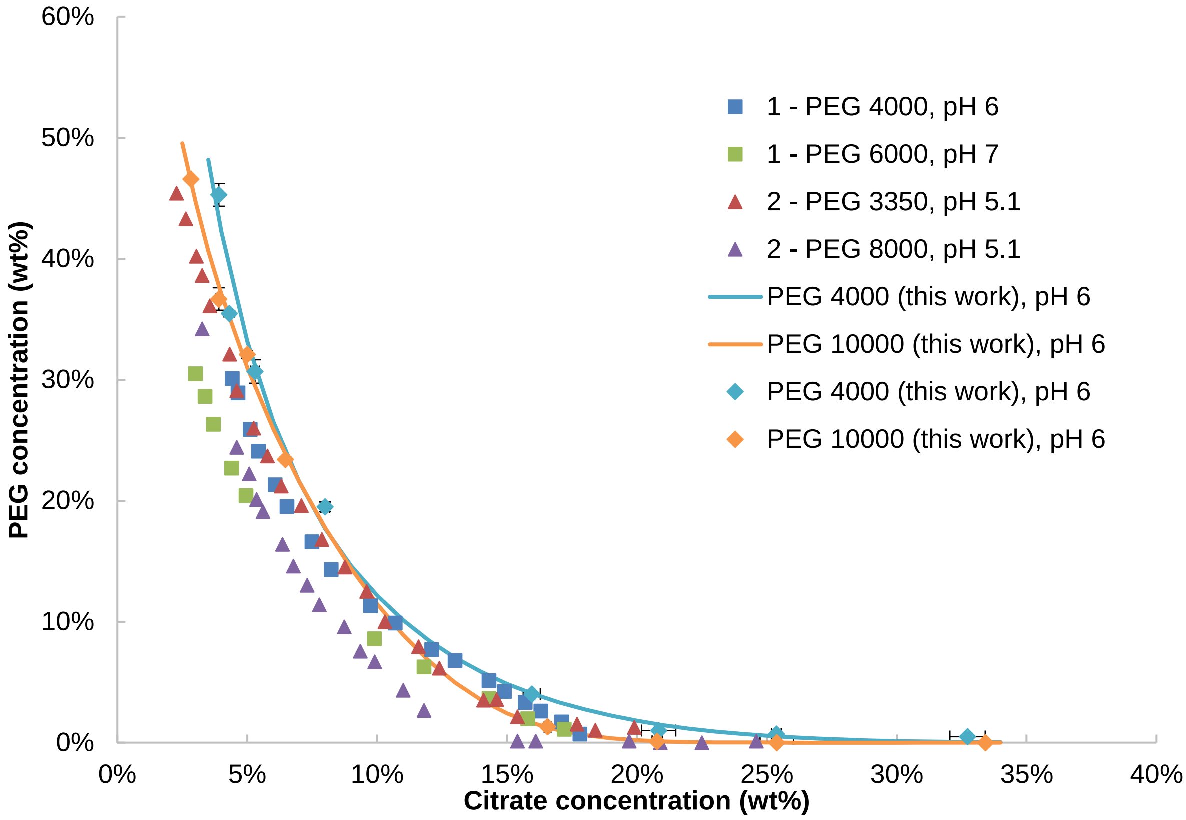

Figure 32. Comparison between PEG – citrate phase diagrams produced in this work to those from literature sources. Points indicate experimental data and literature findings and the lines are the model fit for the PEG MWs shown (Table 13). Literature sources in legend: 1 – Glyk *et al.* (2014), 2 - Tubıo *et al.* (2006). Error bars show standard deviation based on triplicate analysis.

7.3 Two-stage ATPS studies

The component concentrations for the two-stage ATPS experiments were chosen based on previous studies which looked at PEG – citrate ATPS for C-PC purification (Patil *et al.*, 2008; Wang *et al.*, 2012) and the phase diagrams produced in this work. The 'low' (13 wt % PEG; 11 wt% citrate) and 'high' (22 wt% PEG; 14 wt% citrate) concentrations referred to the component concentrations used in first stage, the PEG – citrate ATPS, in the screening experiments. The second stage used a set amount of the PEG (top) phase from the first stage, and diluted this with water before adding MDX, giving a standard MDX concentration of 20 wt% and a consistent PEG concentration estimate of 15 wt% across the tests (see 5.3.8.1).

7.3.1 PEG molecular weight screening

Results from the two-stage screening experiments for the best PEG molecular weight for the two-stage ATPS are presented in Figure 33 and Figure 34. PEG 4000 was found to perform best in the low concentration screening, most visibly in overall C-PC purification (Figure 33). PEG 4000 showed a purification factor of 1.60 ± 0.13 over the two stages, followed by PEG 6000 and PEG 10000, with purification factors of 1.12 ± 0.07 and 0.56 ± 0.31, respectively. This was mostly due to the differences in purification in the first PEG – citrate ATPS stage, where the higher the PEG molecular weight, the lower the purification factor. This result has been documented in previous studies where a PEG – salt ATPS was used for C-PC purification (Patil *et al.*, 2006; Antelo *et al.*, 2015; Chethana *et al.*, 2015).

The second ATPS stage, using the PEG – MDX mixture, found most of the C-PC partitioned to the bottom MDX phase. Each PEG molecular weight gave purification factors of greater than 1.1 over the second stage alone. This still led, however, to the low overall purifications by PEG 6000 and PEG 10000, with PEG 10000 reducing the purity when applied to this two-stage ATPS. The overall recovery over both stages was also highest for PEG 4000, with a recovery of 0.53 ± 0.19. PEG 6000 and PEG 10000 gave lower overall C-PC recoveries of 0.22 ± 0.06 and 0.13 ± 0.10, respectively.

The high relative uncertainties were due to the number of factors going into propagating the uncertainty over the two stages and different phases. Again, this was mainly due to the performance of the different PEG molecular weights in the first stage, using the PEG – citrate ATPS, with similar results being seen in the recoveries over the second, PEG – MDX, ATPS stage.

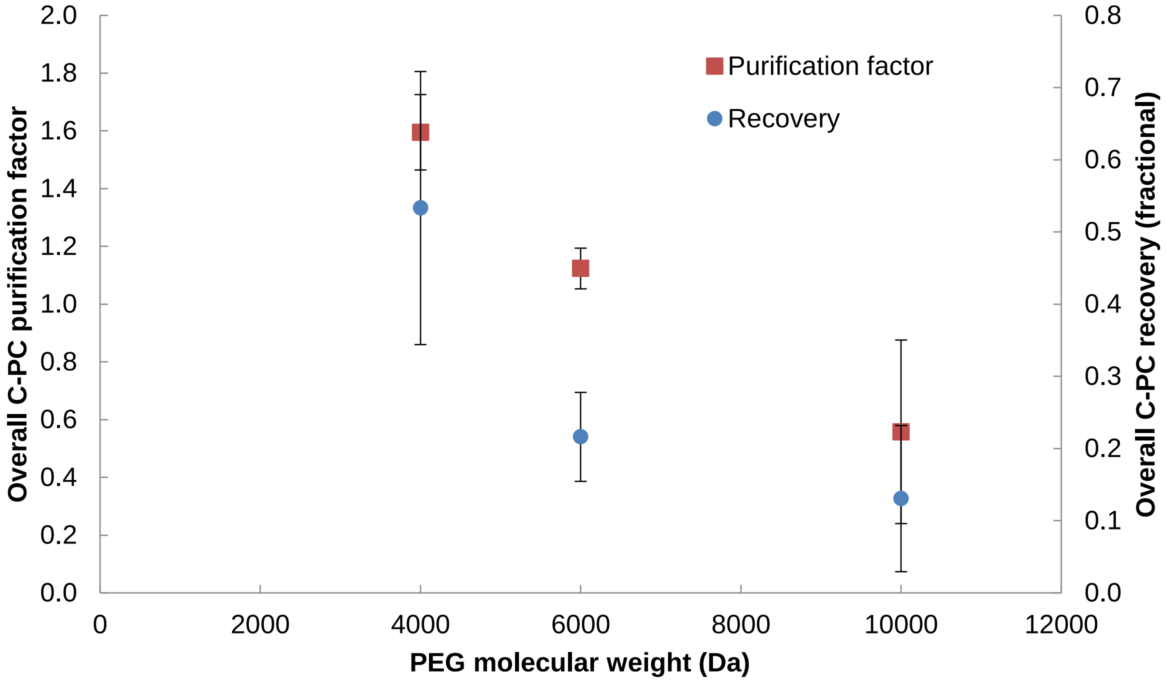

Figure 33. Two-stage ATPS screening results for low (13 wt % PEG; 11 wt% citrate) concentrations of components. Error bars show standard deviation based on duplicated experiments.

Higher purification factors were seen using the 22 wt% PEG – 14 wt% citrate concentration screening, with PEG 4000 performing the best, with an overall C-PC purification factor of 2.11 ± 0.20 over the two stages. PEG 6000 had an overall purification factor of 1.65 ± 0.16 and PEG 10000 purified the C-PC by a factor of 1.02 ± 0.40. These purification factors were far higher than those from the low concentration screening. This was mainly due to the higher purifications seen in the second stage, the PEG – MDX ATPS.

The C-PC recoveries were found to be higher, again, in the lower molecular weight PEGs. The overall C-PC recovery for PEG 4000 was 0.69 ± 0.22, which was followed by 0.52 ±

0.13 and 0.33 ± 0.07 for PEG 6000 and PEG 10000, respectively. These differences in recovery were mainly influenced by the recoveries in the first stage, where the lower PEG molecular weight had higher C-PC recoveries in the PEG – citrate ATPS. This has been documented, where a possible influencing factor is that a higher PEG molecular weight leads to less free space within the phase for C-PC to partition in, leading to precipitation at the interface and partitioning to the salt phase (Patil and Raghavarao, 2007). The second PEG – MDX ATPS had similar recoveries around 0.73 (± 0.05) for each of the molecular weights. The PEG 4000 system produced a final C-PC purity of 1.46 ± 0.08, within the range of cosmetic-grade purity.

Based on these screening results, the best PEG molecular weight to go forward with, when investigating the option of a two-stage ATPS, was PEG 4000. PEG 4000 had the best overall results in terms of C-PC purification and recovery. This was mainly due to the improved performance in the PEG – citrate ATPS stage, while it performed adequately well in the second PEG – MDX ATPS to be better overall. This does not necessarily contradict the previous experiments, where PEG 10000 was found to perform better than PEG 6000 in a PEG – MDX ATPS, since complicating factors (the purification performed in the first stage) likely influenced the performance in the second stage.

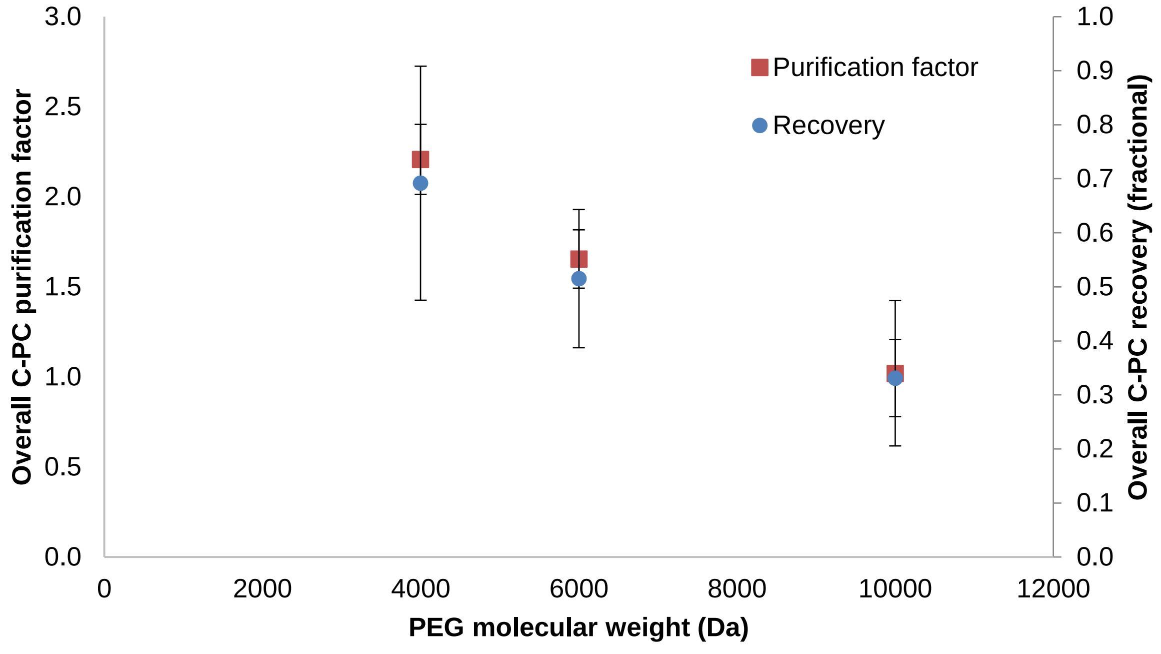

Figure 34. Two-stage ATPS screening results for high (22 wt% PEG; 14 wt% citrate) concentrations of components. Error bars show standard deviation based on duplicated experiments.

7.3.2 PEG – citrate ATPS optimisation

The factorial design for the PEG – citrate ATPS was carried out using PEG 4000 and citrate salts, at pH 6.0. Using factorial design as a statistical tool allowed modelling and the generation of response curves to the data, helping to understand the link between the input variables and the outcomes, over a range of inputs. The 3 levels used were the component concentrations of PEG and citrate of 12, 16 and 20 wt%. These concentrations were based on the phase diagrams produced as well as being in a range encompassing the concentrations used in literature ATPS studies reported for C-PC purification. This resulted in 9 unique concentration combinations (including the central point) being tested, with a further three repeats on the central point (16 wt% PEG and citrate), to determine the experimental uncertainty and provide confidence intervals for predictive values generated by *Statistica*. To observe the effect of the two component concentrations on the C-PC purification factor, recovery and concentration, the factorial design was used to generate a series of response curves using *Statistica.*

7.3.2.1 Effect of component concentrations on C-PC purification factor

The response curve for C-PC purification upon varying component concentrations fitted well with the experimental points, with a low Mean-Squared (MS) residual of 0.00995, the average squared differences between the model response curve and the actual values (Figure 35). The curve showed a clear trend where having high concentration of both components (> 20 wt% PEG and citrate) performed poorly, with purification decreasing in bands. This is seen with the change from dark red shifting to light red, starting from 21 wt% citrate at the right-most corner of the x-y plane, to the point at 21 wt% PEG and 15 wt% citrate, upper-left on the x-y plane. The darkest patch, indicating the highest predicted C-PC purification factor, was seen extending from 18 wt% on the citrate concentration axis to 21 wt%, the highest value included on the axes, and from 11 to 13 wt% in PEG concentration. This could be due to a high citrate concentration and a low PEG concentration creating a low volume ratio, since there would be a greater volume in the bottom citrate phase and a smaller volume in the top PEG phase. The bottom phase therefore has a greater volume to take in partitioned proteins, while C-PC still reports to the top PEG phase and is thus more purified of contaminating proteins. The highest experimental value was a C-PC purification factor of 1.73 at 12 wt % PEG and 16 wt % citrate.

A similar trend has been observed in PEG – phosphate systems, where, at a constant salt concentration of 15 wt%, Chethana *et al.* (2015) found the best C-PC purification at a PEG 4000 concentration of 12 wt%, better than 15 and 20 wt% PEG. Wang *et al.* (2012) also found a better purification factor using 16 wt% PEG 4000 and 20 wt% sodium tartrate, over 18 wt% PEG 4000 and 16 wt% of the salt. In that study it was also found, however, that a lower PEG concentration and a higher salt concentration (14 wt% and 22 wt%, respectively) had a slightly lower purification factor than a PEG concentration of 16 wt% with a salt concentration of 20 wt%. These complicating results highlight the need for testing systems experimentally, since ATPS results can be difficult to predict when using different salts and operating conditions.

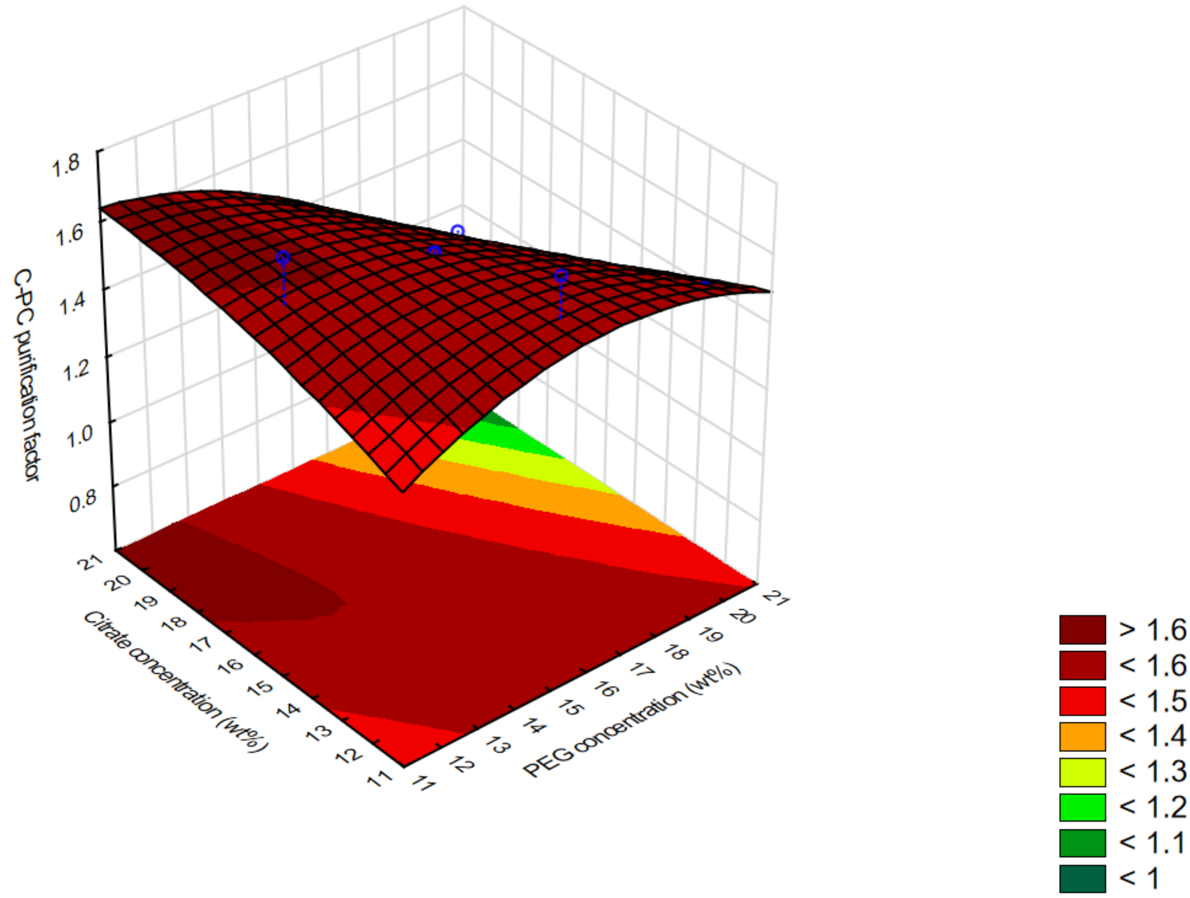

Figure 35. Response curve for C-PC purification factor as a function of PEG and citrate concentrations in a PEG 4000 – citrate ATPS. Blue circles indicate data points from the experiments. Response curves were generated using *Statistica.*

7.3.2.2 Effect of component concentrations on C-PC recovery

The C-PC recovery response curve also had a low MS residual of 0.000829, and in this case the good fit can be seen clearly with the points appearing on the response curve of Figure 36. The PEG – citrate ATPS showed a very high C-PC recovery over this range of component concentrations, with close to 100 % recovery in a wide band stretching across from 21 wt% citrate, 11 wt% PEG (left-most corner) to 11 wt% citrate, 21 wt% PEG (right-most corner). The two regions where recovery was found to decrease were where both components had low concentrations, and less noticeably where both components had high concentrations. A possible mechanism to explain this is that a high salt concentration, citrate in this case, is required to have maximum partitioning of C-PC to the top PEG phase, due to the salting-out effect. This was observed in the studies performed by Wang *et al.* (2012), where higher salt concentrations in the bottom phase lead to better C-PC recoveries. Also noted was that too high concentrations could decrease recovery due to salting out of both top and bottom phases, leading to C-PC precipitation in the interface, which could have caused the decreased recovery in the case where both PEG and citrate concentration were at their highest.

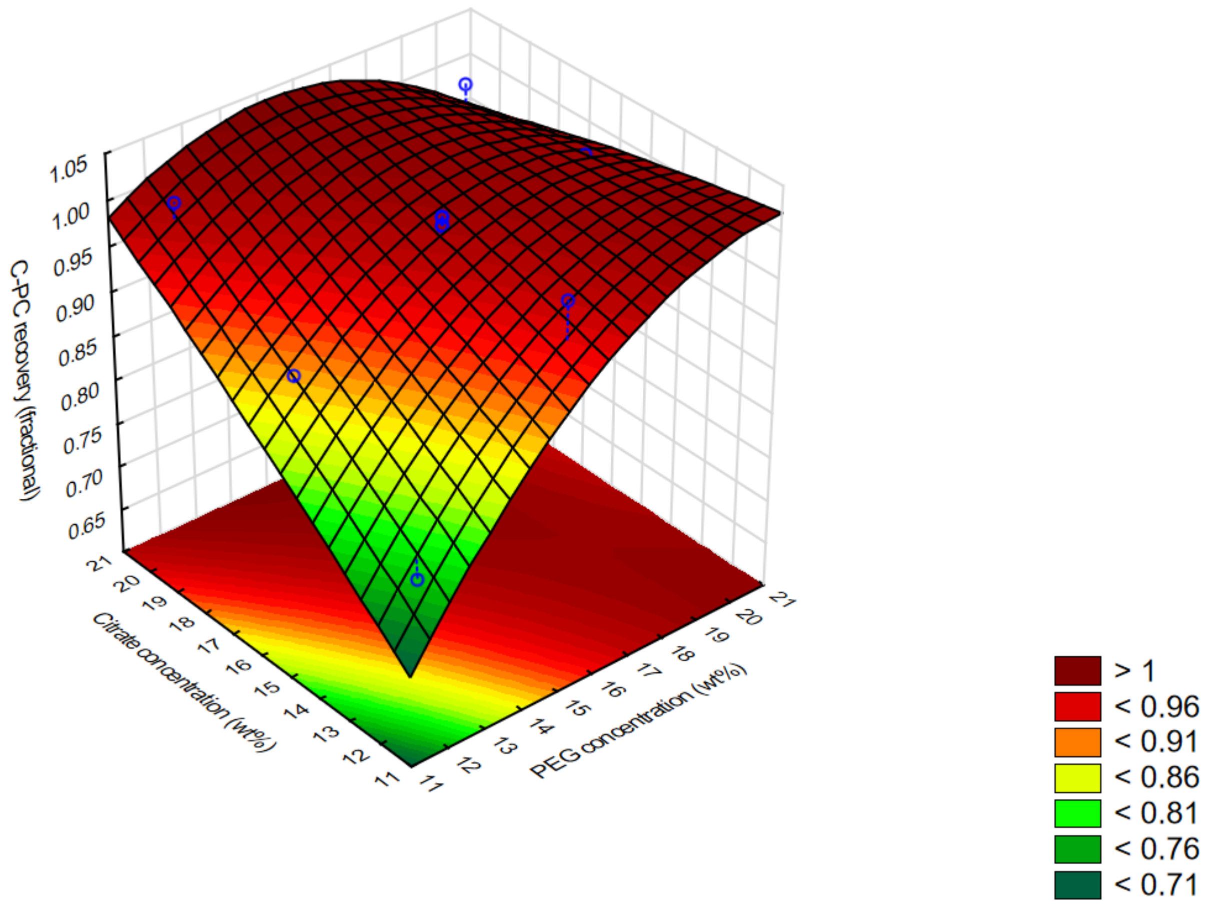

Figure 36. Response curve for C-PC recovery as a function of PEG and citrate concentrations in a PEG 4000 – citrate ATPS. Blue circles indicate data points from the experiments. Response curves were generated using *Statistica.*

7.3.2.3 Effect of component concentrations on C-PC concentration

The C-PC concentration response curve showed a clear relationship with the component concentrations, and the model fit the data well with a very low MS residual of 0.000659 (Figure 37). C-PC concentration increased in a linear plane from the right-most corner of the map, at 11 wt% citrate and 21 wt% PEG, to the left-most corner, at 21 wt% citrate and 11 wt% PEG. This result is likely due to the decreasing volume ratio as citrate concentration increased and PEG concentration decreased, since there would be more of the bottom phase-forming component (i.e. citrate) and less of the top phase-forming component, PEG. This has also been documented by Antelo *et al.* (2010), where a lower volume ratio, due to higher salt (potassium phosphate in this case) and lower polymer concentrations, resulted in higher C-PC concentrations in the PEG phase.

These results favour the use of a low PEG concentration and a higher citrate concentration, which would produce a more concentrated C-PC top phase. More concentrated streams with lower volumes are advantageous in downstream processing, using less energy and having a lower chemical consumption, depending on the subsequent process steps implemented.

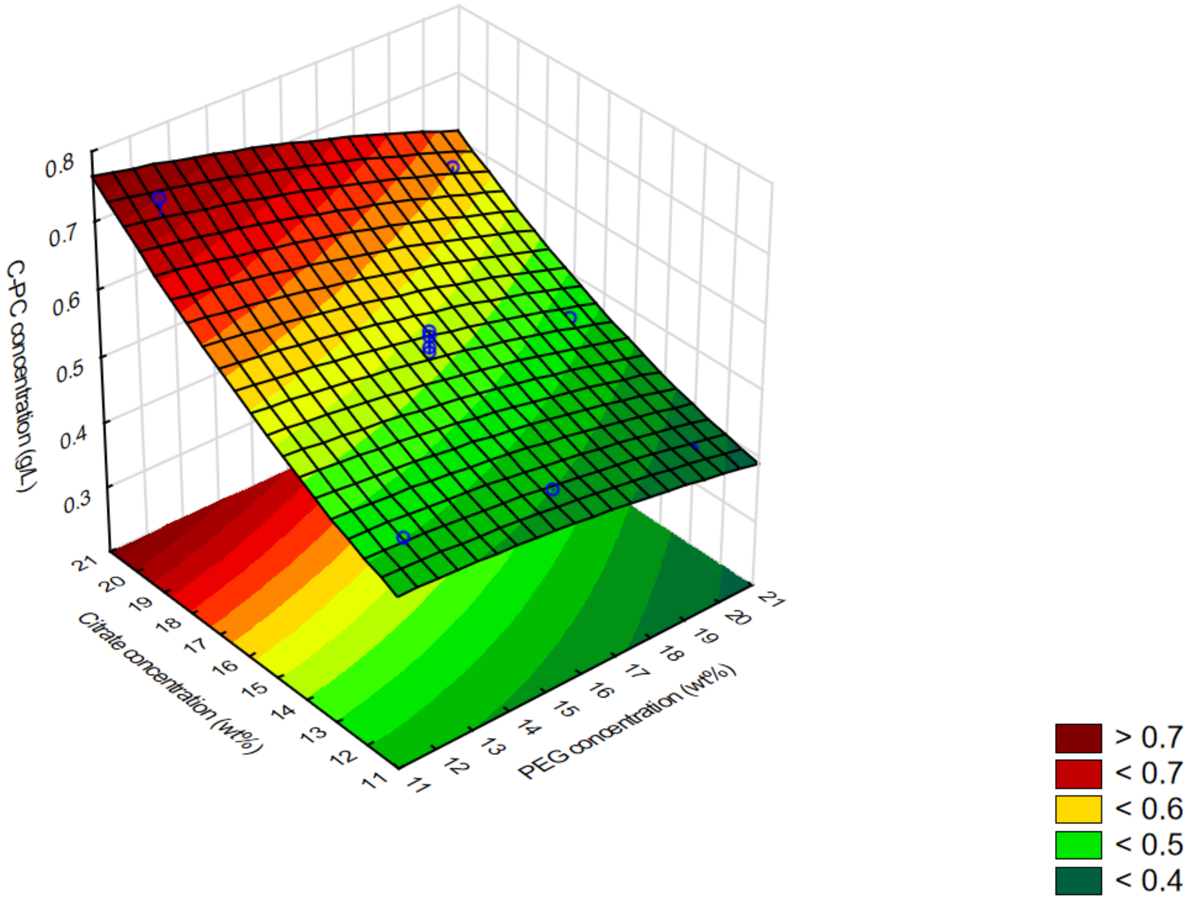

Figure 37. Response curve for C-PC concentration as a function of PEG and citrate concentrations in a PEG 4000 – citrate ATPS. Blue circles indicate data points from the experiments. Response curves were generated using *Statistica.*

7.3.2.4 Influence of tie-line length and volume ratio

Table 14 summarises the relevant results, in terms of C-PC purification, recovery and concentration, from the PEG – citrate ATPS factorial experiment. This was done to make more explicit the possible influence of the volume ratio on C-PC purification in this ATPS, as well as compare this study to the outcomes noted in other studies, where TLL was found to influence C-PC purity. Highlighted in the table are the different tests which had the same PEG concentration, so that within each set of 3, the influence of citrate concentration on TLL and the volume ratio could be shown, and the effect those had on C-PC purification. The TLL and volume ratio were dependent variables in this study, since PEG and citrate concentration needed to be varied in order to alter them, however, they are interesting variables to consider for their secondary influence on the ATPS performance.

At each constant PEG concentration, as the citrate concentration increased the TLL increased and the volume ratio decreased. This was expected based on the phase diagrams for ATPSs, since the higher the salt concentration, the longer the tie-line and the greater the volume expected in the salt phase, resulting in a lower volume ratio. For each highlighted set of 3, excluding the very first result (test 1), the C-PC purification factor was found to decrease as the TLL increased and volume ratio decreased. The explanation given by Rito-Palomares *et al.* (2001) for this was that the free volume in the phases is decreased as the TLL increases, since the phases will have greater differences in density and thus less C-PC and more smaller proteins would partition to the top PEG phase. This does not help prediction, however, since multiple variables are altered to change the TLL, and as the PEG concentration changes, the effect no longer holds. An example is between test 3 and 4; the TLL is lower in test 4, with a higher PEG concentration but lower citrate concentration, while the volume ratio is higher in test 4. The C-PC purification factor, however, is higher in test 4, showing how confounding effects cannot be avoided where multiple variables are changed.

The table also shows clearly the influence of volume ratio on C-PC concentration, where within each set of 3 the concentration increases as the volume ratio decreases. This is to be expected since at higher salt concentrations, the volume of the bottom phase increases, decreasing the volume ratio. With a smaller volume in the top phase the C-PC partitioned there would be more concentrated. This was also clearly shown in Figure 37. The results from the PEG – citrate factorial experiment are taken further to simulate the best predicted concentrations for testing in future studies (Section 7.3.4).

Table 14. Influence of TLL and volume ratio on PEG – citrate ATPS performance

Test	PEG concentration (wt%)	Citrate concentration (wt%)	TLL (%)	Volume ratio (V_R)	C-PC purification factor	C-PC concentration (g/L)	C-PC recovery
1	**12**	**12**	17.9	1.20	1.39	0.483	0.765
2	**12**	**16**	29.7	0.72	1.73	0.540	0.897
3	**12**	**20**	36.4	0.64	1.60	0.738	1.000
4	**16**	**12**	34.0	1.29	1.71	0.448	0.993
5	**16**	**16**	39.5	1.04	1.55	0.539	0.998
6	**16**	**20**	47.2	0.80	1.43	0.632	0.993
7	**20**	**12**	42.4	1.75	1.49	0.405	0.995
8	**20**	**16**	48.5	1.29	1.29	0.487	1.000
9	**20**	**20**	52.4	1.12	1.21	0.606	1.000
5*	**16**	**16**	39.5	1.04	1.54	0.563	0.990
5*	**16**	**16**	39.5	1.04	1.56	0.555	1.000
5*	**16**	**16**	39.5	1.04	1.51	0.531	0.989

* Repeats on central point concentration

7.3.3 PEG – MDX ATPS optimisation

The PEG – MDX ATPS factorial design was done using PEG 4000 and the MDX used in the previous studies. A factorial design allowed the statistical modelling of the effect of PEG and MDX concentrations on the C-PC purification factor, recovery and concentration; this was used to generate response curves using *Statistica.* The PEG and MDX component concentrations were varied at 3 levels, where PEG concentration varied from 12 wt%, to 16 wt% and 20 wt%, based on the phase diagrams produced, and MDX was varied from 20 wt% to 25 wt% and then 30 wt%. The central point (16 wt% PEG and 25 wt% MDX) was repeated a further three times, resulting in 12 experimental runs with 9 unique compositions. A crude C-PC solution was used for this study, despite this being proposed as a second stage to the PEG – citrate ATPS. This was due to the need for highly accurate PEG concentrations by mass, which is not possible when estimating phase compositions from prior ATPS experiments.

7.3.3.1 Effect of component concentrations on C-PC purification factor

There was a distinct trend in the relationship between the component concentrations and the C-PC purification factor (Figure 38). This was evident by the low MS residual value of 0.00124 and the fit of the experimental point to the plane produced by the *Statistica* model. It was found that the C-PC purification factor improved from the back corner of the map, where both PEG and MDX concentrations were high, to the front corner, with low polymer concentrations. The lower end of the MDX concentrations favoured higher purification factors with the dark red bands, indicating purification factors above 1.42, started from about 23 wt% on the MDX concentration axis to about 18 wt% on the PEG concentration axis (at the lower MDX concentration of 18 wt%). The highest C-PC purification factor found on the response curve was above 1.46, higher than that produced in the study from the previous chapter (where a maximum of 1.33 was found). This indicates that further concentration combinations using PEG 10000 could likely have yielded better results in that case. An explanation for the higher purification factors seen are that the lower MDX concentrations lead to a lower volume ratio, which could exclude further contaminating proteins from the bottom phase, increasing the purity of C-PC in the bottom MDX phase.

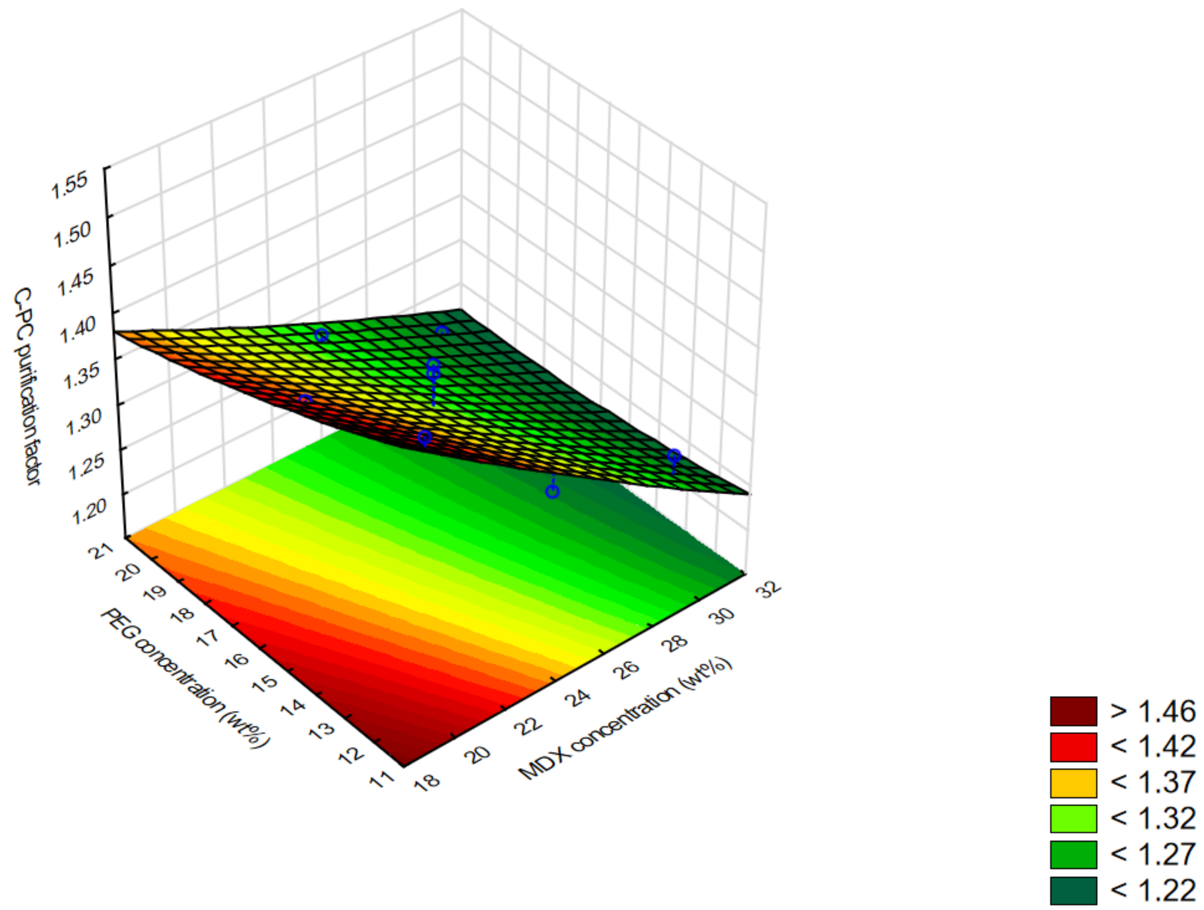

Figure 38. Response curve for C-PC purification factor as a function of PEG and MDX concentrations in a PEG 4000 – MDX ATPS. Blue circles indicate data points from the experiments. Response curves were generated using *Statistica.*

7.3.3.2 Effect of component concentrations on C-PC recovery

The recovery of C-PC within the range of polymer concentrations when modelled presented as a sloped saddle-shape, which fitted the experimental data well at a MS residual of 0.000339 (Figure 39). In this response curve, a lower PEG concentration and intermediate MDX concentration was found to favour C-PC recovery. A high C-PC recovery of above 0.875 was seen in a parabolic band ranging from 12 wt% PEG on the PEG concentration axis, to about 30 wt% MDX on the MDX concentration axis. The highest recoveries were found at the lowest PEG concentration (11 wt%) and at MDX concentrations from 20 to 26 wt%. In this range, a recovery of above 0.9 of the C-PC could be expected in the bottom MDX phase. This showed that the PEG – MDX ATPS required more investigation than the PEG – citrate ATPS when optimising for recovery, since much higher recoveries were observed at a broader range in the PEG – salt system. A possible reason for the higher recoveries at low PEG concentrations was that this leads to a lower overall volume ratio, creating a higher volume in the bottom MDX phase for the partitioning of C-PC. Also contributing to the loss of C-PC could be precipitation at the interface due to high overall polymer concentrations, saturating the two phases and forcing more C-PC to accumulate at the interface.

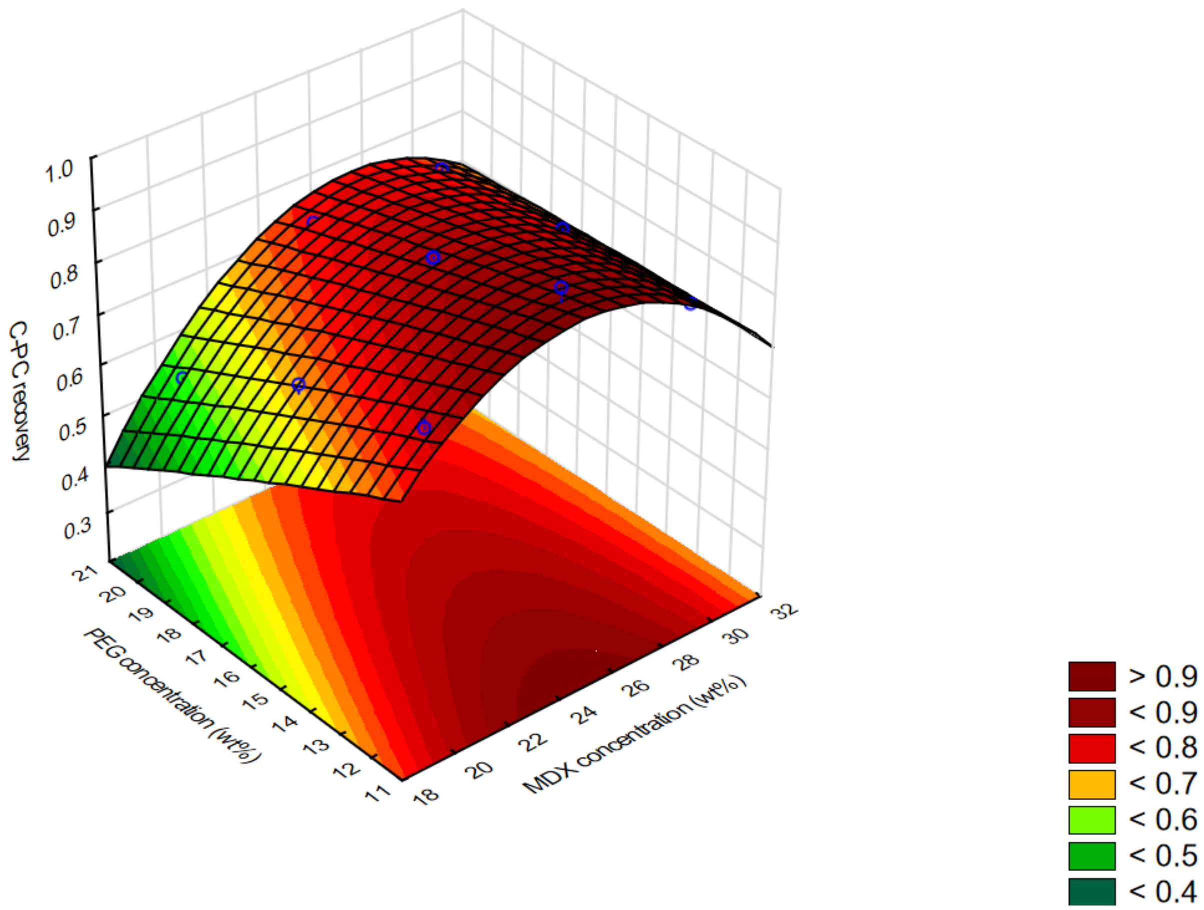

Figure 39. Response curve for C-PC recovery as a function of PEG and MDX concentrations in a PEG 4000 – MDX ATPS. Blue circles indicate data points from the experiments. Response curves were generated using *Statistica.*

7.3.3.3 Effect of component concentrations on C-PC concentration

An asymmetrical saddle shape was seen when C-PC concentration was modelled as a function of the polymer concentrations used in the ATPS, which also showed a good fit at a MS residual of 0.00248 (Figure 40). Here it was found that lower polymer concentrations favoured a high C-PC concentration in the MDX phase. High MDX concentrations, in particular, were found to yield low C-PC concentrations, as seen below along the top right axis at an MDX concentration of 32 wt%. High C-PC concentrations were seen in an arced band ranging from 15 wt% PEG on that axis, to 24 wt% MDX on the MDX concentration axis. Here the concentration was found to be in the range of 1.4 g/L, which increased as the lowest concentrations (11 wt% PEG and 18 wt% MDX) were approached. The higher C-PC concentrations would be due to the greater volume ratios at low MDX concentrations, where there is a smaller bottom phase volume containing the C-PC. This would also be somewhat related to the recovery of C-PC, which was found to be higher in an overlapping region near the bottom corner of the map. Loss of C-PC recovery due to precipitation caused by higher overall polymer concentration could also have affected the concentration of C-PC recovered in the bottom MDX phase.

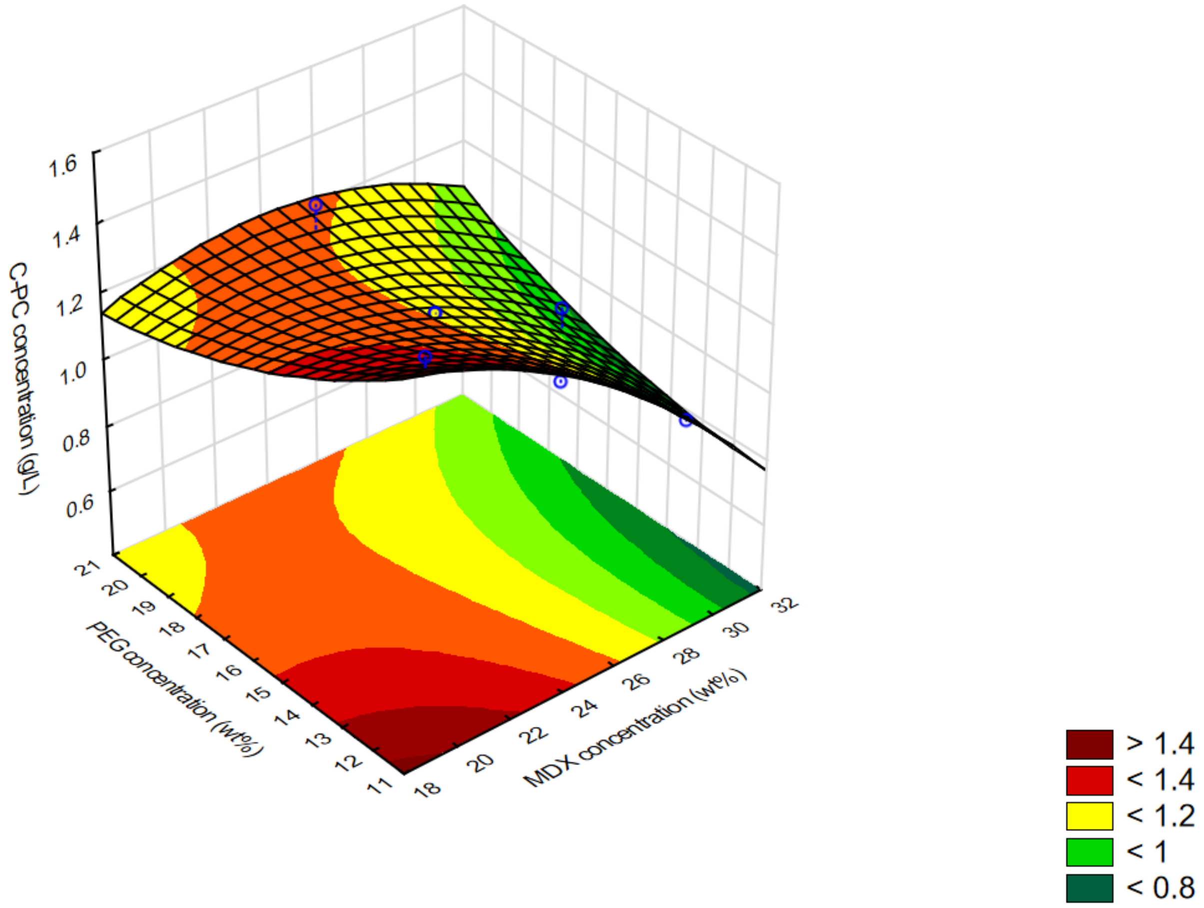

Figure 40. Response curve for C-PC concentration as a function of PEG and MDX concentrations in a PEG 4000 – MDX ATPS. Blue circles indicate data points from the experiments. Response curves were generated using *Statistica*.

7.3.3.4 Influence of tie-line length and volume ratio

To compare results between the different modes of ATPS and have a greater understanding of the PEG – MDX system, the influence of TLL and volume ratio on the ATPS performance was also considered (Table 15). Sets of 3 were again highlighted to show the changes in TLL and volume ratio when MDX concentrations were varied, at a constant PEG concentration. Again, it should be noted that TLL and volume ratio were dependent variables, which vary as the polymer concentrations were varied.

It was found that as TLL increased within each set of 3, the C-PC purification factor decreased. This was also found when looking at the PEG – citrate ATPS results. This seemed to indicate that again, the further apart the compositions of the top and bottom phases, the less purification of C-PC took place into the bottom MDX phase.

The volume ratio decreased as MDX concentration increased within each constant PEG concentration. This was also associated with a decrease in C-PC purification, which was the same as that seen in the PEG – citrate ATPS. The reason for this was unclear, however, since the C-PC is partitioned to the bottom phase in the PEG – MDX system. With a higher volume ratio it is possible that a higher volume in the top phase allows a greater amount of contaminating proteins to partition to the top phase, improving the purity in the bottom MDX phase. The decreasing C-PC concentration within each set of 3 could also be explained by the decreasing volume ratio, since a lower volume ratio means a greater volume in the bottom phase for MDX to partition to, which would decrease the expected concentration.

Recovery of C-PC again showed no clear association with changes in TLL or volume ratio, since values vary within the sets of 3; these were likely a function of the saddle-shape seen in Figure 39.

Table 15. Influence of TLL and volume ratio on PEG – MDX ATPS performance

Test	PEG concentration (wt%)	MDX concentration (wt%)	TLL+ (%)	Volume ratio (V_R)	C-PC purification factor	C-PC concentration (g/L)	C-PC recovery
1	12	20	35.0	1.89	1.45	1.47	0.789
2	12	25	43.4	1.00	1.32	1.22	0.934
3	12	30	52.9	0.77	1.29	0.93	0.791
4	16	20	38.7	1.70	1.39	1.26	0.712
5	16	25	49.1	1.16	1.27	1.19	0.841
6	16	30	57.7	0.96	1.22	1.03	0.787
7	20	20	45.2	2.18	1.35	1.18	0.567
8	20	25	55.5	1.48	1.31	1.28	0.761
9	20	30	64.7	1.04	1.24	1.03	0.762
5*	16	20	49.1	1.12	1.30	1.19	0.840
5*	16	20	49.1	1.12	1.35	1.17	0.826
5*	16	20	49.1	1.12	1.36	1.17	0.826

* Repeats on central point concentration

+ Estimated from PEG 4000 – MDX phase diagrams produced by Machado *et al.* (2012).

7.3.4 Model predictions and discussion

Model predictions for the ATPS performances in terms of C-PC purification, recovery and concentration, were used to simulate the best concentrations for the ATPSs and provide accurate inputs into further attempts to simulate the improved process as a whole. *Statistica* was used for the model predictions based on data from the factorial experiments. These predictions were made for the C-PC purification factor, recovery and concentration for the PEG – citrate ATPS and the PEG – MDX ATPS. These included 95 % confidence intervals based on the repeated experiments, to account for uncertainty in the measurements. The best combination was chosen based mainly on performance in C-PC purification, since this is the main way that processes can add value to the product, which increases in price dramatically with increases in purity. It is also important to achieve cosmetic grade C-PC in the context of this project. The next parameter in terms of importance was C-PC recovery, since that is also closely linked to the value of the final product based on a set input, and then C-PC concentration, which is important for reducing the downstream processing costs, but does not affect the product value. A balance was struck while still attempting to achieve as close to the local optimum as possible for each parameter.

The predicted best concentrations for the PEG 4000 – citrate ATPS was 11 wt% PEG and 20 wt% citrate, and the results are presented in Table 16. This gave an estimated C-PC purification factor of 1.63 ± 0.28, higher than that achieved in all but one of the tests (at 1.73 using 12 wt% PEG and 16 wt% citrate). The C-PC concentration was predicted to be 0.723 ± 0.072 g/L, again higher than all but one of the measured values, which was found at 12 wt% PEG and 20 wt% citrate. The C-PC recovery was 0.956 ± 0.080 which was high despite many of the measured values being higher.

The results were comparable to the C-PC purification found in tests by Wang *et al.* (2012), who found a purification factor of 1.54 using 14 wt% PEG 4000 and 21 wt% citrate, at a recovery of 91 %. This purification factor was lower than some seen in literature on PEG – salt ATPS, however. In PEG 4000 – potassium phosphate ATPS, purification factors of above 2 have been recorded (Patil and Raghavarao, 2007; Sørensen *et al.*, 2013; Antelo *et al.*, 2015). These results point to the superiority of phosphate systems, as previously proved in these studies, yet could also be influenced by other factors, such as differences in conditions used, different *Spirulina* supply and the range of component concentrations used in the experiments. It is possible that the C-PC purification factor could be further improved by testing a greater range of component concentrations.

Table 16. Model-predicted values for C-PC purification by PEG – citrate ATPS, using 11 wt% PEG and 20 wt% citrate as inputs.

PEG 4000 – citrate ATPS	C-PC purification factor	C-PC concentration (g/L)	C-PC Recovery
Predicted value	1.63	0.723	0.956
(-) 95 % confidence	1.36	0.652	0.876
(+) 95 % confidence	1.91	0.795	1.036

For the PEG 4000 – MDX ATPS, the chosen concentrations to simulate was 11 wt% PEG and 22 wt% MDX, with the results presented in Table 17.

This gave an estimated C-PC purification factor of 1.43 ± 0.09, higher than that achieved in all but one of the tests (at 1.45 using 12 wt% PEG and 20 wt% MDX). The C-PC concentration was predicted to be 1.46 ± 0.13 g/L, again higher than all but one of the measured values, which was found at 12 wt% PEG and 20 wt% MDX. The C-PC recovery was 0.868 ± 0.047 which was higher than all the measured values except the recovery found at 12 wt% PEG and 25 wt% MDX.

The C-PC purification found in the factorial experiments were higher than those seen in the previous chapter (6.2.3.1), where the highest purification factor was found to be 1.33 ± 0.01, using 9 wt% PEG 10000 and 25 wt% MDX. This indicates that further studies would likely have produced higher purification in the PEG 10000 – MDX ATPS. The C-PC recovery was lower than those found in the previous experiments, where a recovery of 99 ± 1 % was seen in the PEG 10000 – MDX experiment mentioned above. The concentration achieved in this ATPS was almost double that found in the PEG – citrate ATPS. This was due to the smaller volume into which the C-PC is concentrated in the PEG – MDX ATPS, under these conditions where a high volume ratio was found to perform well. This could provide a strong advantage when it comes to downstream processing.

The purification factor was still lower than the purification produced in the PEG – citrate system, and lower than those found in literature for other PEG – salt systems. This was to be expected, however, as studies done by Patil *et al.* (2006) and Wang *et al.* (2012) considered polymer – polymer ATPS and found that these were up to 1.5 fold less effective in purifying C-PC than PEG – salt systems. This would depend on the conditions used, and starting material, however.

Table 17. Model-predicted values for C-PC purification by PEG – MDX ATPS, using 11 wt% PEG and 22 wt% MDX as inputs.

PEG 4000 – citrate ATPS	C-PC purification factor	C-PC concentration (g/L)	C-PC Recovery
Predicted value	1.43	1.46	0.868
(-) 95 % confidence	1.34	1.33	0.821
(+) 95 % confidence	1.52	1.58	0.915

The overall purification performed in a two-stage process using these concentrations would thus be 2.33 ± 0.41. This would lead to a final C-PC purity number of 1.63 ± 0.29 using the *Spirulina* used in this study, likely within the range of cosmetic grade purity using only these ATPS purification steps.

7.4 Conclusions

This chapter investigated the use of a two-stage ATPS for C-PC purification. This involved first producing phase diagrams for PEG – citrate ATPS of different PEG molecular weights, since this system would be used in the first PEG – citrate ATPS. This was followed by a screening experiment, where three PEG molecular weights were tested using the two-stage procedure, a PEG – citrate ATPS followed by a PEG – MDX ATPS using the PEG top phase from the first ATPS. The best-performing PEG molecular weight was used in two factorial experiments, testing a range of component concentrations for each of the ATPS to explore their effects on the purification, concentration and recovery of C-PC.

The phase diagrams produced showed similar compositions for the top and bottom phases for the three PEG molecular weights tested, 4000, 6000 and 10000 Da. The main difference was the slightly greater biphasic areas found with higher molecular weights, which manifested as the top and bottom being purer in the major component of that phase. The PEG 10000 – citrate equilibrium curve showed that the bottom phase would be almost pure citrate solution (~0 wt% PEG) beyond around 19 wt% citrate, while the PEG 4000 – citrate ATPS had a pure PEG-free bottom phase after around 25 wt% citrate. The equilibrium curves were modelled for each diagram and closely matched the experimental points with very low SSE-values. The phase diagrams produced also resembled those found in literature to a large extent, with the PEG 4000 – citrate phase diagrams most closely matching one produced by Glyk *et al.* (2014), with the same conditions (PEG 4000, pH 6).

The screening experiments found that PEG 4000 performed the best of the three molecular weights tested in both the higher and lower concentration combinations for the two-stage APTS. This was mostly due to the improved performance in the first stage, the PEG – citrate ATPS, where far greater C-PC purification and recoveries were found using the lower molecular weight PEG. The higher concentration screening had a better overall performance, resulting in a C-PC purification factor of 2.11 ± 0.20 for PEG 4000 over the two stages. By comparison, PEG 6000 had a lower purification factor of 1.65 ± 0.16. The overall C-PC recovery for PEG 4000 was 0.69 ± 0.22, followed by 0.52 ± 0.13 for PEG 6000. Thus

PEG 4000 performed best in this integrated system on the basis of recovery and purification. This system produced C-PC with a final purity number of 1.46 ± 0.08, within the range of cosmetic grade, prior to optimisation being done.

The factorial analysis using the PEG 4000 – citrate ATPS performed to investigate further improvements found that C-PC purification was favoured at lower PEG and higher citrate concentrations, within the range of concentrations tested. The recovery of C-PC was high in the PEG – citrate ATPS, only dropping below 90 % as low concentrations were approached for both components (~19 wt% on the citrate concentration axis and ~15 wt% on the PEG concentration axis. The C-PC concentration in the PEG phase was found to increase as citrate concentrations increased and PEG concentrations decreased, which was a consequence of the decreasing volume ratio, producing a more concentrated upper phase. The effect of TLL and volume ratio were also considered within each set of 3 where PEG concentration was constant, although these were dependent on the component concentrations. TLL increased and volume ratio decreased as the citrate concentration was increased, and this increase was associated with a decreased C-PC purification factor and an increased C-PC concentration. Recovery did not seem to be influenced in a clear way by changes in TLL and volume ratio.

A predicted purification factor of 1.63 ± 0.28, C-PC recovery of 0.956 ± 0.080 and a concentration of 0.723 ± 0.072 g/L was found for the PEG 4000 – citrate ATPS, based on the *Statistica* model. The concentrations were chosen to be close to local maxima based on the response curves for these factors, with 11 wt% PEG and 20 wt% citrate being chosen, favouring purification and recovery over concentration. The purification was comparable to that found by Wang *et al.* (2012), who found a purification factor of 1.54 in a PEG 4000 – citrate system. This was lower, however, than some PEG – phosphate salt systems where purification factors above 2 have been observed at recoveries above 90 % (Patil and Raghavarao, 2007; Sørensen *et al.*, 2013; Antelo *et al.*, 2015).

The PEG 4000 – MDX ATPS was also improved using the factorial analysis, which found greater C-PC purities as lower MDX were approached and to a lesser degree, lower PEG concentrations. This was postulated to be due to higher volume ratios and lower TLL at these concentrations, which allow a greater volume in the PEG phase for contaminating proteins to partition, purifying the C-PC in the MDX phase. At lower TLL the polymer concentrations in each phase after separation is lower, changing the way proteins and C-PC partition to these phases. Recovery was found to be favoured at low PEG concentration and moderate (within the range tested) MDX concentrations of around 22 to 26 wt%, where recoveries of above 90 % could be found. The C-PC concentration was strongly favoured at low concentrations of both polymers, which would be due, again, to higher volume ratios, concentrating the C-PC into a smaller MDX volume.

The modelled prediction for the best concentration combination for the PEG 4000 – MDX ATPS was 11 wt% PEG and 22 wt% MDX. This combination predicted a C-PC purification factor of 1.43 ± 0.09, with a recovery of 0.868 ± 0.047 and a C-PC concentration of 1.46 ± 0.13 g/L. The purification was better than that found in the previous experiments on the PEG 10000 – MDX ATPS, while the recovery was slightly lower. This showed that more investigation would likely have yielded better results in that system.

Overall, the optimised C-PC purification performed by both stages together was predicted to be 2.33 ± 0.41. This has the potential to produce cosmetic grade purity (using only these ATPS purification steps) and is comparable to well-performing PEG – salt ATPSs found in literature, with the benefit of having the C-PC in a MDX phase and the advantages of that. These predicted results would ideally have been tested and confirmed in the laboratory, however, this was not possible due to the Coronavirus pandemic lockdown.

The results above were used going forward in proposing alternate approaches and process flowsheet for extracting and purifying C-PC from *Spirulina*.

8 Process route options

8.1 Introduction

Based on the literature review and analyses of the results from this study, some alternate process route options are put forward for extracting C-PC from *Spirulina*. These all include the PEG – MDX ATPS as the main processing step, due to the unique selling-points of ATPS systems and MDX as a polymer (see section 1.2.1), while proposing possible alterations to the other unit procedures from the original patented process. The section focuses on some of the key questions relating to which process configuration can most efficiently produce cosmetic grade C-PC from *Spirulina*, namely:

- Would a 2-stage ATPS using PEG – salt ATPS improve the overall process?
- Can ammonium sulfate use be reduced, or the precipitation step be replaced by UF or an alternative process?
- Can UF or other means be used to recycle PEG and maltodextrin?
- What process route configuration allows for the most resource-efficient C-PC production using ATPS?

In this section, process flowsheets are presented with simulation carried out using SuperPro Designer, a process simulation software. Key results from the simulations (with overall mass balances for the simulated processes in the online open database) are summarised. Assumptions and decisions made along the way were based on a synthesis of the literature and the results obtained from experimental work; the data sources are summarised in Appendix B: Table 19. These include decisions on C-PC purification factors, C-PC recoveries, component splits in different process units used in the flow sheets and concentrations of different components used.

As a starting point, the original process was simulated, using the work done previously on the project as well as results from this study. As the 2nd approach, the process flow sheet was modified for the inclusion of a two-stage ATPS, studied in Chapter 7. This was due to the poorer C-PC purification seen when using only a PEG – MDX ATPS, where most purification was done in successive ammonium sulphate precipitation steps. Consequently, the number of precipitation steps could also be reduced, saving on ammonium sulfate usage and processing time. In Approach 3, the citrate phase of the PEG – citrate ATPS was purified using UF, to remove the contaminating proteins and recycle the citrate salts. UF was also used to purify the C-PC from the MDX phase of the second ATPS stage in this 3rd variation. The combination of microfiltration, for sterilising the product of bacteria and spores, and UF replaced the 3 precipitation stages of the original process. This still allowed high purity C-PC to be produced, and could potentially increase C-PC yield while reducing ammonium sulfate usage.

The two-stage process added complexity to the overall process, which lead to a fourth proposed route. This involved going back to using a single PEG – MDX ATPS, and having a pre-treatment step before removing the cell debris. The pre-treatment included adding activated carbon and chitosan, which adsorb organic compounds, and has been found to be extremely effective in literature studies (see Section 2.2.2). This would increase the amount of biomass removed during centrifugation as well as increase the purity of the C-PC crude extract fed to the ATPS by adsorbing contaminating proteins. This pre-treatment step would again reduce the need for purification by precipitation, so 2 precipitation stages were included in this proposed process.

The fifth and final process iteration built on the pre-treatment process, involved replacing the second precipitation stage with microfiltration. This was considered as the preceding simulation findings suggested that the C-PC purity was high enough after the initial precipitation stage. Filter sterilisation could then be used effectively to remove bacterial contamination to within allowable limits, while saving on ammonium sulfate use and reducing C-PC losses associated with precipitation.

These were the five options that were chosen for presentation. Multiple aspects of each could be interchanged, however, depending on the needs and purpose of the process in question. UF was not considered in the pre-treatment processes since these were attempts to reduce the complexity of the process and have not been seen used with PEG – MDX ATPS in literature. Costing and economic analyses for each process route were not done, as these were outside of the scope of this part of the overall project and are dependent on further clarification of the specific process requirements and goals. This has great impact on which process is most viable, however, and will be briefly discussed in qualitative terms.

Process simulation flowsheets

8.1.1 Original process

The original process was simulated as per the method given in Section 5.3.2, and is presented in Figure 41**.** The exception to this was the polymer concentrations used in the PEG – MDX ATPS. The original process used 5 wt% PEG 10000 and 30 wt% MDX. This was changed to 11 wt% PEG and 22 wt% MDX, based on results from Section 7.3.3. Although PEG 4000 was used to determine this concentration, PEG 10000 would likely produce even better results, since it performed best in the single polymer-polymer ATPS.

Biomass removal in the centrifugation stage was assumed at 96 % going forward (Uduman *et al.*, 2010). Proteins and C-PC recovery were assumed based on average C-PC data from the centrifuge stages found in Chapter 6. For the PEG – MDX ATPS, the purification was based on the previous chapter (7), with total protein recovery in the MDX phase being inversely proportional to the amount of C-PC purification done in the phase. This was assumed due to the ratioed-relationship in purity number between C-PC and total protein absorbances.

The precipitation stages had purity numbers that were based on the purification achieved in the previous work in developing the process. Recoveries were assumed based on the ammonium sulfate saturation and studies performed on C-PC fractionation (Song *et al.*, 2013). Freeze drying was performed as the drying step, with negligible losses due to the nature of the process. Appendix B: Table 19 provides detailed process inputs and appendix

A.8 gives the stream tables for the simulation. Appendix A.9 gives the simulation file for this scenario.

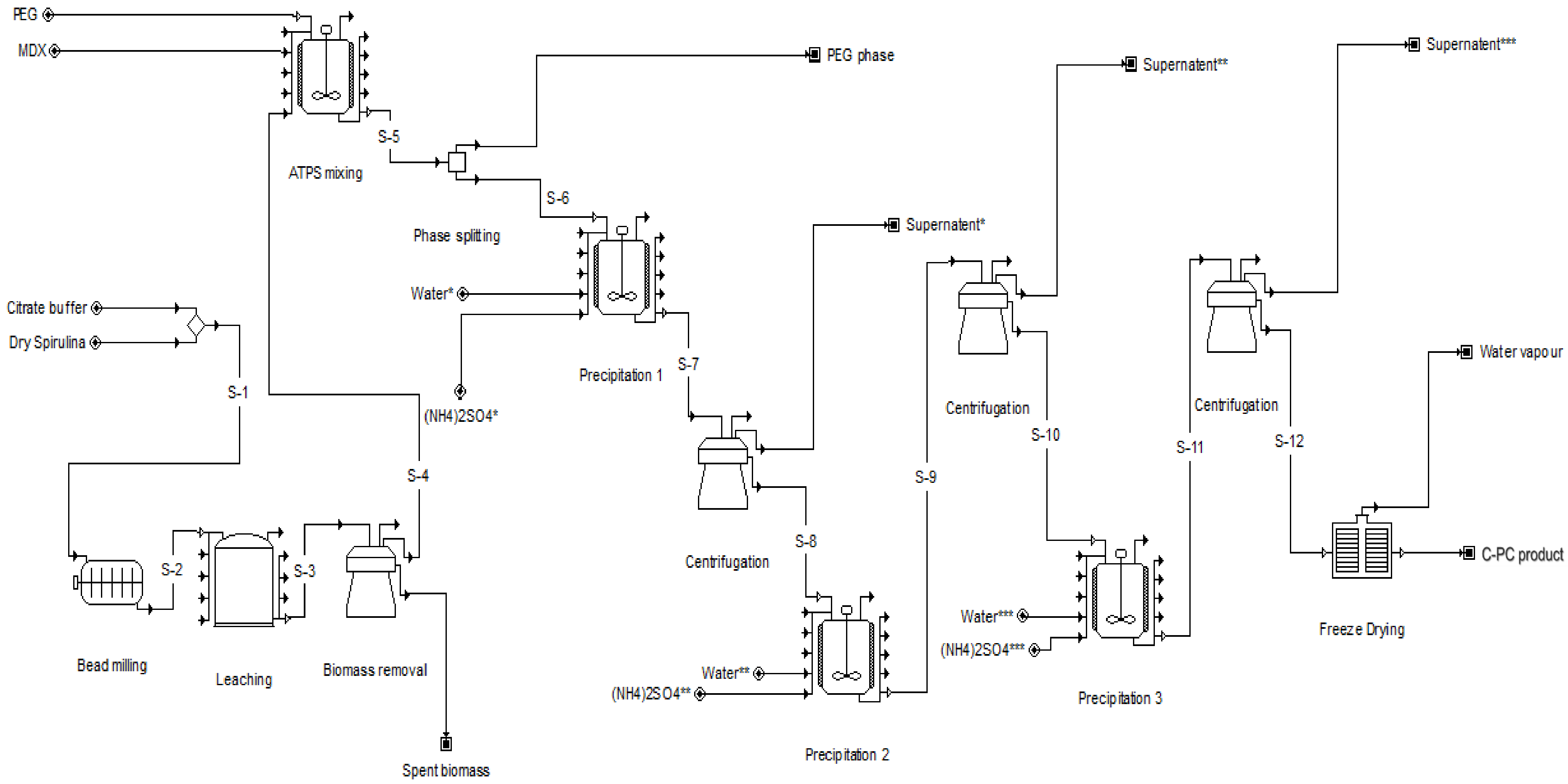

Figure 41. Original C-PC process flowsheet compiled using SuperPro Designer

CeBER

8.1.2 Two-stage ATPS process

The two-stage ATPS process added a PEG – citrate ATPS before the PEG – MDX ATPS in the original process (Figure 42). This leads to greater purification, as well as fewer required ammonium sulfate precipitation stages. The added ATPS stage is likely to reduce overall bacterial counts, due to the tendency of biomass to migrate to the interface of the phases; another reason fewer precipitation stages would be required (Antelo *et al.*, 2010).

PEG 4000 would be used in this two-stage ATPS process, based on the results in Section 7.3.1. The component concentrations used are as modelled in Section 7.3.4, with 11 wt% PEG and 20 wt% in the first ATPS and 11 wt% PEG and 22 wt% MDX in the second ATPS. The C-PC purification and recovery are also taken from work done in that section.

The process proposed here uses a greater amount of citrate salts, while reducing the usage of ammonium sulfate (due to fewer precipitation stages). This is an advantage with respect to the environmental impact of the process, since citrate salts are readily biodegradable and do not have the same potentially detrimental impact on water quality as ammonium sulfate.

This process could also produce C-PC at a faster rate than the original patented process, since the precipitation stages can take particularly long to equilibrate before carefully removing the supernatants. This would need to be confirmed at large scale to compare to the time taken for the added ATPS stage, however.

The C-PC was finally spray dried, as this is a much more scalable option, has a higher throughput and is becoming the standard for C-PC drying (2.5.2). MDX is added before the spray drying, to act as a heat protectant, and protect the C-PC from oxidation once it is in powdered form. Appendix B: Table 19 gives more detailed process inputs and appendix A.10 gives the stream tables for the simulation. Appendix A.11 gives the simulation file for this scenario.

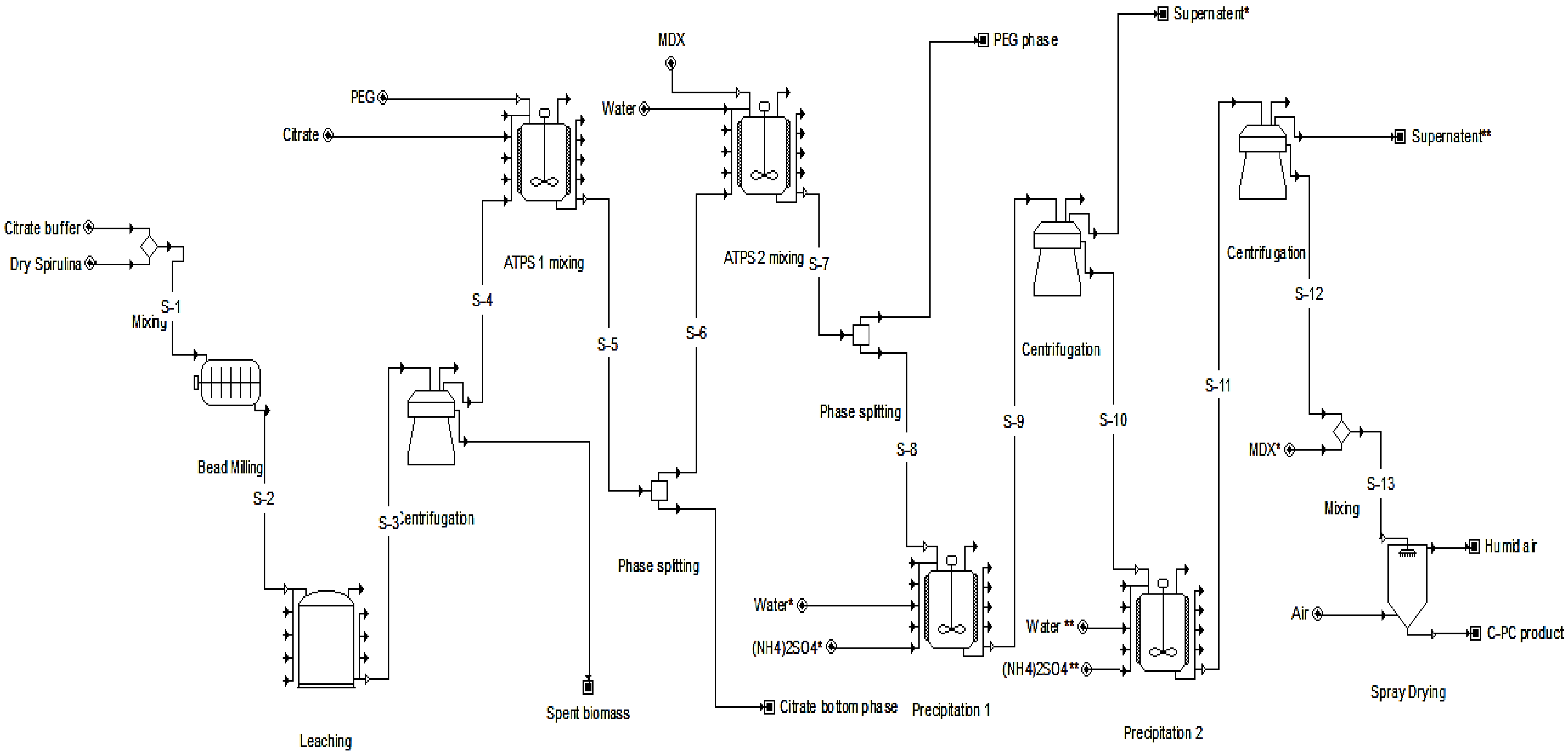

Figure 42. Two-stage ATPS process flowsheet for C-PC extraction compiled using SuperPro Designer

CeBER

8.1.3 Two-stage ATPS process with recycle and ultrafiltration

This option again considered a process using two ATPS stages, one being a PEG – citrate ATPS and the second one a PEG – MDX ATPS (Figure 43). The specifications were based on the experiments and model predictions in the previous chapter (7). The proposed process would use PEG 4000, the PEG molecular weight that performed best in this configuration.

A recycle option was included in this process option, where the citrate bottom phase is recycled by using UF to remove contaminating proteins. Since the citrate phase after PEG – citrate ATPS is highly pure with a negligible PEG concentration, UF could be used without the issues that come up when polymers are involved (see 3.2.3).

It was found that for the top phase of the second (PEG – MDX) ATPS, recycling is not a realistic option. The top phase contained moderate concentrations of both PEG and MDX, which could not be sent back to the first ATPS, since a PEG – citrate ATPS is untested with the addition of MDX. This stream could also not be cleaned by UF without massive dilution to reduce viscosity, which would make the polymer solutions unusable in the process.

As an alternative to the multiple precipitation steps, a microfiltration step was included for the filter sterilisation of the C-PC containing MDX phase after the ATPS stages. This could remove the majority of, or essentially all, contaminating microbes and microbial spores.

To remove the MDX from the C-PC product, UF is also an option, instead of the precipitation train. This would require considerable dilution due to the high polymer concentration, however, and has not been done practically (while C-PC has been purified from a PEG phase by UF, see 2.4.2). Otherwise, precipitation could be retained here as a means of removing the majority of the MDX from the C-PC product. Both have a positive influence on the purification of C-PC.

Again, the C-PC was spray dried to produce the final product. Some residual MDX would be present in the C-PC product, which acts as a thermo-protectant. See appendix A.12 for the process stream tables and Appendix B: Table 19 for simulation inputs. See appendix A.13 for the simulation file for this scenario.

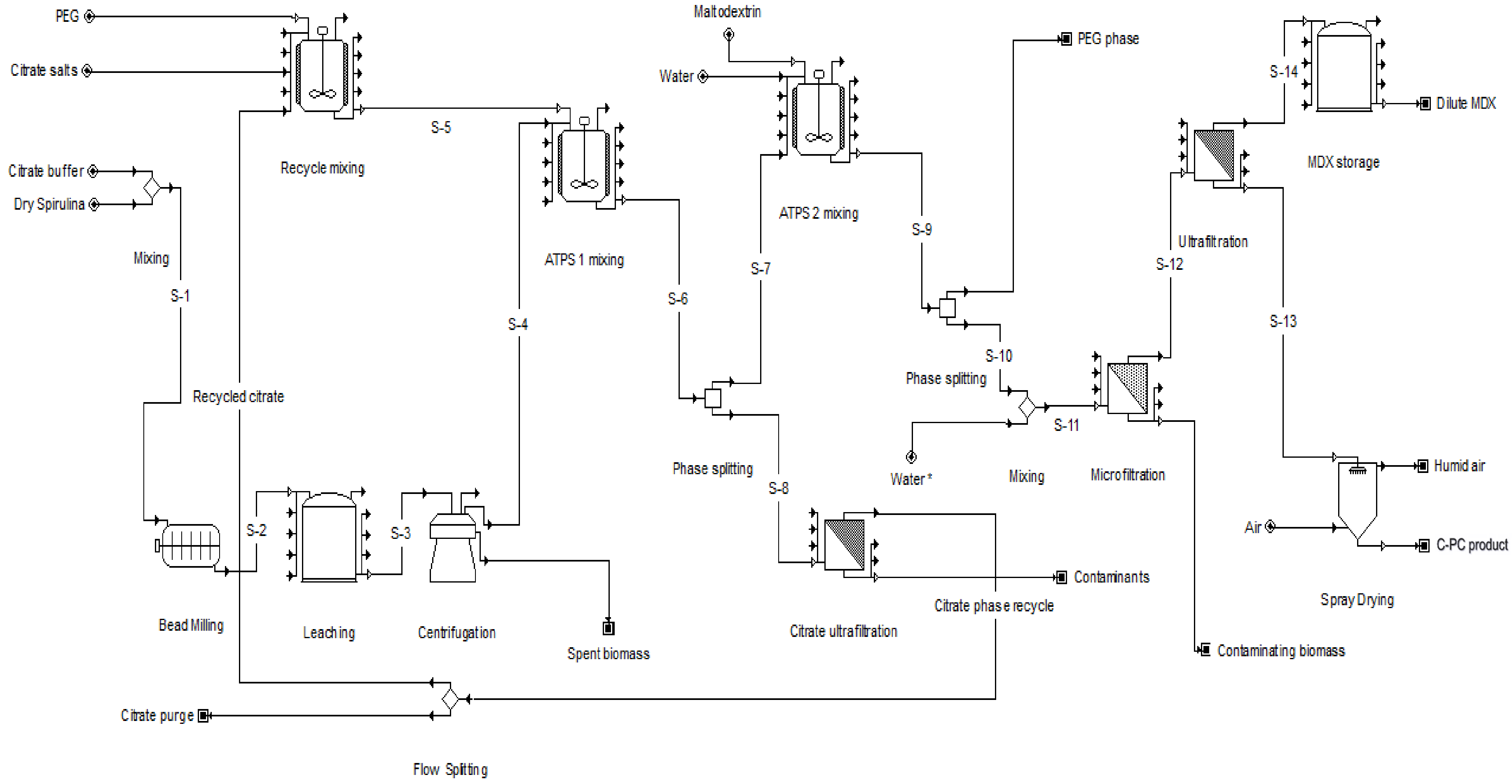

Figure 43. Modified C-PC process with two-stage ATPS compiled using SuperPro Designer

8.1.4 ATPS process with pre-treatment

Having considered using two ATPS stages for purifying the C-PC, a process using a single stage but with additional pre-treatment was proposed (Figure 44). This was to avoid the increased complexity of using two ATPS stages, and the increased number of process steps and units required. This proposed process includes a pre-treatment step at the leaching and biomass removal stage, to improve C-PC purity and to make biomass removal more efficient.

The pre-treatment step involves employing activated carbon and chitosan as adsorption agents to help remove biomass and contaminating proteins. These would be added during the last minutes of the leaching step and before centrifugation for biomass removal. A C-PC purification factor of 2 – 7 can be expected from this treatment, without the need for an extra process unit (see 2.2.2). This would also help remove more biomass, reducing equipment fouling and contamination in downstream units.

Having the pre-treatment, it would be necessary to include only one ATPS step(PEG – MDX) which improves the ease of recovering the C-PC in this process. PEG 10000 would likely be used, having performed the best when only considering the single PEG – MDX ATPS (see 6.2.3.2). This combination would produce C-PC of high purity, well above cosmetic grade, while not substantially increasing the complexity of the overall process.

The process would likely require only two precipitation stages, in order to remove bacterial contamination from the final product. This would save on processing time as well as ammonium sulfate usage. These precipitation stages could also be more geared toward C-PC recovery, rather than purification, due to the purification performed in the pre-treatment step.

Spray drying is again the proposed drying step. See Appendix B: Table 19 for simulation inputs and A.14 for the process stream tables. Appendix A.15 gives the simulation file for this scenario.

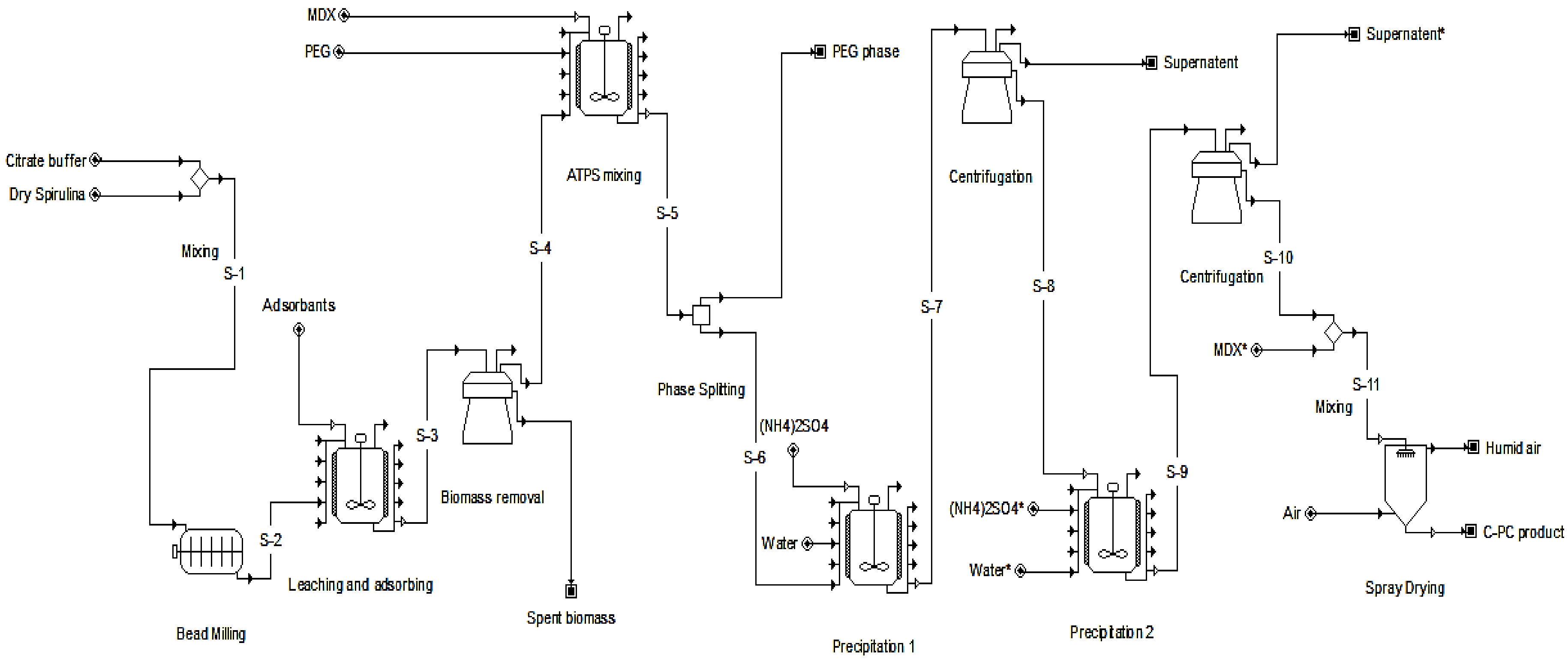

Figure 44. Pre-treatment C-PC ATPS process flowsheet compiled using SuperPro Designer

8.1.5 ATPS process with pre-treatment and filter sterilisation

This final option was presented as perhaps the most realistic option, based on the studies performed and literature review, presented in Figure 45. This involved using a pre-treatment step, employing activated carbon and chitosan as adsorption agents to help remove biomass and contaminating proteins. These would be added during the last minutes of the leaching step and before centrifugation for biomass removal. A C-PC purification factor of 2 – 7 can be expected from this treatment, without the need for an extra process unit (see 2.2.2). This would also help remove more biomass, reducing equipment fouling and contamination in downstream units.

Having the pre-treatment, it would be necessary to include only one ATPS step, which would be the PEG – MDX for the ease of recovering the C-PC in this process. PEG 10000 would likely be used, having performed the best when only considering the single PEG – MDX ATPS. This combination would produce C-PC of high purity, well above cosmetic grade, while not substantially increasing the complexity of the overall process. A single precipitation step was used to recover the C-PC, since it is tested and can achieve high recovery and remove the majority of the MDX from the C-PC product.

To remove the contaminating biomass before product drying, a microfiltration unit was again used, which could easily reduce bacterial contamination and spores without the need for more precipitation steps. The product would then be mixed with a small amount of MDX, added as a heat- and oxidation-protectant, before being spray-dried to achieve a powdered C-PC product of high purity. See appendix A.16 for the process stream tables and Appendix B: Table 19 for more detailed simulation inputs. See appendix A.17 for the simulation file for this scenario.

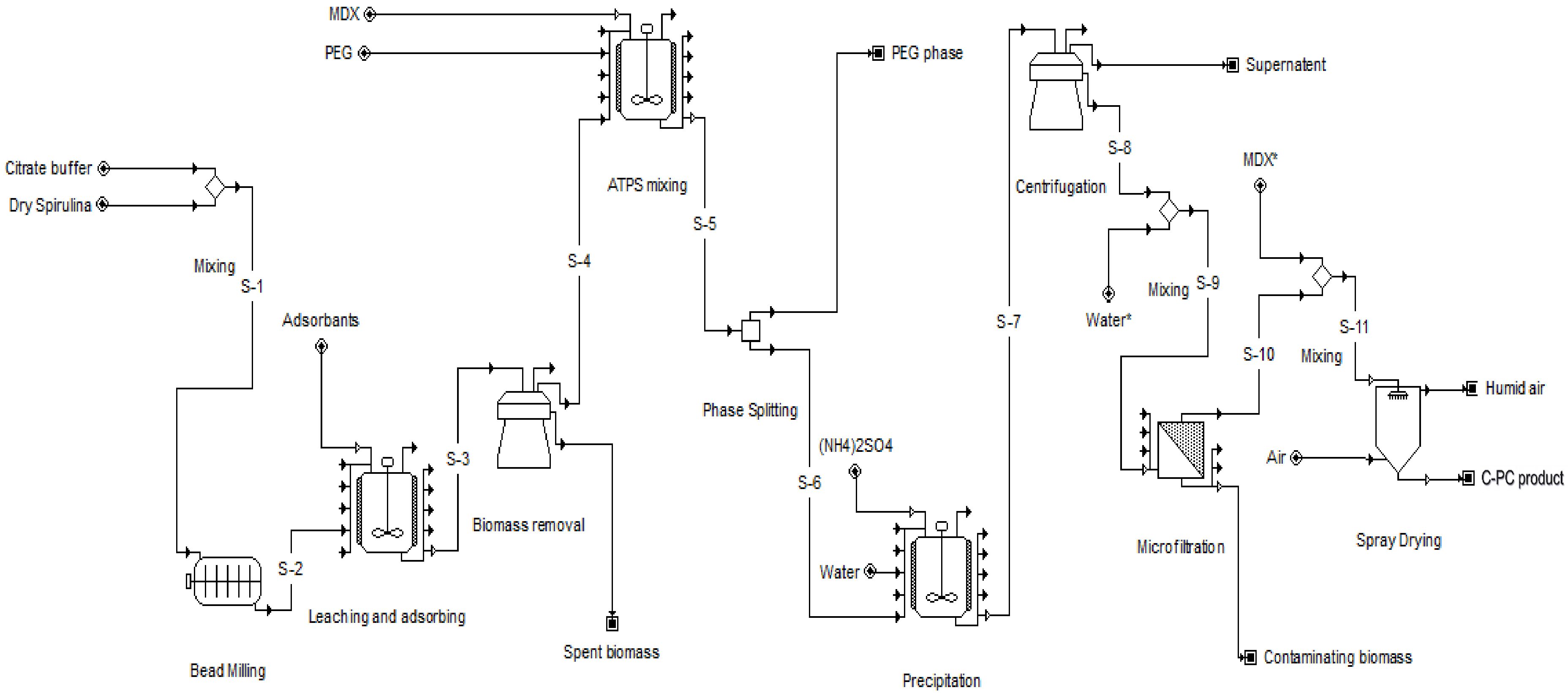

Figure 45. Pre-treatment C-PC ATPS process flowsheet with filter sterilisation compiled using SuperPro Designer

CeBER

8.2 Process comparison and conclusions

A comparison was done of the process simulations. The different overall C-PC recoveries and purities achieved are presented in Table 18. Consumables usage was also considered.

All five processes produced very high purity C-PC, well above cosmetic grade (purity number > 1.5). The two pre-treatment processes are estimated to produce the highest purity C-PC (possibly greater than 4). This is mainly due to the high purification factors found in studies using adsorbents on the crude extract, and having precipitation as a means of product recovery. Conservative figures were still used for both unit operations, and it would also be possible to favour recovery over purification for each of the process options presented. This is especially true if extremely high purity C-PC were not required, as in food and cosmetic applications.

The final pre-treatment process (using filter sterilisation) had the highest recovery, with an overall C-PC recovery of 47.7 % from the starting crude solution. This was followed by the pre-treatment process using two precipitation steps. The generally low recoveries were mainly due to the initial biomass removal stage, where only about 68 % of the C-PC is recovered from the leached solution, while the rest remains entrained in the biomass. Classical filtration with a washing step could possibly reduce this loss of C-PC, although this seems to be less favoured for algae (Al hattab *et al.*, 2015). The original process, with the three stages of precipitation at different $(NH_4)_2SO_4$ saturations, lead to the lowest recovery, despite using freeze drying as the drying method. The four alternate processes incurred losses in recovery due to the spray-drying method used, although these could be made up for by higher throughput and lower costs. The two-stage ATPS process with UF was the most resource intensive with respect to polymer, citrate salts, and water usage, while the original process had the highest use of ammonium sulfate, all of which add to production costs and waste treatment costs.

The number of separate unit procedures was highest with the two-stage ATPS process with added membrane stages for recycling of citrate and C-PC recovery from the MDX phase. The other processes had fewer unique process units required, and each had many units that could be reused for multiple purposes, such as the centrifuges and mixing tanks.

The original process had the greatest estimated time for three batches to be completed, at 67.3 h. Three batches were chosen since batches could overlap based on unit scheduling, and this would give a more realistic perspective on the time taken to produce C-PC. The original process had three precipitation stages which required equilibration of the $(NH_4)_2SO_4$ solutions and then separation by centrifuge, as well as a long freeze-drying cycle contributing to the long batch-times. The processes with two ATPS stages could both achieve three consecutive batches within 36.0 h. The first pre-treatment process produces batches the fastest, with three batches taking 21.8 h, and the pre-treatment process with filtration takes 24.1 h for three batches. These were the fastest due to only having the single ATPS, requiring less time for phases separation. The pre-treatment step is also fast and simple.

In this study the economics of the processes were not quantified, however it is certain that the higher the consumables usage, the smaller the gross profit margins could be. Expensive units, such as centrifugation and ultrafiltration, for example, also greatly shift the feasibility and desirability of implementing certain of the proposed options. Capital cost would need to be balanced with operating costs and production rate, since each process uses centrifugation in multiple procedures, which could be the same unit reused, saving capital cost, or could be multiple units, potentially increasing production rate.

Each of the processes were found to produce products with small amounts of MDX, citrate salts and $(NH_4)_2SO_4$, all of which have GRAS status, and could be safely used in food or cosmetics depending on the desired properties of the products. The processes can also easily be adjusted to accommodate the desired product purities.

Table 18. Key results for different process route options

Process	Original process	Two-stage ATPS process	Two-stage ATPS (with UF and recycle)	Pre-treatment process	Pre-treatment process with filtration
C-PC product purity*	3.77	3.33	2.47	>4.00	>4.00
Overall C-PC recovery ^	38.7 %	39.1 %	39.5 %	42.7 %	47.7 %
PEG usage	113 g/batch	105 g/batch	230 g/batch	116 g/batch	116 g/batch
MDX usage	226 g/batch	210 g/batch	460 g/batch	233 g/batch	233 g/batch
Citrate usage	48.4 g/batch	208 g/batch	163 g/batch	48.4 g/batch	48.4 g/batch
$(NH_4)_2SO_4$ usage	933 g/batch	710 g/batch	-	710 g/batch	350 g/batch
Process water usage	3.14 L/batch	2.91 L/batch	41.9 L/batch	2.63 L/batch	11.7 L/batch
Time taken for 3 batches	67.3 h	32.0 h	36.0 h	21.8 h	24.1 h

* Purity is highly uncertain, due to the purification factors being used from other studies, where different crude extracts and degree of processing differ widely.

^ Recovery based on total C-PC leached into the crude solution.

9 Conclusions and recommendations

9.1 Conclusions of the study

The aim of this study was to evaluate and improve the ATPS process developed for purifying and producing C-PC from *Spirulina*, and to explore various process routes surrounding the ATPS. The project focused on the use of the PEG – MDX ATPS as the core unit in the overall process, and attempted to improve it in order to produce a C-PC product of cosmetic grade (purity number >1.5). Greater understanding of the mass balance and equilibrium relationships in the ATPS were also sought, to allow improvement in the overall process and simulate the various options proposed, aiding further research.

For the *Spirulina* sourced for this research, the optimal leaching time could be reduced to 2 h, giving higher purity C-PC while also reaching the maximum C-PC concentration**.** The lower leaching time achieves a reduction in the risk of heavy bacterial loads causing contamination in the final product, as well as reduced equipment fouling in the process.

The phase diagrams produced for the PEG – MDX ATPS gave a greater understanding of the mass balance as well as the equilibrium involved in the ATPS. These showed that a near-pure MDX bottom phase was achievable in a PEG – MDX ATPS, as the bottom phase reached above 22 to 25 wt % MDX, meaning that no PEG would need to be removed in recovering C-PC from the bottom phase. These were used to guide studies on the impact of component concentrations on the purity, recovery and concentration of C-PC produced.

In evaluating the patented process using the PEG – MDX ATPS for C-PC purification, this work suggested the use of PEG 10000 as the best molecular weight for a single PEG – MDX ATPS. At 9 wt % PEG 10000 and 20 wt % MDX, C-PC was concentration by a factor of 1.65 ± 0.10 and a C-PC purification factor of 1.21 ± 0.01, with a 95.1 ± 7.8 % recovery. Cosmetic grade C-PC was not achieved with a single ATPS and would require use of the precipitation train based on the results from Chapter 6.

The two-stage ATPS, using PEG – citrate followed by the PEG – MDX ATPS, was proposed and tested to achieve the aim of producing cosmetic grade C-PC without the need for multiple precipitations (chapter 7). The study found that PEG 4000 performs best in this system, due to the improved recoveries in the PEG – citrate stage at lower PEG molecular weights. A C-PC purification factor of 2.11 ± 0.20 was found in the screening for the two stages, with PEG 6000 second best at a purification factor of 1.65 ± 0.16. This produced cosmetic grade C-PC after the two ATPS stages, achieving one of the main aims of the study.

For the factorial experiment which investigated PEG and citrate concentrations in a 2^3 factorial design using the selected PEG 4000, a predicted C-PC purification factor of 1.63 ± 0.28 at a recovery of 95.6 ± 8.0 % was found. This was predicted at 11 wt% PEG 4000 and 20 wt% citrate after modelling the ATPS results using *Statistica*. The modelled prediction for the PEG 4000 – MDX ATPS factorial design (also 2^3, investigating PEG and MDX concentrations), gave a C-PC purification factor of 1.43 ± 0.09, with a recovery of 86.8 ± 4.7

% at the best chosen concentrations of 11 wt% PEG and 22 wt% MDX The factorial experiments indicated that above cosmetic grade C-PC could be produced using the best concentrations found for each ATPS stage.

In summary, the aims of this thesis project were achieved. Leaching was studied using a new *Spirulina* sample, showing the necessity of testing the dried *Spirulina* received from each supplier, owing to the differing cell integrity and strength based on cultivation and drying conditions. The leaching time could be greatly reduced to 2 h (previously 24 h) and no bead-milling was required in this case. The PEG – MDX ATPS was studied and a greater understanding of the mass balance was obtained with phase diagrams. Cosmetic grade C-PC could also be produced using the two-stage process alone, before any precipitation steps. These results, together with findings from literature were used to propose and simulate possible process alternatives, presented in Chapter 8. These process alternatives form the basis for further study proposed for the project going forward.

The process simulations chapter (Chapter 8) looked more closely at the key questions designed to test potential for process improvement or improved process unit operations for producing cosmetic grade C-PC. Specifically, the following were addressed:

- Can ammonium sulfate use be reduced, or the precipitation step be replaced by UF or an alternative process?
- Can UF or other means be used to recycle PEG and maltodextrin?
- What process configuration allows for the most efficient C-PC production using ATPS?

Combining synthesis from literature with current findings, it could be concluded that a process employing pre-treatment with activated carbon and chitosan, has potential to produce cosmetic grade C-PC using *Spirulina* as the starting material. An activated carbon and chitosan pre-treatment stage would lead to greater C-PC purification by adsorbing more contaminating proteins, and remove more biomass by adsorption, improving performance in the ATPS and possibly decreasing downstream contamination.

The recommended process also employed a single PEG – MDX ATPS, which could benefit from further study in order to test the model predications made. With pre-treatment increasing the C-PC purity, the ATPS could favour C-PC recovery and concentration over purification, as the predicted final purity number of the C-PC product in the fifth process option is greater than 4.0, well above cosmetic grade.

A microfiltration step for reducing microbial contamination in the final product was proposed, as this would potentially save consumable chemical costs associated with using multiple ammonium sulfate precipitations to this purpose, since precipitation had the dual purpose of purification (which the process will no longer be as reliant on) and contamination removal. In this vain, a single precipitation stage was chosen to remove MDX and purify C-PC. This reduces ammonium sulfate use and batch time over the three precipitations used in the base-case process. A recycle was found not to be feasible with this process, due to the high polymer concentrations leading to high viscosity, making it impractical to separate PEG from MDX using membrane processes. Spray-drying of the final product was selected as the drying method of choice, owing to its scalability and potential cost-effectiveness as a drying method.

9.2 Recommendations for future work

A thorough techno-economic study should be performed for the process flowsheet proposed in Section 8.1.4. Through this analysis, further refinement may be proposed. Further, test work to experimentally validate the various steps proposed should also be undertaken, both at lab scale and to assess the upscaling of the process. The ATPS in particular warrants study of scale-up of its operation, with particular emphasis on phase equilibration and effective separation, as well as the equipment needed. Experimentally, there are many options for development going forward:

- The leaching of the *Spirulina* should be studied for each new sample, since the cyanobacterial samples differ depending on the source
- Continuously stirred C-PC leaching from the disrupted *Spirulina* should be used, to possibly further decrease time needed
- The proposed pre-treatment step should be experimentally tested. If promising, it could be optimised with the *Spirulina* used in the work, starting with the results from the reviewed literature (2.2.2)
- At a large scale, the biomass removal step should be reassessed, and the costs-benefit analysis of filtration over centrifugation explored
- The ATPS performance as a function of scale needs to be explored. Further, the method of phase separation should be considered (noting that a simple mixer-settler may be suitable at large scale depending on throughput)
- A single stage precipitation should be explored based on the proposed process, and optimised if promising
- Filter sterilisation using a microfiltration unit should be tested for its ability to reduce bacterial contamination
- Spray drying should be tested, and it should be determined whether the addition of MDX (and/or other carriers) is necessary to improve recovery

While not yet presented in the proposed process, the possibility of recycling the PEG top phase in a process using only a PEG – MDX ATPS requires consideration. Here, a conceivable option would be using activated carbon filtration. Literature could not be found for using activated carbon for recycling polymer streams, but it was found to selectively adsorb contaminating proteins in a crude *Spirulina* extract, which could be applied to a PEG phase containing these proteins. The viscosity of a high-concentration polymer stream would likely be a challenge to overcome, and could warrant further study and economic evaluation.

The market for C-PC is projected to be growing at 5 to 7 % annually, presenting an opportunity for companies to fill in the gaps in production. Additional uses for the pigment are studied and published at a growing rate, leading to the potential demand for higher purity C-PC. The work presented here could potentially lead to a lucrative commercial process for supplying the growing demand for high quality C-PC for food and cosmetics, and could lay the foundation for further work to produce reagent-grade C-PC for pharmaceutical and research purposes.

References

Abakoura, B. 2018. *Interfacial behavior of colored protein fractions from Spirulina platensis*. PhD Thesis. Liege University.

Abalde, J., Torres, E., Betancourt, L., Cid, A. and Barwell, C. 1998. 'Purification and characterization of phycocyanin from the marine cyanobacterium *Synechococcus* sp. IO9201', *Plant Science*, 136(1), pp. 109–120. doi: 10.1016/s0168-9452(98)00113-7.

Antelo, F. S., Anschau, A., Costa, J. A. V and Kalil, S. J. 2010. 'Extraction and Purification of C-phycocyanin from *Spirulina platensis* in Conventional and Integrated Aqueous Two-Phase Systems', *Journal of Brazilian Chemical Society*, 21(5), pp. 921–926.

Antelo, F. S., Costa, J. A. V. and Kalil, S. J. 2015. 'Purification of C-phycocyanin from *Spirulina platensis* in aqueous two-phase systems using an experimental design', *Brazilian Archives of Biology and Technology*, 58(1), pp. 1–11. doi: 10.1590/S1516-8913201502621.

Asenjo, J. A. and Andrews, B. A. 2011. 'Aqueous two-phase systems for protein separation: A perspective', *Journal of Chromatography A*, 1218(49), pp. 8826–8835. doi: 10.1016/j.chroma.2011.06.051.

Benavides, J. and Rito-Palomares, M. 2005. 'Potential aqueous two-phase processes for the primary recovery of colored protein from microbial origin', *Engineering in Life Sciences*, 5(3), pp. 259–266. doi: 10.1002/elsc.200420073.

Boussiba, S. and Richmond, A. . 1979. 'Isolation and characterization of phycocyanins from the blue-green alga *Spirulina platensis'*, *Archives of Microbiology*, 120(2), pp. 155-159.

Chethana, S., Nayak, C. A. and Madhusudhan, M. C. 2015. 'Single step aqueous two-phase extraction for downstream processing of C-phycocyanin from *Spirulina platensis'*, *Journal of Food Science and Technology*, 52(4), pp. 2415–2421. doi: 10.1007/s13197-014-1287-9.

Cunha, T. and Aires-Barros, R. 2003. 'Large-Scale Extraction of Proteins', *Molecular Biotechnology*, 20(1), pp. 029–040. doi: 10.1385/mb:20:1:029.

Dewi, E. N., Purnamayati, L. and Kurniasih, R. A. 2016. 'Antioxidant activities of phycocyanin microcapsules using maltodextrin and carrageenan as coating materials', *Jurnal Teknologi*, 2, pp. 45–50.

Dewi, E. N., Purnamayati, L. and Kurniasih, R. A. 2017. 'Physical characteristics of phycocyanin from *spirulina* microcapsules using different coating materials with freeze drying method Physical Characteristics of Phycocyanin from *Spirulina* Microcapsules using Different Coating Materials with Freeze Drying Meth', *IOP Conf. Series: Earth and Environmental Science*, 55. doi: 10.1088/1742-6596/755/1/011001.

Dubois, M., Gilles, K. A., Hamilton, J. K., Rebers, P. A. and Smith, F. 1956. 'Colorimetric Method for Determination of Sugars and Related Substances', *Analytical chemistry*, 28(3), pp. 350–356.

Dufosse, L., Galaup, P., Yaron, A., Malis, S., Blanc, P., Murthy, N. C., Ravishankar, G. A. and Durand, G. 2005. 'Microorganisms and microalgae as sources of pigments for food use : a scientific oddity or an industrial reality ?', *Trends in Food Science and Technology*, 16, pp. 389–406. doi: 10.1016/j.tifs.2005.02.006.

Eriksen, N. T. 2008. 'Production of phycocyanin — a pigment with applications in biology , biotechnology , foods and medicine', *Applied microbiology and biotechnology*, 80(1), pp. 1–14. doi: 10.1007/s00253-008-1542-y.

Fekrat, F., Nami, B., Ghanavati, H., Ghaffari, A. and Shahbazi, M. 2019. 'Optimization of chitosan / activated charcoal-based purification of *Arthrospira platensis* phycocyanin using response surface methodology', *Journal of Applied Phycology*. Journal of Applied Phycology, 31, pp. 1095–1105. doi: 10.1007/s10811-018-1626-8.

Furuki, T., Maeda, S., Imajo, S., Hiroi, T., Amaya, T., Hirokawa, T., Ito, K. and Nozawa, H. 2003. 'Rapid and selective extraction of phycocyanin from *Spirulina platensis* with ultrasonic cell disruption', *Journal of Applied Phycology*, 15(1979), pp. 319–324.

Geckeler, K. E. and Court, H. 1996. 'Removal of Hazardous Substances from Water Using Ultrafiltration in Conjunction with Soluble Polymers', *Environmental Science and Technology*, 30(3), pp. 725–734. doi: 10.1021/es950326l.

Glazer, A. N. 1994. 'Phycobiliproteins - A Family of Valuable , Widely Used Fluorophores Phycobiliproteins - a family of valuable , widely used fluorophores', *Journal of Applied Phycology*, 6, pp. 105–112. doi: 10.1007/BF02186064.

Glyk, A., Scheper, T. and Beutel, S. 2014. 'Influence of Different Phase-Forming Parameters on the Phase Diagram of Several PEG − Salt Aqueous Two-Phase Systems', *Journal of Chemical and Engineering Data*, 59, pp. 850–859. doi: 10.1021/je401002w.

Graverholt, O. S. and Eriksen, N. T. 2007. 'Heterotrophic high-cell-density fed-batch and continuous-flow cultures of *Galdieria sulphuraria* and production of phycocyanin', *Applied Microbiology and Biotechnology*, 77(1), pp. 69–75. doi: 10.1007/s00253-007-1150-2.

Griffiths, M., Harrison, STL, Smit, D. and Maharajh, M. 2016. 'Major commercial products from micro- and macroalgae', in Bux, F. and Chisti, Y. (eds) *Algae Biotechnology: Products and Processes*. Cape Town: Springer International Publishing, pp. 269–300. doi: http://dx.doi.org/10.1007%2F978-3-319-12334-9_14.

Griffiths, M., Burke, M., Pott, R., Fagan-Endres, M. and Harrison, STL. 2016. *Phycocyanin production from Spirulina, Project close out report, UCT TIA Seed Fund*. Cape Town.

Grossman, P. D. and Gainer, J. L. 1988. 'Correlation of Aqueous Two-Phase Partitioning of Proteins with Changes in Free Volume', *Biotechnology Progress*, 4(1), pp. 6–11. doi: 10.1002/btpr.5420040103.

Guan, S. 2016. *Liquefaction of its residues to produce bio-crude oil*. MSc Thesis. University of Illinois.

Harrison, R. G., Todd, P., Rudge, S. R. and Petrides, D. P. 2013. 'Laboratory exercises in bioseparations', in *Bioseparations Science and Engineering*. New York: Oxford University Press, pp. 511–530.

Harrison, STL, Burke, M., Pott, R. and Fagan-Endres, M. 2019. 'Method for purifying phycocyanin'. International Bureau: World Intellectual Property Organization, WO2019034955A1.

Al hattab, M., Ghaly, A. and Hammoud, A. 2015. 'Microalgae Harvesting Methods for Industrial Production of Biodiesel : Critical Review and Comparative Analysis Fundamentals of Renewable Energy and Applications', *Journal of Fundementals of Renewable Energy and Applications*, 5(2). doi: 10.4172/20904541.1000154.

Hatti-Kaul, R. 2000. *Aqueous Two-phase Systems: Methods and Protocols*. Totowa, New Jersey: Humana Press.

Herrera, A. ., Boussiba, S. ., Napoleone, V. . and Hohlberg, A. . 1989. 'Recovery of c-phycocyanin from the cyanobacterium *Spirulina maxima'*, *Journal of Applied Phycology*, 1(4), pp. 325–331. doi: 10.1007/BF00003469.

Hu, M., Zhai, Q., Jiang, Y., Jin, L. and Liu, Z. 2004. 'Liquid - Liquid and Liquid - Liquid - Solid

Equilibrium in PEG + Cs_2SO_4 + H_2O', *Journal of Chemical Engineering Data*, pp. 1440–1443. doi: 10.1021/je0498558.

Hustedt, H. 1986. 'Extractive enzyme recovery with simple recycling of phase forming chemicals', *Biotechnology Letters*, 8(11), pp. 791–796.

Ilter, I., Akyil, S., Koc, M., Demirel, Z., Dalay, M. C. and Ertekin, K. F. 2017. 'Microencapsulation of phycocyanin by spray drying technique', *Journal of Biotechnology*, 256.

Iqbal, M., Tao, Y., Xie, S., Zhu, Y., Chen, D., Wang, X., Huang, L., Peng, D., Sattar, A., Shabbir, M. A. B., Hussain, H. I., Ahmed, S. and Yuan, Z. 2016. 'Aqueous two-phase system (ATPS): an overview and advances in its applications', *Biological Procedures Online*, 18(1), pp. 1–18. doi: 10.1186/s12575-016-0048-8.

Kuar, G., Khattar, J. I. S., Singh, D. P., Singh, Y. and Nadda, J. 2009. 'Microalgae: a Source of Natural Colours', *Algal Biology and Biotechnology*, (July 2016), pp. 129–149.

Kuddus, M., Singh, P., Thomas, G. and Al-hazimi, A. 2013. 'Recent Developments in Production and Biotechnological Applications of C-Phycocyanin', *BioMed Research International*, 2013. doi: 10.1155/2013/742859.

Kurniasih, R. A., Purnamayati, L., Amalia, U. and Dewi, E. N. 2018. 'Formulation and Characterization of Phycocyanin Microcapsules within Maltodextrin- Alginate', *Agritech*, 38(1), pp. 23–29. doi: 10.22146/agritech.16752.

Li, Y., Zhang, Z., Paciulli, M. and Abbaspourrad, A. 2020. 'Extraction of phycocyanin — A natural blue colorant from dried *spirulina* biomass : Influence of processing parameters and extraction techniques', *Journal of Food Science*, 85(3), pp. 727–735. doi: 10.1111/1750-3841.14842.

Machado, F. L. C., Dos Reis Coimbra, J. S., Zuniga, A. D. G., Da Costa, A. R. and Martins, J. P. 2012. 'Equilibrium data of aqueous two-phase systems composed of poly(ethylene glycol) and maltodextrin', *Journal of Chemical and Engineering Data*, 57(7), pp. 1984–1990. doi: 10.1021/je3002442.

Minkova, K. M., Tchernov, A. A., Tchorbadjieva, M. I., Fournadjieva, S. T., Antova, R. E. and Busheva, M. C. 2003. 'Purification of C-phycocyanin from *Spirulina* (*Arthrospira*) *fusiformis*', *Journal of Biotechnology*, 102(1), pp. 55–59. doi: 10.1016/S0168-1656(03)00004-X.

Mitchinson, C. and Pain, R. H. 1985. 'Effects of sulphate and urea on the stability and reversible unfolding of β-lactamase from *Staphylococcus aureus*: implications for the folding pathway of β-lactamase', *Journal of molecular biology*, 184(2), pp. 331–342. doi: 10.1016/0022-2836(85)90384-5.

Moreno, J., Rodríguez, H., Vargas, M. A., Rivas, J. and Guerrero, M. G. 1995. 'Nitrogen-fixing cyanobacteria as source of phycobiliprotein pigments. Composition and growth performance of ten filamentous heterocystous strains', *Journal of Applied Phycology*, 7(1), pp. 17–23. doi: 10.1007/BF00003545.

Murty, V. R., Rajasekar, V., Raja, S., Thivaharan, V. and Ramesh, V. 2012. 'Aqueous Two Phase Systems for the Recovery of Biomolecules – A Review', *Science and Technology*, 1(1), pp. 7–16. doi: 10.5923/j.scit.20110101.02.

De Oliveira, R. M., Dos Reis Coimbra, J. S., Minim, L. A., Da Silva, L. H. M. and Fontes, M. P. F. 2008. 'Liquid-liquid equilibria of biphasic systems composed of sodium citrate + polyethylene(glycol) 1500 or 4000 at different temperatures', *Journal of Chemical and Engineering Data*, 53(4), pp. 895–899. doi: 10.1021/je7004209.

Papamichael, N., Borner, B., Hustedt, H., Forschung, B., Weg, M. and Braunschweig, D.-

1992. ‘Continuous Aqueous Phase Extraction of Proteins : Automated Processing and Recycling of Process Chemicals’, *Journal of Chemical Technology & Biotechnology*, 54, pp. 47–55. doi: 0268-2575/92/$05.0.

Patil, G., Chethana, S., Sridevi, A. S. and Raghavarao, K. S. M. S. 2006. ‘Method to obtain C-phycocyanin of high purity’, *Journal of Chromatography A*, 1127(1–2), pp. 76–81. doi: 10.1016/j.chroma.2006.05.073.

Patil, G., Chethana, S., Madhusudhan, M. C. and Raghavarao, K. S. M. S. 2008. ‘Fractionation and purification of the phycobiliproteins from *Spirulina platensis’*, *Bioresource Technology*, 99(15), pp. 7393–7396. doi: 10.1016/j.biortech.2008.01.028.

Patil, G. and Raghavarao, K. S. M. S. 2007. ‘Aqueous two phase extraction for purification of C-phycocyanin’, *Biochemical Engineering Journal*, 34(November 2006), pp. 156–164. doi: 10.1016/j.bej.2006.11.026.

Pott, R. 2018. ‘The release of the blue biological pigment cytolysis of live *Spirulina* sp . Coloration Technology’, *Coloration Technology*, 135(1), pp. 17–21. doi: 10.1111/cote.12373.

Purnamayati, L., Dewi, E. N. and Kurniasih, R. A. 2018. ‘Phycocyanin stability in microcapsules processed by spray drying method using different inlet temperature Phycocyanin stability in microcapsules processed by spray drying method using different inlet temperature’, *Earth and Environmental Science*, 116.

Raghavarao, K. S. M. S., Rastogi, N. K., Gowthaman, M. K. and Karant, N. G. 1995. ‘Aqueous Two-Phase Extraction for Downstream Processing of Enzymes / Proteins’, *Advances in Applied Microbiology*, 41, pp. 97–171.

Ramos, A., Acién, F. G., Fernández-sevilla, J. M., González, C. V and Bermejo, R. 2011. ‘Development of a process for large-scale purification of C-phycocyanin from *Synechocystis aquatilis* using expanded bed adsorption chromatography’, *Journal of Chromatography B*, 879(7–8), pp. 511–519. doi: 10.1016/j.jchromb.2011.01.013.

Ramyadevi, D., Subathira, A. and Saravanan, S. 2012. ‘Phase compositions of aqueous two-phase systems formed by poly (ethylene glycol) and maltodextrin at different temperatures’, *International Journal of Chemical Sciences and Applications*, 3(2), pp. 289–292.

Report Hive Research 2019. *Global Phycocyanin Market Research Report 2020 by Manufacturers, Regions, Types and Applications*, *Report Hive Research*. Available at: https://www.reporthive.com/Report/2112499/phycocyanin-market (Accessed: 1 April 2020).

Rito-Palomares, M., Nuez, L. and Amador, D. 2001. ‘Practical application of aqueous two-phase systems for the development of a prototype process for c-phycocyanin recovery from *Spirulina maxima’*, *Journal of Chemical Technology and Biotechnology*, 76(12), pp. 1273–1280. doi: 10.1002/jctb.507.

Rogner, M., Nixon, P. J. and Diner, B. A. 1990. ‘Purification and characterization of Photosystem I and Photosystem II core complexes from wild-type and phycocyanin-deficient strains of the cyanobacterium *Synechocystis* PCC 6803’, *Journal of Biological Chemistry*, 265(11), pp. 6189–6196.

Scheer, H. and Kufer, W. 1977. ‘Conformational Studies on C-Phycocyanin from *Spirulina platensis’*, *Journal of Biosciences*, 32(7–8), pp. 513–519. doi: 10.1515/znc-1977-7-806.

Sekar, S. and Chandramohan, M. 2008. ‘Phycobiliproteins as a commodity : trends in applied research , patents and commercialization’, *Journal of Applied Phycology*, 20, pp. 113–136. doi: 10.1007/s10811-007-9188-1.

Shkinev, V. M., Eva, G. A. V., Spivakov, B. Y. A., Geckeler, K. E. and Bayer, E. 1987.

‘Enrichment of Arsenic and Its Separation from Other Elements by Liquid-Phase Polymer-Based Retention’, *Separation Science and Technology*, 22(11), pp. 2165–2173.

Shukia, S. P., Singh, J. S., Kashyap, S., Giri, D. D. and Kashyap, A. K. 2008. ‘Antarctic cyanobacteria as a source of phycocyanin: An assessment’, *Indian Journal of Marine Sciences*, 37(4), pp. 446–449.

Silva, L. H. M. and Meirelles, A. J. A. 2001. ‘Phase equilibrium in polyethylene glycol / maltodextrin aqueous two-phase systems’, *Carbohydrate Polymers*, 42(2000), pp. 273–278.

Song, W., Zhao, C. and Wang, S. 2013. ‘A large-scale preparation method of high purity c-phycocyanin’, *International journal of bioscience, biochemistry and bioinformatics*, 3(4), pp. 293–297. doi: 10.7763/IJBBB.2013.V3.216.

Sørensen, L., Hantke, A. and Eriksen, N. T. 2013. ‘Purification of the photosynthetic pigment C-phycocyanin from heterotrophic *Galdieria sulphuraria’*, *Journal of the Science of Food and Agriculture*, 93(12), pp. 2933–2938. doi: 10.1002/jsfa.6116.

Srinivas, N. D. 2000. *Aqueous two-phase extraction for the downstream processing of enzymes*. PhD Thesis. University Of Mysore. doi: 10.1016/S0065-2164(08)70309-5.

Stec, B., Troxler, R. F. and Teeter, M. M. 1999. ‘Crystal Structure of C-Phycocyanin from Cyanidium caldarium Provides a New Perspective on Phycobilisome Assembly’, *Biophysical Journal*, 76(6), pp. 2912–2921. doi: 10.1016/S0006-3495(99)77446-1.

Stewart, D. and Farmer, F. 1982. ‘Extraction, identification, and quantitation pigments from phototrophic plankton’, *Limnology and Oceanography*, 29(2), pp. 392–397.

Tan, Z., Li, F., Xu, X. and Xing, J. 2012. ‘Simultaneous extraction and purification of aloe polysaccharides and proteins using ionic liquid based aqueous two-phase system coupled with dialysis membrane’, *Desalination*, 286, pp. 389–393. doi: 10.1016/j.desal.2011.11.053.

Tanuja, S., Srinivas, N. D., Gowthaman, M. K. and Raghavarao, K. S. M. S. 2000. ‘Aqueous two-phase extraction coupled with ultrafiltration for purification of amyloglucosidase’, *Bioprocess Engineering*, 23, pp. 63–68. doi: https://doi.org/10.1007/s004499900123.

Tubıo, G., Pellegrini, L., Nerli, B. B. and Pico, G. A. 2006. ‘Liquid - Liquid Equilibria of Aqueous Two-Phase Systems Containing Poly (ethylene glycols) of Different Molecular Weight and Sodium Citrate’, pp. 209–212. doi: 10.1021/je050332p.

U.S. Food and Drug Administration 2019. *Listing of Specific Substances Affirmed as GRAS: Sec. 184.1444 Maltodextrin.*, *U.S. FDA*. Available at: https://www.accessdata.fda.gov/scripts/cdrh/cfdocs/cfcfr/cfrsearch.cfm?fr=184.1444 (Accessed: 14 April 2020).

Uduman, N., Qi, Y., Danquah, M. K., Forde, G. M. and Hoadley, A. 2010. ‘Dewatering of microalgal cultures: a major bottleneck to algae-based fuels.’, *Journal of renewable and sustainable energy*, 2(1), p. 12701.

Vandamme, D., Foubert, I. and Muylaert, K. 2013. ‘Flocculation as a low-cost method for harvesting microalgae for bulk biomass production’, *Trends in Biotechnology*, 31(4), pp. 233–239. doi: 10.1016/j.tibtech.2012.12.005.

Vernès, L., Granvillain, P., Chemat, F. and Vian, M. 2015. ‘Phycocyanin from Arthrospira Platensis . Production , Extraction and Analysis Phycocyanin from *Arthrospira platensis* . Production , Extraction and Analysis’, *Current Biotechnology*, 4(October). doi: 10.2174/2211550104666151006002418.

Wang, F., Cui, Z.-G., Liu, Y.-H., Shao, L.-L. and Ma, Y. 2016. ‘Application of TMA-PEG to promote C-phycocyanin extraction from *S. platensis* in the PEG ATPS’, *Process*

Biochemistry, 52(November 2016), pp. 283–294. doi: 10.1016/j.procbio.2016.11.006.

Wang, W., Zhang, X., Xu, C. and Cheng, H. 2012. 'Purification and Concentration of C-Phycocyanin from *Spirulina Platensis* Using Aqueous Two-Phase System', *Applied Mechanics and Materials*, 138–139, pp. 995–1001. doi: 10.4028/www.scientific.net/AMM.138-139.995.

Wingfield, P. T. 2016. 'Protein Precipitation Using Ammonium Sulfate', *Current Protocols in Protein Science*, 13(1), p. A-3F. doi: 10.1002/0471140864.psa03fs13.Protein.

Yoshikawa, N. and Belay, A. 2008. 'Single-Laboratory Validation of a Method for the Determination of c-Phycocyanin and Allophycocyanin in *Spirulina* (*Arthrospira*) Supplements and Raw Materials by Spectrophotometry', *Journal of AOAC International*, 91(3), pp. 650–655.

Appendix A: ZivaHub Open Data UCT files

A.1 Leaching study data

DOI: 10.25375/uct.13901744

A.2 Phase diagrams PEG – MDX data

DOI: 10.25375/uct.13901738

A.3 Phase diagrams PEG – citrate data

DOI: 10.25375/uct.13901750

A.4 PEG – MDX ATPS evaluation studies

DOI: 10.25375/uct.13901747

A.5 Two-stage ATPS screening experiments

DOI: 10.25375/uct.13901753

A.6 PEG – citrate ATPS factorial design data

DOI: 10.25375/uct.13901741

A.7 PEG – MDX ATPS factorial design data

DOI: 10.25375/uct.13901735

A.8 Original patented process stream tables

DOI: 10.25375/uct.13901873

A.9 Original patented process simulation file

DOI: 10.25375/uct.15079065

A.10 Two-stage ATPS process stream tables

DOI: 10.25375/uct.13901873

A.11 Two-stage ATPS process simulation file

DOI: 10.25375/uct.15079065

A.12 Two-stage ATPS process with recycle and UF stream tables

DOI: 10.25375/uct.13901873

A.13 Two-stage ATPS process with recycle and UF simulation file

DOI: 10.25375/uct.15079065

A.14 First iteration pre-treatment process stream tables

DOI: 10.25375/uct.13901873

A.15 First iteration pre-treatment process simulation file

DOI: 10.25375/uct.15079065

A.16 Pre-treatment process with filter sterilisation stream tables

DOI: 10.25375/uct.13901873

A.17 Pre-treatment process with filter sterilisation simulation file

DOI: 10.25375/uct.15079065

Appendix B: Simulation inputs

Table 19. Process simulation inputs and rationale expanded

Unit procedure/ parameter in question	Values used	Reference	Rationale
C-PC content in *Spirulina*	5.3 $g_{C\text{-}PC}$/100g	Leaching study (6.2.1)	Only leachable C-PC is useful in simulation
Leaching time	2 h	Leaching study (6.2.1)	Maximum time needed to fully leach C-PC from sample
Biomass removal	96 %	Uduman *et al.* *(*2010)	Centrifugation used. Same value used in pre-treatment process for prudence due to not testing
C-PC recovery over biomass removal	68 %	ATPS study (6.2.3)	Solids concentration in waste stream adjusted to achieve observed recovery
Split factors for ATPS phases	See simulation files	PEG – MDX (6.2.2, 6.2.3 & 7.3.3) PEG – MDX (7.2.1 & 7.3.2)	Based on component splits from phase diagrams produced, and C-PC recoveries and purification from the ATPS studies
Precipitation stages concentrations	From patent method	Presented in Section 5.3.2.4	Based on patented process, using three stages at different $(NH_4)_2SO_4$ saturations
Precipitation stages recoveries	Depending on stage and saturation	Song *et al.* (2013)	Depending on saturation different amounts of C-PC and proteins are precipitated, affecting purity and recovery
Precipitation stages purifications	Purification factors of 1.1, 2.3 and 1.6 for the 3 stages. 2.0 used for pre-treatment process	Patent close-out report (Griffiths, Burke, *et al.*, 2016)	Purifications used as per data shown in Figure 11. Good starting point despite different starting purity. Pre-treatment process used an intermediate value as starting point
Ultrafiltration for citrate recycle	100 % protein rejection (and biomass)	Harrison *et al.* (2013)	Versatile unit with variable membrane pore-sizes, and a large MW difference between components. Also testing required for accurate results

Table 20. Process simulation inputs and rationale continued

Unit procedure/ parameter in question	Values used	Reference	Rationale
Recycle ratio for citrate recycle	90 % recycled	-	Assumption for a decent starting point, also does not overload the system with liquid volume
Microfiltration for biomass removal	100 % biomass rejection coefficient	Harrison *et al.* (2013)	Based on relative molecular sizes of membrane cut-offs and biomass size, can choose to have complete removal/sterilisation
Ultrafiltration for C-PC recovery	80 % C-PC recovery	Tanuja *et al.* (2000); Sørensen *et al.* (2013)	In the range found when using UF to purify proteins from MDX, and previous studies where C-PC was purified from PEG
Pre-treatment purification factor and recovery	Purification factor of 2.0. Recovery of 90 % (adjusted after stage)	See Section 2.2.2 (multiple sources)	Prudent assumption, purification factors of 2 – 7 have been found in different studies, and high recoveries possible when lower purification targeted
Spray drying	Recovery of 80 % chosen, with residual MDX from ATPS as carrier	Ilter *et al.* (2017) & see Section 2.5.2	Assumed as a start point. This step needs testing and optimisation, varying results found in literature, with highest being 87 % from source mentioned
Freeze drying	Recovery of 100 % Time taken of 15 h	This work	No degradation expected when freeze-drying and no significant residue loss. Time taken suggested by *Superpro* and makes sense from this experimental work